Analysis of Plastic Deformation According to Von Mises' Theory With Application to the South Silverton Area, San Juan County Colorado

GEOLOGICAL SURVEY PROFESSIONAL PAPER 378-B

Analysis of Plastic Deformation According to Von Mises' Theory With Application to the South Silverton Area, San Juan County Colorado

By DAVID J. VARNES

THE SOUTH SILVERTON MINING AREA, SAN JUAN COUNTY, COLORADO

GEOLOGICAL SURVEY PROFESSIONAL PAPER 378-B

UNITED STATES GOVERNMENT PRINTING OFFICE, WASHINGTON : 1962

UNITED STATES DEPARTMENT OF THE INTERIOR

STEWART L. UDALL, *Secretary*

GEOLOGICAL SURVEY

Thomas B. Nolan, *Director*

For sale by the Superintendent of Documents, U.S. Government Printing Office
Washington 25, D.C.

CONTENTS

	Page
Abstract	B–1
Introduction	1
Principal features of the theory of elasticity	3
Stress	3
Types of stress	3
Variation with orientation of stress at a point	4
Stresses in static equilibrium	7
Strain	8
Definitions and notation	8
Stress-strain relations in the elastic state	11
Condition of compatibility	12
Plane strain and plane stress	12
The stress function	13
The plastic state	14
Definitions	14
Criteria of failure	15
Relation between load and deformation in the plastic state	17
Generalized expression for slip lines in plane plastic strain (cartesian coordinates)	20
Prandtl's compressed strip	21
Statement of the problem	21
Slip lines	22
Stresses	22
Velocity field	23
Formulas in polar coordinates	25
Stress notation and equilibrium equations	B–25
Strain and velocities	26
Relations of plastic stress to rate of strain in plane strain	26
Generalized expressions for slip lines in plane plastic strain	27
Generalized expressions for stresses in plane plastic strain	29
Geometric properties of slip lines	30
Application to the South Silverton area	31
General statement	31
Analysis of the western shear system	35
Statement of the problem	35
Derivation of slip lines	36
Normal stresses	39
Velocities	40
Analysis of the eastern shear system	41
Statement of the problem	41
Derivation of slip lines	43
Normal stresses	44
Comparison of slip-line fields and actual fault patterns	46
Western part	46
Eastern part	46
Discussion of results	46
References cited	48

ILLUSTRATIONS

[Plates are in pocket]

			Page
PLATE	1.	First flow diagram.	
	2.	Second flow diagram.	
FIGURE	1.	Stresses on a cubic element in equilibrium	B–4
	2.	Stresses on a triangular element in equilibrium	4
	3.	*A*, Mohr's circle of stress. *B*, Physical plane corresponding to stress plane	6
	4.	Stresses on small rectangular element	8
	5.	Components of displacement	8
	6.	*A*, Homogeneous infinitesimal strain. *B*, Mohr's circle for strains	9
	7.	Stress-strain relations	14
	8.	State of stress at failure, Coulomb criterion	16
	9.	Parabolic envelope of stress circles	18
	10.	Stress circle envelope, constant shear stress	19
	11.	Physical arrangement in Prandtl's strip	21
	12.	Directions of principal stress and shear on rectangular element in Prandtl's strip	22
	13.	Net of principal shear stress trajectories in compressed strip	23
	14.	Stresses on triangular element in polar coordinates	25
	15.	Generalized geologic map of part of the Silverton caldera	31
	16.	Principal fracture systems of South Silverton area	33
	17.	Simplified structural pattern	34
	18.	Slip lines between inclined lines (Nádai)	36
	19.	Compressed wedge, idealization	37
	20.	Compression of wedge, boundary velocities	40
	21.	Compressed annular ring	42
	22.	Sketch map of subsided block	45
	23.	Comparison of actual faults with theoretical pattern	47

THE SOUTH SILVERTON MINING AREA, SAN JUAN COUNTY, COLORADO

ANALYSIS OF PLASTIC DEFORMATION ACCORDING TO VON MISES' THEORY, WITH APPLICATION TO THE SOUTH SILVERTON AREA, SAN JUAN COUNTY, COLORADO

By DAVID J. VARNES

ABSTRACT

The patterns of faults in the South Silverton mining area are analyzed according to Von Mises' theory of plasticity in plane strain. Initial sections are devoted to standard derivations of basic equations concerning stress, to criteria of failure, and to plastic stress-strain relations in plane strain. Generalized differential equations are derived for slip lines in polar coordinates and applied in the later sections of the report to the two basic problems presented by the Silverton district.

The first problem is that of determining the slip-line pattern to be expected if a wedge is compressed in plane strain so that material flows toward the large end. This simulates the inferred mode of deformation in the western part of the district. The orientation of certain faults are used as boundary conditions for solution of the differential equations and the whole of the slip-line field is reconstructed from partial knowledge of the fault system. Equations for the conjugate shears are exponential in form. A compatible velocity field is derived.

The second problem is that of constructing the slip-line field generated by radial stresses, in plane strain, within a segment of a ring around the southeast border of the subsided block of the Silverton caldera. The geometry of certain faults is again used to reconstruct the whole theoretical pattern. Although the equations of the slip lines are exponential in form, they represent orthogonal epicycloids and hypocycloids. The distribution of stresses required to form the slip lines in the eastern district are computed. They appear compatible with stresses to be expected due to wedging of a graben area at the northeast corner of the subsided block.

Theoretical slip-line fields for both the western and eastern parts of the district are compared with the actual fault pattern. Although there are differences, the agreement is, on the whole, satisfactory.

INTRODUCTION

An examination of the mining area southeast of Silverton, Colo., indicated that the veins and faults form a pattern that might be amenable to theoretical analysis. The present paper, which is a companion report to that on the general geology and ore deposits of the area (Prof. Paper 378–A), presents one of the several possible types of analyses that may be applied to a study of the fault pattern.

The purpose of such an analysis is to better understand the mechanical system within which the faults were formed. If one or several theoretical systems may be found that simulate the relations observed in the field to a reasonable degree, it may then be possible to make inferences or extrapolations regarding features that cannot be observed directly. For example, if the interest is in ores that occur in veins along faults and if the complete pattern of faults can be inferred from exposures of parts of the pattern, then this inferred pattern perhaps may be used to advantage in exploring areas that are less well known or covered by younger deposits.

This analysis of the Silverton fault systems seeks to test the possibility that some information about the whole of a fault pattern within a structural unit may be derived from knowledge only of certain parts. Because the analysis is essentially the solution of a boundary-value problem, the type of information derived from the solution depends upon the type of information that is put in. Several approaches are possible; the emphasis in this report is upon orientation of faults. The strikes of faults along certain lines, which are generally the boundaries of the structural units, are known. From these partial data the full theoretical pattern of strikes of faults in the interior of the units is derived by analysis. The pattern of theoretical strikes of faults is then compared with the actual pattern by direct superposition on the geologic map. By this kind of test, some opinion may be formed concerning the usefulness of this particular type of analysis to the study of other fault systems where the full pattern is not actually known.

This analysis differs in several respects from the

types of theoretical analyses of geologic structures that have appeared with increasing excellence and frequency in the geological literature. It is, first of all, a specific study in which analysis is applied to actual structures in a relatively small area, rather than to idealized or generalized classes of geologic structures. The absence of scale models or other experimental methods of study that might be used to supplement the theoretical results is perhaps a disadvantage; but it is hoped that, if so, this deficiency is in part made up by direct comparison with nature.

Further, the analysis proceeds from a formal theory of plasticity that allows permanent deformation, rather than from the theory of elasticity, which excludes faulting or any other type of permanent deformation. Perhaps this is a matter having more logical import than practical necessity, since the usual procedure of mentally transforming principal shear-stress trajectories in an elastic medium into real faults in a permanently deformed medium has been used with some success. Yet, it seems prudent to avoid this logical hiatus, if possible, and to explore the use of theories of plasticity that actually may admit discontinuities, even though at present these theories perhaps incorporate other features that are not wholly satisfactory.

Finally, the South Silverton analysis differs significantly from others in the type of information that is regarded as "known." All theoretical analyses of fault patterns with which the writer is familiar specify either stresses or displacements upon the boundaries. From these the regions that are potentially unstable according to an assumed yield criterion are calculated, and the directions of potential faults are drawn at some constant angle to the trajectories of principal stress. In the present analysis the orientation of faults at the boundaries of structural units is considered to be known. Through the yield criterion, this may be translated in to the angle γ between the algebraically largest principal stress and the coordinate system. The angle γ then becomes the fundamental unknown in the boundary-value problem. The assumption of a certain distribution to the values of γ upon the boundaries does not require specification of the exact magnitude of all normal stresses or strains, but it does determine the general form of the equations by which they may be expressed. Once γ has been solved for throughout the body the expressions for the stresses and strains may be derived. Included in the derived expressions for stresses are constants whose values may be determined from other information at hand. The compatibility of the derived stress and strain or of strain-rate fields must be checked.

Stresses are quantities that cannot be observed directly; their direction and magnitude may only be inferred from their effects. Therefore, the method of analyzing fault patterns in this paper in which the observed orientation of faults at certain boundaries is used to reconstruct the whole potential fault pattern within the boundaries, appears to be more direct, in situations where it can be applied, than methods that depend upon complete knowledge of boundary stresses.

The theoretical analysis of plastic deformation proceeds from a choice among several types of "ideal" materials. The specific properties of these ideal materials are determined fundamentally by the assumption of certain mathematical relations involving, for instance, the stresses and the stress-strain relations at the beginning of plastic deformation. The consequences of these assumptions are then followed out, leading to an analysis of the expected behavior of the ideal substance under various stress systems. An interpretation may then be made as to whether the ideal material represents any real material to a tolerable degree of accuracy.

Since analyses of ideal materials furnish, at best, only approximations to the behavior of real materials, it is naturally advantageous to begin with the simplest mathematical assumptions for stress-strain relations and for the stresses at the yield point. The simple theory then may be elaborated as necessary to bring it more into agreement with observation. The simplest and most thoroughly studied theory, which is adopted for use in this report, is that developed independently by Lévy (1870) and by Von Mises (1913). The choice of the Lévy-Mises' theory was also influenced by the fact that it leads to systems of shear fractures, in plane strain, that intersect at right angles. The strikes of principal conjugate faults in the Silverton area do, in fact, intersect at nearly right angles. An analysis based upon Coulomb's yield criterion, but with a small angle of internal friction (3°), appears to be even more appropriate for some parts of the Silverton area.

This report can be divided into three main parts. The first is a section in which notations and sign conventions are presented and the fundamental equations pertaining to stress and strain and to stress-strain relations of an ideal material in the elastic state are derived. In the second section, the concept of plastic, or permanent, deformation is introduced, and the derivations are continued with emphasis on those parts that lead to differential

equations for slip lines. To illustrate an application to a particularly simple boundary-value problem in cartesian coordinates, the slip lines, stresses, and velocities in Prandtl's compressed strip are derived. The applicable equations (on the summary line of plate 1) are next reiterated in polar coordinates because the polar coordinate system better fits the curved and inclined boundaries of the structural units in the Silverton area. The derivation of slip lines and stresses are based on two assumptions, which, farther on, are to be applied respectively to the two parts of the Silverton area. The derivations in this section are then terminated at the point where detailed boundary conditions must be inserted in order to reach a solution. The third section contains the analysis of actual fault patterns in the mapped area.

Some of the mathematical manipulations are a little complicated, and several digressions into points of general interest tend to obscure the main thread of the argument. Hence the reader may wish to refer occasionally to plates 1 and 2, which show the operations diagrammatically.

It is a pleasure to acknowledge the help of many people who are concerned with the mechanics of rock deformation. The continued and patient interest of my colleagues, E. B. Eckel, W. S. Burbank, and James Gilluly, has been an essential aid. At a very early stage in the analysis the writer corresponded with A. Nádai. After the analysis was substantially complete, the results were discussed with M. K. Hubbert, John Handin, D. V. Higgs, and, particularly, H. Odé of the Shell Development Co.; and with Professors W. F. Brace and E. Orowan of the Massachusetts Institute of Technology; with Professors D. C. Drucker, R. T. Shield, and E. T. Onat of Brown University, and Professor D. T. Griggs of the University of California, Los Angeles. The writer is indebted to all those mentioned for suggestions, stimulation, and criticism.

The geological fieldwork on which this analysis is based was done with financial cooperation from the Colorado State Geological Survey Board and the Colorado Metal Mining Fund.

PRINCIPAL FEATURES OF THE THEORY OF ELASTICITY

STRESS

TYPES OF STRESS

Stress is the intensity of force, measured in terms of force per unit area of the surface upon which it acts, such as pounds per square inch or kilograms per square centimeter. The magnitude of stress at a point is more precisely defined as the limit of the ratio of force to area as the area around the point becomes infinitesimally small.

In investigating the stresses within a body subject to external or internal forces, it is convenient to imagine that the measurements of stress are made upon an infinitesimal surface. However complicated the forces may be that are applied to the body, the internal stresses can always be resolved into two kinds: normal stress, either tension or compression, that acts perpendicular to the imaginary reference surface, and shearing stress that acts in the plane of the reference surface. As this small surface is imagined to move about and turn within the body, the normal and shearing stresses on it will vary in a continuous and regular manner, assuming that the body under stress is itself free from discontinuities. If the small surface be kept at a point and rotated about an axis in its plane, the amounts of normal and shearing stress vary both in absolute magnitude and in their ratio to each other, according to the angle at which the surface lies. Stress at a point cannot, therefore, be represented adequately by a single vector of a certain magnitude and direction. Stress is a physical quantity of higher complexity than a vector; it is a tensor, and it can be defined only by stating its components in some coordinate system. The state of stress at a point is completely defined in cartesian coordinates, for example, if the nine normal and shear stress components acting on three mutually perpendicular faces of a small cubic element around the point are known.

A variety of notations for stress have been, and still are, used in various countries and by various workers. The notation used in this paper follows that which appears to be gaining some measure of acceptance. In it, normal stresses are designated by the Greek letter sigma (σ) and shear stresses by the Greek letter tau (τ). The direction of stress is indicated by a subscript. Normal stress is positive if it produces tension and is negative if it produces compression. This convention of sign is commonly reversed by some writers, especially in the field of engineering.

The components of shear stress that act parallel with coordinate axes are designated by appropriate subscripts. In three dimensional cartesian coordinates, the first subscript of τ_{yz} indicates that the shear operates in a plane that is normal to the y axis; the second subscript indicates that, within this plane, the line of action of τ_{yz} is parallel with the z axis. The sign of shearing stress is taken to be positive if it produces a counterclockwise moment about an interior point as viewed from the positive end of a coordinate axis. Figure 1 shows stresses

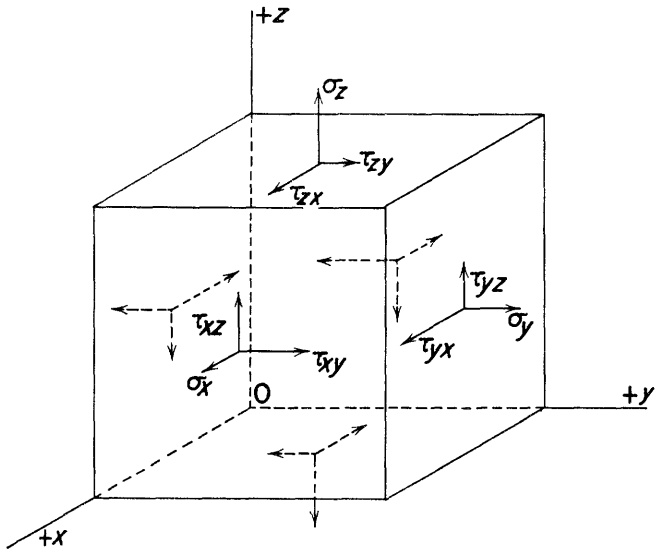

FIGURE 1.—Stresses on a cubical element in equilibrium.

on a cubical element in equilibrium. The shear stress τ_{yz} is shown acting in the positive direction and is opposed by τ_{zy} acting in the negative direction. This convention for the sign of shear is different from that of Timoshenko (1934, p. 4), who adopts the convention that all stresses as shown in figure 1 are positive. Timoshenko's convention is not consistent, however, with the sign of shear stress determined from the construction of Mohr's circle.

Of the nine stress components shown in figure 1, three are necessarily of the same absolute magnitude:

$$|\tau_{xy}| = |\tau_{yx}| \quad (1.1)$$

$$|\tau_{zy}| = |\tau_{yz}| \quad (1.2)$$

$$|\tau_{xz}| = |\tau_{zx}|. \quad (1.3)$$

The six quantities σ_x, σ_y, σ_z, τ_{xy}, τ_{yz}, and τ_{zx}, if known, completely determine the state of stress.

This paper will be concerned mostly with stress analysis in two dimensions, either in the x, y plane of x, y, z space, or in the r, θ plane of r, θ, z space. Under these conditions it will be assumed that σ_x and σ_y, or σ_r and σ_θ, do not vary along the z coordinate, and the displacements of all points are confined to the planes perpendicular to z. This is known as a state of plane deformation or plane strain.

Stresses within the interior of a body may originate in several ways. They may be generated by forces applied to the surface if the body is prevented from moving. There are also body forces that depend upon fundamental properties of matter and act throughout the interior of the body. The most familiar are those of gravity and inertia, which affect each particle independently of the stresses due to boundary forces. Electrical and magnetic fields also may produce body forces in certain materials. Hydrostatic pressure, flow or fluid through a permeable material, of flow of heat produce interior stresses that usually must be considered separately from stresses due to boundary forces. The presence of body forces complicates some of the mathematical operations in stress analysis.

VARIATION WITH ORIENTATION OF STRESS AT A POINT

The components of stress that act on any particular plane are related through certain basic equations to the stresses that act on other planes at other orientations. The triangle shown in figure 2 represents the plan view of a very small prism of unit thickness in the z direction. Assume that the top and bottom planes of the triangle parallel to the x, y plane of the paper are free from shearing stress (conditions of plane stress or plane strain). Then only the stresses shown need be considered in determining equilibrium of the element in the x, y plane. Assume also that the stress components σ_x, σ_y, and τ_{xy} are known at point O, and the problem is to determine what σ_μ and τ_μ are on some other plane, say AB, which is oriented so that its normal makes an angle μ with the x axis. The prism is so small that the variation of the stresses along the sides from point O may be neglected and the stresses that really act at O are shown as acting on the midpoints of the sides of the triangle. As dx and dy become infinitesimally small, the relations between the stresses on the triangle become the relations between stresses on planes at various orientations at a point.

According to the adopted convention, τ_{xy} in this diagram is positive, τ_{yx} is negative but of the same absolute magnitude as τ_{xy}, and τ_μ has as yet an unknown sign. Assume for the time being both σ_μ and τ_μ are directed as shown.

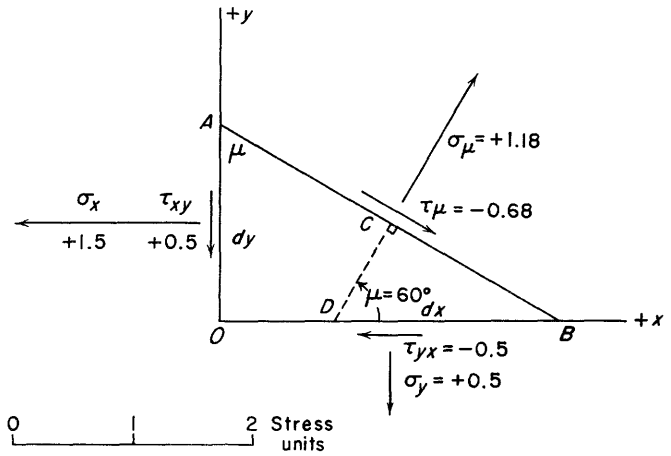

FIGURE 2.—Stresses on a triangular element in equilibrium.

The stresses σ_μ and τ_μ must be such that the triangular element shall remain in static equilibrium. The condition of equilibrium is satisfied if

$$\sigma_\mu = \frac{\sigma_x + \sigma_y}{2} + \frac{\sigma_x - \sigma_y}{2}\cos 2\mu + \tau_{xy}\sin 2\mu, \tag{2.1}$$

and τ_μ acts clockwise in amount

$$\tau_\mu = -\frac{\sigma_x - \sigma_y}{2}\sin 2\mu + \tau_{xy}\cos 2\mu = -0.68. \tag{2.2}$$

To find the value of μ, say μ' that gives the extreme value (maximum or minimum) of σ, let the partial derivative of σ with respect to μ be zero:

$$\frac{\partial\sigma}{\partial\mu} = 0 = -2\,\frac{\sigma_x - \sigma_y}{2}\sin 2\mu' + 2\tau_{xy}\cos 2\mu', \tag{2.3}$$

which reduces to

$$\frac{2\tau_{xy}}{\sigma_x - \sigma_y} = \tan 2\mu' \qquad \text{at an extreme value of } \sigma. \tag{2.4}$$

At $\mu = \mu'$, τ has the value of

$$\tau_{\mu'} = -\frac{\sigma_x - \sigma_y}{2}\sin 2\mu' + \tau_{xy}\cos 2\mu' = 0. \tag{2.5}$$

Under a given state of stress there are two values of μ that define planes on which extreme values of σ and zero of τ act. This can be seen from equation 2.4 in which tan 2μ has identical values at $\mu = \mu'$ and $\mu = \mu' + 90°$. The two values μ' and $\mu' + 90°$ define two mutually perpendicular planes, called the principal planes. The normal stresses acting on these planes are called principal stresses.

The algebraically largest principal stress (tension is positive) is designated σ_1; the algebraically least principal stress is designated σ_3. The intermediate principal stress, σ_2, acts in a direction perpendicular to the plane that includes the lines of action of σ_1 and σ_3.

Similarly, to find the value of μ, say μ'', that gives extreme values of shearing stress, let

$$\frac{\partial\tau}{\partial\mu} = 0 = \frac{\sigma_x - \sigma_y}{2}2\cos 2\mu'' + \tau_{xy}\,2\sin 2\mu'', \tag{2.6}$$

which reduces to

$$\frac{2\tau_{xy}}{\sigma_x - \sigma_y} = -\cot 2\mu''. \tag{2.7}$$

Equating 2.7 and 2.4 gives

$$\tan 2\mu' = -\cot 2\mu'',$$

which reduces to

$$\mu'' = \mu' - 45°, \text{ at extreme values of } \tau. \tag{2.8}$$

Shear stresses, therefore, reach their maximum values on planes that make angles of 45° with the principal planes.

The coordinates x and y can be chosen in any arbitrary direction relative to the stress field. Equations 2.1 and 2.2 may therefore be regarded in a more general sense as defining the normal and shear stress on any plane whose normal makes an angle μ with one of another pair of mutually perpendicular planes, if the stresses on the latter pair of planes is known, and as the means for transforming expressions for stress components from one orthogonal coordinate system to another.

To particularize σ, let σ be σ_1, the algebraically largest principal stress. The angle μ will have in this instance the special value μ', which henceforth in this paper will be designated as γ.

The angle γ is measured counterclockwise from the positive direction of the x axis to the direction of action of σ_1. Equations 2.1 and 2.2 can then be rewritten as:

$$\sigma_1 = \frac{\sigma_x + \sigma_y}{2} + \frac{\sigma_x - \sigma_y}{2}\cos 2\gamma + \tau_{xy}\sin 2\gamma \tag{2.9}$$

$$\tau = 0 = -\frac{\sigma_x - \sigma_y}{2}\sin 2\gamma + \tau_{xy}\cos 2\gamma. \tag{2.10}$$

The other and algebraically least principal stress, σ_3, acts on a plane that is oriented at $\gamma + 90°$ to the plane on which σ_1 acts, hence:

$$\sigma_3 = \frac{\sigma_x + \sigma_y}{2} - \frac{\sigma_x - \sigma_y}{2}\cos 2\gamma - \tau_{xy}\sin 2\gamma \tag{2.11}$$

$$\tau = 0 = \frac{\sigma_x - \sigma_y}{2}\sin 2\gamma - \tau_{xy}\cos 2\gamma. \tag{2.12}$$

Transferring $\frac{\sigma_x + \sigma_y}{2}$ to the left in equation 2.9, squaring 2.9, squaring 2.10, and adding gives

$$\left(\sigma_1 - \frac{\sigma_x + \sigma_y}{2}\right)^2 = \left(\frac{\sigma_x - \sigma_y}{2}\right)^2 + \tau^2_{xy}. \tag{2.13}$$

Treating equations 2.11 and 2.12 similarly gives

$$\left(\sigma_3 - \frac{\sigma_x + \sigma_y}{2}\right)^2 = \left(\frac{\sigma_x - \sigma_y}{2}\right)^2 + \tau^2_{xy}. \tag{2.14}$$

Because σ_1 is defined as the algebraically largest principal stress, these last two equations may be written in the following form:

$$\sigma_1 = \frac{\sigma_x + \sigma_y}{2} + \left[\left(\frac{\sigma_x - \sigma_y}{2}\right)^2 + \tau^2_{xy}\right]^{1/2} \tag{2.15}$$

$$\sigma_3 = \frac{\sigma_x + \sigma_y}{2} - \left[\left(\frac{\sigma_x - \sigma_y}{2}\right)^2 + \tau^2_{xy}\right]^{1/2}. \tag{2.16}$$

On the other hand, σ_1, σ_3, and γ, may be known and σ_x, σ_y, and τ_{xy} may be the unknown stresses to be determined. In this event, expressions for σ_x, σ_y, and τ_{xy}, in terms of principal stresses can be obtained by a series of algebraic manipulations on equations 2.9, 2.10, and 2.11 to yield

$$\frac{\sigma_1 - \sigma_3}{2} = \frac{\sigma_x - \sigma_y}{2}\cos 2\gamma + \tau_{xy}\sin 2\gamma. \tag{2.17}$$

Next, multiply 2.10 by cos 2γ, and 2.17 by sin 2γ, and add, giving

$$\frac{\sigma_1 - \sigma_3}{2}\sin 2\gamma = \tau_{xy}. \tag{2.18}$$

Multiply 2.10 by ($-\sin 2\gamma$) and 2.17 by $\cos 2\gamma$ and add, giving

$$\frac{\sigma_1 - \sigma_3}{2} \cos 2\gamma = \frac{\sigma_x - \sigma_y}{2} . \qquad (2.19)$$

Note that by adding 2.15 and 2.16 one may obtain

$$\sigma_1 + \sigma_3 = \sigma_x + \sigma_y. \qquad (2.20)$$

The mutually perpendicular axes, x and y, have no fixed relation to the directions of σ_1 an σ_3 (γ does not appear in equation 2.20). Therefore, equation 2.20 states that the sum of normal stresses on mutually perpendicular planes is a constant, at any given point, no matter how these pairs of planes may be oriented. In mathematical terminology, the sum of normal stresses is an invariant of the stress tensor under the operation of coordinate transformation.

Substituting equation 2.20 into 2.19 gives

$$\sigma_y = \frac{\sigma_1 + \sigma_3}{2} - \frac{\sigma_1 - \sigma_3}{2} \cos 2\gamma, \qquad (2.21)$$

$$\sigma_x = \frac{\sigma_1 + \sigma_3}{2} + \frac{\sigma_1 - \sigma_3}{2} \cos 2\gamma \qquad (2.22)$$

and, as before,

$$\tau_{xy} = \frac{\sigma_1 - \sigma_3}{2} \sin 2\gamma. \qquad (2.18)$$

The relations among the stresses on various planes and the angle between the planes, as expressed in all of the preceding equations, can be most clearly visualized through a graphical construction devised by Otto Mohr (1882) and shown in figure 3.

Figure 3 is a graph, constructed in σ and τ coordinates, which shows the stresses on the triangular element in the real physical x, y plane of figure 2. Every point on the circle O' in figure 3 represents the stress on a line such as OA or AB in figure 2. The σ and τ coordinates of the point on the circle give the magnitude of the stresses that operate on the line. Such lines in figure 2 are, of course, actually projections of planes that are parallel to the z axis. Figure 3A is constructed by plotting the point A' according to the known stress on OA shown in figure 2. That is, σ_x is equal to plus 1.5 units and τ_{xy} is equal to plus 0.5 units (positive τ_{xy} is plotted downward). Point B' is plotted in the same way, according to the stresses on OB. A circle is then drawn through A' and B' from a center O' on the σ axis. The stresses on a line AB, whose normal makes an angle μ with the x axis in figure 2, are given by the point C' in figure 3A. Point C' is located on the circle at an angle 2μ measured counterclockwise from $O'A'$. By plotting $+\tau$ downward, the angle 2μ may be laid off from $O'A'$ in the same sense as μ in figure 2. The coordinates of C' may also be computed from equations 2.1 and 2.2. The magnitudes of principal stresses are

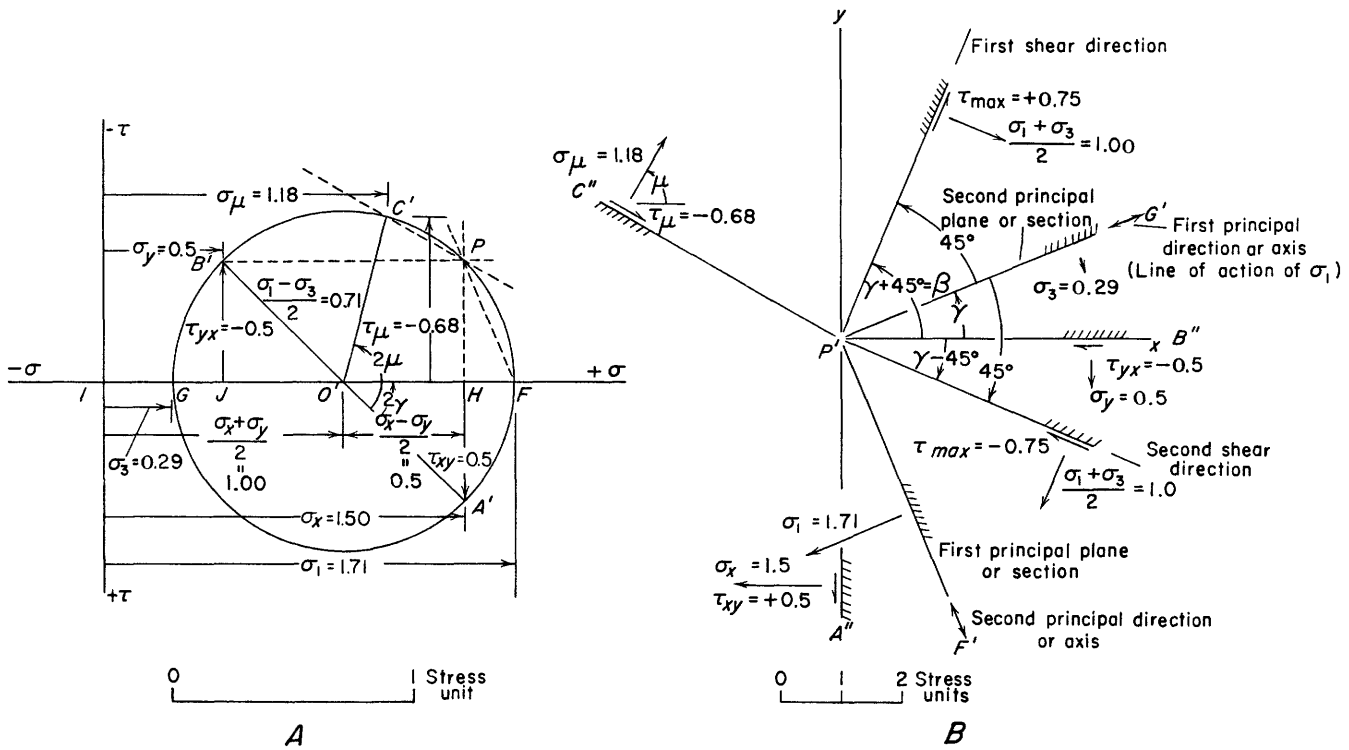

FIGURE 3.—*A*, Mohr's circle of stress. *B*, Physical plane (x, y) corresponding to stress plane (σ, τ) shown on *A*.

given by σ_1 equal to IF and σ_3 equal to IG. Maximum shearing stress is equal to the radius of the circle.

Point C' also may be located graphically in another way. This method makes use of an actual physical relationship between figure 2 and figure 3A. Point P in figure 3A has an important property, namely, that if a line is drawn through P parallel to any line through or bounding the body in figure 2, this line in figure 3A will intersect the stress circle at coordinates which specify the stress acting upon the line in figure 2. Thus, if PC' is drawn parallel to AC, point C' defines the stresses on AC. Point P is called the pole of the stress circle.

The relationship between the actual physical diagram shown in figure 2 and the representation of stress in figure 3A perhaps may be seen more clearly by reference to figure 3B. In figure 3B all the traces of the various planes are shown in their actual orientations with the actual stresses operating on them. Corresponding lines in figures 2 and 3 are parallel. For instance, a line through P and F in figure 3A gives the orientation of the line upon which σ_1 acts (normal to the line of action of σ_1). This line is shown as line $P'F'$ in figure 3B. In addition, figure 3B shows the conventions adopted in this paper for first and second principal planes and directions of first and second shears.

If the quantities σ_1, σ_3 and γ are given, one may determine σ_x, σ_y and τ_{xy} either by computing from equations 2.21, 2.22 and 2.18 or by the following graphical procedure. Lay off, as in figure 3A, the values σ_1 and σ_3 on the σ axis and construct the circle passing through F and G. Next, lay off 2γ clockwise from the line $O'F$. The line oriented at 2γ from $O'F$ meets the circle at A', which gives the value for σ_x and τ_{xy}. Next, lay off the line $O'H = (\cos 2\gamma)\ (\sigma_1 - \sigma_3)/2$ from the center O', in the opposite direction from $O'H$, to locate point J, and erect a perpendicular to the σ axis from J in the opposite direction to HA'. This line meets the circle at B'. Point B' defines the stresses σ_y and τ_{yx}.

In the parts of this paper that deal with the analysis of actual geologic structures, considerable attention is given to determining the equations of pairs of lines across which the principal stresses or the shearing stresses have extreme values. These are called, respectively, the principal-stress trajectories and the maximum-shearing-stress trajectories. As shown in figure 3B, the angle γ defines the direction of action of σ_1 at any point. This direction is the first principal direction, or axis, and also the tangent to the principal-stress trajectory across which σ_3 acts, or along which σ_1 acts. Thus, if γ is known at each point, a differential equation may be written for the stress trajectory. If the equation of the trajectory along which σ_1 acts (σ_1 trajectory) is expressed as a function,

$$y = f(x), \tag{2.23}$$

then:

slope of stress trajectory

$$= \frac{df(x)}{dx} = \tan\gamma = \frac{\sin 2\gamma}{1 + \cos 2\gamma}. \tag{2.24}$$

Using the connection between γ and stresses, the slope of the σ_1 stress trajectory may also be written as

$$\frac{df(x)}{dx} = \frac{\tau_{xy}}{\{[(\sigma_x - \sigma_y)/2]^2\}^{1/2} + \tau^2_{xy} + (\sigma_x - \sigma_y)/2} \tag{2.25}$$

If expressions for the stresses σ_x, σ_y and τ_{xy} can be written in terms of x and y, then equation 2.25 becomes a differential equation in x and y only, the solution of which gives the equation of the σ_1 trajectory.

The differential equation of a trajectory of maximum shear may be derived in a similar manner. If the equation of the trajectory of the first shear direction is expressed as a function

$$y = F(x), \tag{2.26}$$

then:

the slope of first shear trajectory

$$= \frac{dF(x)}{dx} = \tan(\gamma + 45°) \tag{2.27}$$

$$= \frac{\cos 2\gamma}{1 - \sin 2\gamma}, \tag{2.28}$$

or, in terms of stresses,

$$\frac{dF(x)}{dx} = \frac{\sigma_x - \sigma_y}{2\{[(\sigma_x - \sigma_y)/2]^2 + \tau^2_{xy}\}^{1/2} - 2\tau_{xy}}. \tag{2.29}$$

STRESSES IN STATIC EQUILIBRIUM

The preceding development showed how the stresses at a point vary with the orientation of the plane on which they are measured. These relations permit the determination of the angle γ if the stresses are known at the point. But, in order to write the differential equation for the stress or shear trajectories in terms of x and y, it clearly must be known how γ or the stresses vary with the coordinates.

One of the fundamental mathematical expressions for determining the distribution of stresses, both in the theory of elasticity and in the theory of plasticity, states that each part of a stressed body remains in static equilibrium. If the stresses on each small element of a body are to balance each other so that the element does not accelerate, then certain simple relations must prevail between the stresses in various directions. Expressed in differential equations, these relations form the foundations for further analysis.

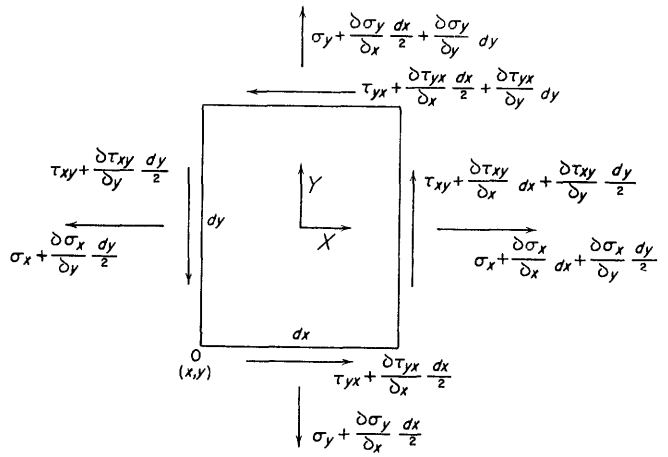

FIGURE 4.—Stresses on a small rectangular element in static equilibrium in plane strain or plane stress.

The equations of equilibrium are derived by requiring all the stresses on an infinitesimally small piece of the body to be in static equilibrium. For convenience, the boundaries of the small element are made parallel to the coordinate system in use. Suppose that the symmetry of the whole stressed body makes it convenient to use rectangular x, y coordinates. Consider the stresses acting upon the midpoints of the sides dx and dy of the very small rectangle shown in figure 4. All stresses are shown in their positive directions. Let the stresses at point O be σ_x, σ_y, τ_{xy} and τ_{yx} and let X and Y be the components of body force per unit volume. The force on each side will be the average stress, at midpoint, multiplied by the area of that side. The thickness of the rectangle in the z direction is taken to be equal to unity.

Stresses acting in the x, y plane, but on planes perpendicular to z (τ_{zx}, τ_{zy}), are assumed not to change through the thickness of the elemental rectangular prism; that is, $\partial\tau_{zx}/\partial z = 0$, $\partial\tau_{zy}/\partial z = 0$, and these stresses do not enter into the consideration of equilibrium of the element in figure 4. As will be shown later, this is equivalent to assuming a state of plane strain or of plane stress.

The forces summed in the x direction and equated to zero reduce to:

$$\frac{\partial\sigma_x}{\partial x} - \frac{\partial\tau_{yx}}{\partial y} + X = 0. \tag{3.1}$$

Since $\tau_{yx} = -\tau_{xy}$, 3.1 becomes

$$\frac{\partial\sigma_x}{\partial x} + \frac{\partial\tau_{xy}}{\partial y} + X = 0. \tag{3.2}$$

Similar summing of forces in the y direction yields:

$$\frac{\partial\sigma_y}{\partial y} + \frac{\partial\tau_{xy}}{\partial x} + Y = 0. \tag{3.3}$$

By extension of the same method, and this time considering all the stresses on the rectangular prism, it may be shown that the corresponding equations of equilibrium for stresses in three dimensions are:

$$\begin{aligned} \frac{\partial\sigma_x}{\partial x} + \frac{\partial\tau_{xy}}{\partial y} + \frac{\partial\tau_{xz}}{\partial z} + X = 0. \\ \frac{\partial\sigma_y}{\partial y} + \frac{\partial\tau_{xy}}{\partial x} + \frac{\partial\tau_{yz}}{\partial z} + Y = 0. \\ \frac{\partial\sigma_z}{\partial z} + \frac{\partial\tau_{zx}}{\partial x} + \frac{\partial\tau_{yz}}{\partial y} + Z = 0. \end{aligned} \tag{3.4}$$

These relations were first developed by Cauchy about 1828. Analogous equations of equilibrium can be developed for other coordinate systems. The equations of equilibrium pertain only to stresses. They contain no commitment about mode of deformation and hence may be applied to any region of an elastic or plastic body in which the expressed derivatives are continuous.

STRAIN

DEFINITIONS AND NOTATION

Strain is the measure of intensity of deformation. Strain due to tension or compression is measured by elongation or shortening per unit of length; strain due to shear is measured by the change in the original angle between two planes. When loads are imposed on a body, each interior point undergoes a small displacement u, which in general, varies in direction and magnitude from place to place. This displacement has components u_x, u_y, and u_z parallel to a cartesian coordinate as shown for point O in figure 5. Elastic displacement varies continuously with the coordinates, so that the displacement of a neighboring point P will in general be somewhat different from that at O and the matter between O' and P' is put into a state of strain.

Consider the displacements of the points O, A, B and P of figure 6 in two-dimensional strain. After

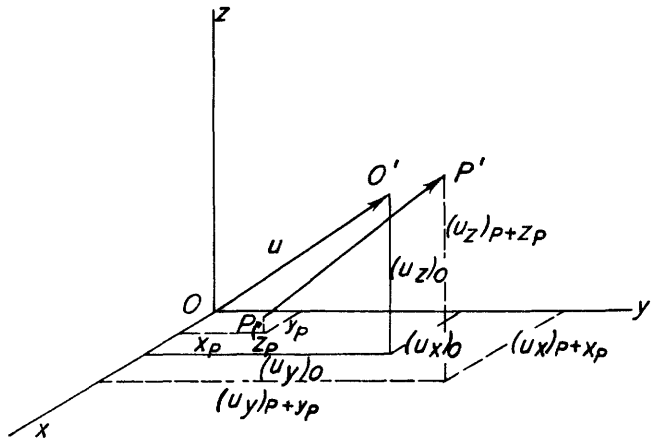

FIGURE 5.—Components of displacement in strain as point O moves to O' and a neighboring point P moves to P'.

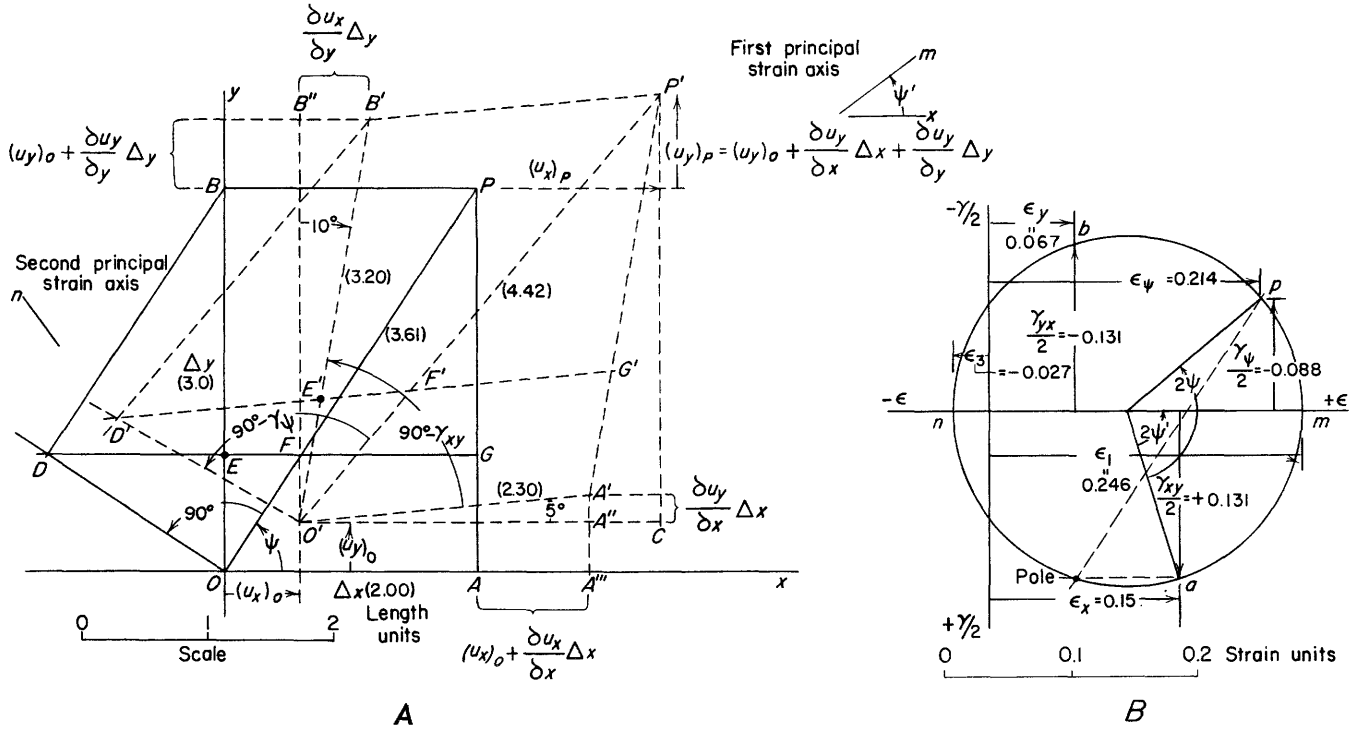

FIGURE 6.—*A*, Homogeneous infinitesimal strain of a rectangle *OAPB* into a parallelogram *O' A' P' B'*. *B*, Mohr's circle for strains.

deformation, the points are at O', A', B' and P', respectively.

The x component of displacement at P $(x + \triangle x, y + \triangle y)$ can be determined from that at O (x, y) according to Taylor's theorem. Where $u_x = f(x, y)$ and $(u_x)_O$ denotes u_x at O and $(u_x)_P$ denotes u_x at P we may write

$$(u_x)_P = (u_x)_O + \frac{\partial (u_x)_O}{\partial x}\Delta x + \frac{\partial (u_x)_O}{\partial y}\Delta y + \frac{1}{2!}\left[\frac{\partial^2 (u_x)_O}{\partial x^2}(\Delta x)^2 + 2\frac{\partial^2 (u_x)_O}{\partial x \partial y}\Delta x \Delta y + \frac{\partial^2 (u_x)_O}{\partial y^2}(\Delta y)^2\right] + \frac{1}{3!}\left[\text{third derivatives and cubes of deltas}\right] + \ldots,$$

where the dots indicate terms of increasingly higher derivatives and powers. All derivatives must exist and be continuous. Taylor's theorem is not restricted to small $\triangle x$ and $\triangle y$, but we shall assume that $\triangle x$ and $\triangle y$ are so small that their products, squares, and higher powers are negligible compared to the quantities themselves. In other words, we investigate strain in the immediate vicinity of O. According to Taylor's theorem, the displacement $(u_x)_A$ at A, becomes, since $\triangle y$ vanishes, simply

$$(u_x)_A = (u_x)_O + \frac{\partial (u_x)_O}{\partial x}\Delta x.$$

The strain of line OA during deformation may be defined as

$$\text{strain of } OA = \frac{O'A' - OA}{OA}.$$

The length $O'A'$ is given by

$$O'A' = [(O'A'')^2 + (A'A'')^2]^{1/2},$$

but the quantity $(A' A'')^2$ may be neglected because it is certainly smaller than $(\triangle y)^2$.
Hence:

$$O'A' = O'A' = OA''' - (u_x)_O$$

$$O'A' = \Delta x\left(1 + \frac{\partial (u_x)_O}{\partial x}\right),$$

and

$$\text{strain of } OA = \frac{\partial (u_x)_O}{\partial x}.$$

Introducing the notation for strain we may define the x component of strain at O as

$$\epsilon_x = \frac{\partial u_x}{\partial x},$$

and, similarly,

$$\epsilon_y = \frac{\partial u_y}{\partial y}.$$

The change in direction of the line OA to the position $O'A'$ is given by the angle $A''\ O'\ A'$, which if small, is closely approximated by its tangent, so that

$$A''O'A' = \frac{\partial u_y}{\partial x},$$

similarly,

$$B''O'B' = \frac{\partial u_x}{\partial y}$$

The change in angle

$$AOB - A'O'B' = \frac{\partial u_y}{\partial x} + \frac{\partial u_x}{\partial y}$$

represents a shearing strain denoted by γ_{xy}. The shearing strain is positive if the initial right angle becomes smaller and negative if it becomes larger. The quantities $\partial u_x/\partial y$ and $\partial u_y/\partial x$ are, in general, not equal. To restore the angle $A'O'B'$ to a position symmetric with the x and y axis it would be necessary to rotate it counterclockwise as a rigid body through a small angle $\hat{\omega}$ given by

$$\hat{\omega} = \tfrac{1}{2}\left(\frac{\partial u_x}{\partial y} - \frac{\partial u_y}{\partial x}\right).$$

If $\hat{\omega} = 0$ the deformation is said to be irrotational.

The definitions of strain components in three dimensions are

$$\epsilon_x = \frac{\partial u_x}{\partial x}, \quad \epsilon_y = \frac{\partial u_y}{\partial y}, \quad \epsilon_z = \frac{\partial u_z}{\partial z}$$

$$\gamma_{xy} = \frac{\partial u_x}{\partial y} + \frac{\partial u_y}{\partial x}, \quad \gamma_{xz} = \frac{\partial u_x}{\partial z} + \frac{\partial u_z}{\partial x}, \quad \gamma_{yz} = \frac{\partial u_y}{\partial z} + \frac{\partial u_z}{\partial y} \quad (4.1)$$

Considering again the two-dimensional strain of OP in figure 6A, it may be seen that the new length of OP is given by

$$(O'P')^2 = (O'C)^2 + (CP')^2, \quad (4.2)$$

and the strain ϵ of OP is given by

$$\epsilon = \frac{O'P' - OP}{OP}. \quad (4.3)$$

Following more or less the derivation presented by Jaeger (1956, p. 38–40), we may write equation 4.2 as

$$(O'P')^2 = \left[\Delta x\left(1 + \frac{\partial (u_x)_o}{\partial x}\right) + \frac{\partial (u_x)_o}{\partial y}\,\Delta y\right]^2 + \left[\Delta y\left(1 + \frac{\partial (u_y)_o}{\partial y}\right) + \frac{\partial (u_y)_o}{\partial x}\,\Delta x\right]^2. \quad (4.4)$$

In the expansion of equation 4.4 the products and squares of the derivatives of $(u_x)_o$ and $(u_y)_o$ are neglected. This restricts the discussion to infinitesimal strains. The products and squares of Δx and Δy here may not be neglected because either a product or square of these quantities occurs in every term. If the symbols for strain are introduced, we have

$$(O'P')^2 = (\Delta x)^2 + (\Delta y)^2 + 2\epsilon_x (\Delta x)^2 + 2\epsilon_y (\Delta y)^2 + 2\Delta x \Delta y \gamma_{xy}. \quad (4.5)$$

Now, let

$$\Delta x = OP \cos \Psi$$
$$\Delta y = OP \sin \Psi,$$

and the square root of equation 4.5 be taken, again neglecting squares and products of strains. The result is

$$O'P' = OP + OP\,(\epsilon_x \cos^2 \Psi + \epsilon_y \sin^2 \Psi + \sin \Psi \cos \Psi\, \gamma_{xy}). \quad (4.6)$$

From equation 4.3, the strain of OP (whose direction is Ψ) is now

$$\epsilon_\Psi = \epsilon_x \cos^2 \Psi + \epsilon_y \sin^2 \Psi + \gamma_{xy} \sin \Psi \cos \Psi, \quad (4.7)$$

$$\epsilon_\Psi = \frac{\epsilon_x + \epsilon_y}{2} + \frac{\epsilon_x - \epsilon_y}{2} \cos 2\Psi + \frac{1}{2}\gamma_{xy} \sin 2\Psi. \quad (4.8)$$

By neglecting the terms involving products and squares of Δx and Δy in Taylor's theorem, in effect, we specified that displacements can be expressed as linear functions of the coordinates. If the body is so strained that displacements can be expressed in this way, the strain is said to be homogeneous. The characteristics of homogeneous strain (in three dimensions) are listed by Love (1944, p. 36–37) as follows:

(i) Straight lines remain straight. (ii) Parallel lines remain parallel. (iii) All straight lines in the same direction are extended, or contracted, in the same ratio. (iv) A sphere is transformed into an ellipsoid, and any three orthogonal diameters of the sphere are transformed into three conjugate diameters of the ellipsoid. (v) Any ellipsoid of a certain shape and orientation is transformed into a sphere, and any set of conjugate diameters of the ellipsoid is transformed into a set of orthogonal diameters of the sphere. (vi) There is one set of three orthogonal lines in the unstrained state which remain orthogonal after the strain; the directions of these lines are in general altered by the strain. In the unstrained state they are the principal axes of the ellipsoid referred to in (v); in the strained state, they are the principal axes of the ellipsoid referred to in (iv) * * *

The strain shown in figure 6A is not only assumed to be homogeneous in the vicinity of point O but it is also infinitesimal, since the squares and products of the strains themselves are neglected. It will be understood that the expressions for strain derived in this section refer only to homogenous infinitesimal strain at a point.

By using the first three of the characteristics listed by Love, one may develop the expression for the shearing strain γ_ψ, which is associated with the direction OP determined by Ψ. The shearing strain γ_ψ is defined as the change in angle between lines originally oriented at Ψ and $\Psi + 90°$. In figure 6A, this is angle POD minus angle $P'O'D'$. Point D is determined by the intersection of a line from O perpendicular to OP with a line from B parallel with OP. Line DG is drawn parallel with the x axis. After strain points E, F, and G are at E', F'' and G', whose locations are determined by the relations:

$$O'E' = OE\frac{OB}{O'B'} \quad O'F' = OF\frac{OP}{O'P'} \quad A'G' = O'E'. \quad (4.9)$$

The new position of D now lies on the prolongation of $G'E'$. Since BD is parallel to OP, the new position of D also lies on a line from B' parallel to $P'O'$. Thus, D' is located. The shearing strain is angle POD minus angle $P'O'D'$.

In the triangle $O'D'F'$

$$(D'F')^2 = (O'D')^2 + (O'F')^2 - 2(O'D')(O'F')\cos(F'O'D'). \tag{4.10}$$

However,

$$\text{angle } F'O'D' = P'O'D'$$
$$D'F' = DF(1+\epsilon_x)$$
$$DF = BP = OA$$
$$O'D' = OD(1+\epsilon_{\Psi+90^\circ}) = OA\sin\Psi(1+\epsilon_{\Psi+90^\circ})$$
$$O'F' = OF(1+\epsilon_\Psi) = OA\cos\Psi(1+\epsilon_\Psi).$$

Hence (4.10) becomes

$$(OA)^2(1+\epsilon_x)^2 = (OA)^2\sin^2\Psi(1+\epsilon_{\Psi+90^\circ})^2 + (OA)^2\cos^2\Psi(1+\epsilon_\Psi)^2 - 2(OA)^2\sin\Psi\cos\Psi(1+\epsilon_\Psi)(1+\epsilon_{\Psi+90^\circ})\cos(90^\circ-\gamma_\Psi). \tag{4.11}$$

The expression $\epsilon_{\Psi+90^\circ}$ can be obtained from (4.7) through substitution of $\Psi + 90^\circ$ for Ψ. If products and squares of strains are neglected, and if γ_Ψ is so small that $\sin\gamma_\Psi = \gamma_\Psi$ the shearing strain is given by:

$$\frac{\gamma_\Psi}{2} = -\frac{\epsilon_x - \epsilon_y}{2}\sin 2\Psi + \frac{\gamma_{xy}}{2}\cos 2\Psi \tag{4.12}$$

Equations 4.8 and 4.12 define extensions and shears on an arbitrary plane, oriented at angle Ψ to the x axis, in terms of the strain components in the coordinate directions. These equations are of the same form as equations 2.1 and 2.2 that defined normal shearing stresses on a plane whose normal is inclined at an angle μ with the x axis, in terms of stress components in the coordinate directions. Note, however, that γ_Ψ and γ_{xy} are each multiplied by one-half.

This formal correspondence allows us to infer at once that the form of the relations among stresses obtained by use of the equation 2.2 is also true for relations among strains. Strains reach extreme values that may be designated as ϵ_1, ϵ_3, and γ_{max} at certain values of Ψ; $\epsilon_x + \epsilon_y = \epsilon_1 + \epsilon_3$, and the relations between strains may be represented by Mohr's circle in $(\epsilon, \gamma/2)$ coordinates as in figure 6B. The angle Ψ' is the angle between the x axis and the direction of ϵ_1, the greatest elongation.

Figure 6B is constructed as if the strains actually shown in figure 6A were infinitesimal instead of finite. Thus

$$\epsilon_x = \frac{2.30 - 2.00}{2.00} = +.15$$

$$\epsilon_y = \frac{3.20 - 3.00}{3.00} = +.67$$

$$\gamma_{xy} = 15^\circ = .262 \text{ radians.}$$

The circle in figure 6B also has a pole. Lines drawn through the pole intersect the strain circle at coordinates which define the strain in the direction of the line. The line pole–a in figure 6B is parallel to OA in figure 6A, the line pole–p is parallel to OP, the line pole–m is parallel to Om and so on. If the strains in figure 6A were infinitesimal, the coordinates of p would give the values of ϵ_Ψ and $\gamma_\Psi/2$ that might be obtained by measuring lines and angles in figure 6A.

The strains actually shown in figure 6A are, of course, exaggerated in order to be seen and are hence rather large. It may be instructive to compare the strains of OP as shown in figure 6A with those computed from equations 4.8 and 4.12 and with those measured from Mohr's circle.

	Strains shown on figure 6A	Strains computed from equations 4.8 and 4.12	Strains measured from Mohr's circle
ϵ_Ψ	+0.224	+0.214	+0.214
$\gamma_\Psi/2$	$-5°40' = -0.099$ radians	−.0887	−.088

Comparison of these figures will give some idea of the error involved in applying the formulas for infinitesimal homogeneous strains to finite homogeneous strains.

It is important to observe that if the tensor of stress and the tensor of strain are coaxial, then $\Psi' = \gamma$. The axes of principal stress and of principal strain then coincide. This is equivalent to stating that stresses are related to strains by a scalar factor, not a vector. The factor may be a constant, as in elasticity, or a scalar function of the coordinates, as in Von Mises' theory of plasticity. The principal axis of stress and strain are, in general, not coincident unless the material is isotropic.

STRESS-STRAIN RELATIONS IN THE ELASTIC STATE

If an isotropic, perfectly elastic, rectangular prism with sides parallel to x, y, and z is submitted to a uniform stress σ_x, the unit elongation is given by Hooke's law

$$\epsilon_x = \frac{\sigma_x}{E}, \tag{5.1}$$

in which E is the modulus of elasticity for material under tension, or Young's modulus. The material simultaneously contracts equal amounts in the y

and z directions as it elongates in the x direction. The contractions are given by

$$\epsilon_y = -\nu\frac{\sigma_x}{E}, \qquad \epsilon_z = -\nu\frac{\sigma_x}{E}, \tag{5.2}$$

in which ν is Poisson's ratio.

If the prism is subjected to three principal axial stresses σ_x, σ_y, and σ_z, the strains corresponding to each stress may be superposed, and the result is:

$$\begin{aligned} \epsilon_x &= (1/E)[\sigma_x - \nu(\sigma_y + \sigma_z)], & \gamma_{xy} &= \tau_{xy}/G \\ \epsilon_y &= (1/E)[\sigma_y - \nu(\sigma_x + \sigma_z)], & \gamma_{yz} &= \tau_{yz}/G \\ \epsilon_z &= (1/E)[\sigma_z - \nu(\sigma_x + \sigma_y)], & \gamma_{zx} &= \tau_{zx}/G. \end{aligned} \tag{5.3}$$

Conversely, expressions for stresses in terms of strains are given by:

$$\begin{aligned} \sigma_x &= \lambda e + 2G\epsilon_x & \tau_{xy} &= G\gamma_{xy} \\ \sigma_y &= \lambda e + 2G\epsilon_y & \tau_{yz} &= G\gamma_{yz} \\ \sigma_z &= \lambda e + 2G\epsilon_z & \tau_{zx} &= G\gamma_{zx}; \end{aligned} \tag{5.4}$$

in which

$$G = \frac{E}{2(1+\nu)}$$

= modulus of elasticity for material under shear,

$$\lambda = \frac{\nu E}{(1+\nu)(1-2\nu)}, \tag{5.5}$$

and

$e = \epsilon_x + \epsilon_y + \epsilon_z$ = volume strain.

CONDITION OF COMPATIBILITY

The six components of strain given in equation 4.1 are functions of only three components of displacement u_x, u_y, u_z. Hence, the components of strain cannot be independent of each other. The relations between the various components of strains can be determined from equations 4.1 by differentiating ϵ_x twice with respect to y, ϵ_y twice with respect to x, and γ_{xy} once with respect to y and once with respect to x. The result is the first of the six equations given below: the others are obtained by similar operations, as explained by Timoshenko (1934, p. 196).

$$\begin{aligned} \frac{\partial^2\epsilon_y}{\partial x^2} + \frac{\partial^2\epsilon_x}{\partial y^2} &= \frac{\partial^2\gamma_{xy}}{\partial x\partial y}, & 2\frac{\partial^2\epsilon_x}{\partial y\partial z} &= \frac{\partial}{\partial x}\left(-\frac{\partial\gamma_{yz}}{\partial x} + \frac{\partial\gamma_{zx}}{\partial y} + \frac{\partial\gamma_{xy}}{\partial z}\right) \\ \frac{\partial^2\epsilon_y}{\partial z^2} + \frac{\partial^2\epsilon_z}{\partial y^2} &= \frac{\partial^2\gamma_{yz}}{\partial y\partial z}, & 2\frac{\partial^2\epsilon_y}{\partial x\partial z} &= \frac{\partial}{\partial y}\left(\frac{\partial\gamma_{yz}}{\partial x} - \frac{\partial\gamma_{zx}}{\partial y} + \frac{\partial\gamma_{xy}}{\partial z}\right) \\ \frac{\partial^2\epsilon_z}{\partial x^2} + \frac{\partial^2\epsilon_x}{\partial z^2} &= \frac{\partial^2\gamma_{zx}}{\partial x\partial z}, & 2\frac{\partial^2\epsilon_z}{\partial x\partial y} &= \frac{\partial}{\partial z}\left(\frac{\partial\gamma_{yz}}{\partial x} + \frac{\partial\gamma_{zx}}{\partial y} - \frac{\partial\gamma_{xy}}{\partial z}\right). \end{aligned} \tag{6.1}$$

Equations 6.1 express the mutual compatability of the components of strain. By means of the relation between stress and strain given by Hooke's law, the condition of compatibility in elasticity can also be expressed in terms of stresses. If body forces are absent or constant, these expressions are, according to Timoshenko (1934, p. 198):

$$\begin{aligned} (1+\nu)\nabla^2\sigma_x + \frac{\partial^2 S}{\partial x^2} &= 0, & (1+\nu)\nabla^2\tau_{yz} + \frac{\partial^2 S}{\partial y\partial z} &= 0 \\ (1+\nu)\nabla^2\sigma_y + \frac{\partial^2 S}{\partial y^2} &= 0, & (1+\nu)\nabla^2\tau_{zx} + \frac{\partial^2 S}{\partial x\partial z} &= 0 \\ (1+\nu)\nabla^2\sigma_z + \frac{\partial^2 S}{\partial z^2} &= 0, & (1+\nu)\nabla^2\tau_{xy} + \frac{\partial^2 S}{\partial x\partial y} &= 0 \end{aligned} \tag{6.2}$$

in which

$$S = \sigma_x + \sigma_y + \sigma_z, \tag{6.3}$$

and

$$\nabla^2 \text{ is Laplace's operator } \left(\frac{\partial^2}{\partial x^2} + \frac{\partial^2}{\partial y^2} + \frac{\partial^2}{\partial z^2}\right). \tag{6.4}$$

The six equations of compatibility 6.2 and the three equations of equilibrium 3.4 furnish nine equations containing six unknowns σ_x, σ_y, σ_z, τ_{xy}, τ_{yz}, τ_{xz}. Theoretically, at least, the means are thereby at hand to solve for the stresses completely, provided that the conditions of stress or strain on the boundaries are known. The boundary conditions are used to evaluate the constants of integration that appear in the solution.

The solution of these second-order partial-differential equations may present difficult mathematical problems. A direct method of simplification is to restrict the analysis to two dimensions. In two-dimensional analysis a further choice is to be made between analysis for a state of plane strain and analysis for a state of plane stress.

PLANE STRAIN AND PLANE STRESS

Plane strain and plane stress are hypothetical states assumed to exist for the purpose of practical analysis. The assumption of one or the other of these ideal conditions greatly simplifies the mathematics in problems of stress and strain, and, since they represent broad classes of practical problems to a considerable degree of accuracy, these concepts have been widely used.

In plane strain one assumes the existence of a direction such that all deformation is confined to planes that are perpendicular to this direction, and further, that the stresses and strains do not vary with distance along this direction. Rectangular coordinates are usually chosen so that this direction parallels the z axis. The principal strain ϵ_z vanishes. We have from equations 4.1 and the last of equations 5.3, and if E remains finite,

$$\begin{aligned} \epsilon_z &= 0 && \text{Plane strain} \\ \gamma_{yz} &= \frac{\partial u_y}{\partial z} + \frac{\partial u_z}{\partial y} = 0, && \tau_{yz} = 0 \\ \gamma_{zx} &= \frac{\partial u_x}{\partial z} + \frac{\partial u_z}{\partial x} = 0, && \tau_{zx} = 0 \\ \sigma_z &= \nu(\sigma_x + \sigma_y), && \frac{\partial}{\partial z}(\sigma, \tau, \epsilon, \gamma) = 0. \end{aligned} \tag{7.1}$$

A state of plane strain is more or less closely approached in sections distant from the ends of a

long cylindrical or prismatic body loaded by forces that are normal to the long axis and do not vary along its length.

The equations of equilibrium 3.4 become, in the state of plane strain, respectively:

$$\frac{\partial \sigma_x}{\partial x}+\frac{\partial \tau_{xy}}{\partial y}+X=0$$
$$\frac{\partial \sigma_y}{\partial y}+\frac{\partial \tau_{xy}}{\partial x}+Y=0 \qquad \text{Equilibrium in plane strain}$$
$$\frac{\partial}{\partial z}[\nu(\sigma_x+\sigma_y)]+Z=0. \qquad (7.2)$$

The stress-strain relations of equation 5.3 become:

$$\epsilon_x=(1/E)[(1-\nu^2)\,\sigma_x-\nu(1+\nu)\,\sigma_y]$$
$$\epsilon_y=(1/E)[(1-\nu^2)\,\sigma_y-\nu(1+\nu)\,\sigma_x]$$
$$\epsilon_z=0 \qquad \text{Stress-strain in plane strain (strains in terms of stresses)}$$
$$\gamma_{xy}=2(1+\nu)\,\tau_{xy}/E, \qquad (7.3)$$

or, from equation 5.4:

$$\sigma_x=\lambda(\epsilon_x+\epsilon_y)+2G\,\epsilon_x$$
$$\sigma_y=\lambda(\epsilon_x+\epsilon_y)+2G\,\epsilon_y \qquad \text{Stress-strain in plane strain (stresses in terms of strains)}$$
$$\sigma_z=\lambda(\epsilon_x+\epsilon_y)$$
$$\tau_{xy}=G\,\gamma_{xy}. \qquad (7.4)$$

In a state of plane stress, one of the principal normal stresses vanishes. The direction of zero principal stress is again taken as parallel to the z axis. All stresses act in planes perpendicular to z, hence

$$\sigma_z=0,$$
$$\tau_{xz}=0,\gamma_{xz}=0 \qquad \text{Plane stress}$$
$$\tau_{yz}=0,\gamma_{yz}=0. \qquad (7.5)$$

It is usually further assumed that the other stress components do not vary with distance along z.

The equations of equilibrium and stress-strain relations are, respectively:

$$\frac{\partial \sigma_x}{\partial x}+\frac{\partial \tau_{xy}}{\partial y}+X=0 \qquad \text{Equilibrium in plane stress}$$
$$\frac{\partial \sigma_y}{\partial y}+\frac{\partial \tau_{xy}}{\partial x}+Y=0. \qquad (7.6)$$

$$\epsilon_x=(1/E)(\sigma_x-\nu\sigma_y) \qquad \text{Stress-strain relations in}$$
$$\epsilon_y=(1/E)(\sigma_y-\nu\sigma_x) \qquad \text{plane stress (strains in}$$
$$\epsilon_z=(-\nu/E)(\sigma_x+\sigma_y) \qquad \text{terms of stresses)}$$
$$\gamma_{xy}=(1/G)\,\tau_{xy}, \qquad (7.7)$$

$$\sigma_x=\lambda e+2G\,\epsilon_x=2G(\epsilon_x-\epsilon_z) \qquad \text{Stress-strain relations in}$$
$$\sigma_y=\lambda e+2G\,\epsilon_y=2G(\epsilon_y-\epsilon_z) \qquad \text{plane stress (stresses in}$$
$$\lambda e=-2G\,\epsilon_z \qquad \text{terms of strains)}$$
$$\tau_{xy}=G\,\gamma_{xy}. \qquad (7.8)$$

THE STRESS FUNCTION

To assume that a state either of plane stress or of plane strain exists also allows considerable simplification of the compatibility equations. The equations of equilibrium may be combined with the equations of compatibility to form a single equation valid for both plane stress and plane strain, providing that body forces are zero or are constant. If body forces are zero this equation is:

$$\frac{\partial^4 F}{\partial x^4}+2\frac{\partial^4 F}{\partial x^2\partial y^2}+\frac{\partial^4 F}{\partial y^4}=0, \qquad (8.1)$$

in which F is Airy's stress function, which is related to stresses by the expressions

$$\sigma_x=\frac{\partial^2 F}{\partial y^2},\ \sigma_y=\frac{\partial^2 F}{\partial x^2} \text{ and } \tau_{xy}=-\frac{\partial^2 F}{\partial x\partial y}. \qquad (8.2)$$

The problem of elastic-stress analysis then becomes one of finding an expression for F, in terms of the coordinates, that both satisfies the stress-function equation and which yields stresses that satisfy the known boundary conditions.

As there are an infinite number of solutions to the stress-function equation, the selection of the one that satisfies actual conditions may present a great deal of difficulty. A number of rigorous solutions have been obtained for problems that involve relatively simple geometric shapes or relatively simple distributions of boundary and body forces. Various approximate methods may be employed if the mathematical difficulties of a rigorous solution are very great. Some solutions in the form of infinite series have been obtained that fulfill the requirements to a satisfactory degree of accuracy. The usual procedure is to try a first expression for F (say F_1). The computed boundary stresses are then compared with information that may be available concerning the real boundary stresses. If the two do not agree, another function F_2 is added to F_1 to remove part or all of the discrepancy and the process repeated until either an exact solution is obtained or the increasing complexity of the expression begins to outweigh the advantage of greater accuracy. Most rigorous or semirigorous solutions result in very complicated expressions for stresses that are best presented in the form of tables or graphs.

In engineering practice, elasticity analyses are usually made to determine the stresses expected to act on or within an elastic structure. By use of the elastic constants of the materials, strains may also be calculated. In geology, elasticity analyses are more often used to explain the pattern of deformation of masses of rock than to compute stresses. Geologists have been, therefore, primarily interested either in the directions of principal stress, if potential failure is by tension, or in the directions of maximum shearing stress, if potential failure is by flowage or faulting.

Examples of the use of Airy's elastic-stress function in analysis of large-scale geologic structures have been presented by Hafner (1951), possibly for

the first time in American geological literature. Such analyses of elastic-stress distribution should be continued. But the theoretical bases should also be more closely examined as investigations progress from studies of elasticity to studies of geologic structures that involve finite and permanent deformation. Some of the features of permanent or plastic deformation are considered in the following section.

THE PLASTIC STATE

DEFINITIONS

The concept of the plastic state originates in the observation that the response of many solid materials to uniaxial stress changes greatly in character, and more or less abruptly, when the load reaches a certain value. For example, the load-deformation curve for a wire or rod of ductile metal under tension may have the general shape shown in figure 7. In the range *OP* the material conforms to Hooke's law (strain is proportional to stress), and the original shape and volume is recovered upon release of stress. At point *P*, the proportional limit, the relation of stress to strain becomes nonlinear. The proportional limit is usually close to the elastic limit, *E*, beyond which there is permanent deformation. By definition, the material becomes plastic if stressed beyond the elastic limit. The yield strength is taken as equal to the stress at which a specified amount of permanent strain, say 0.002, occurs. Some materials, such as mild steel, have a well-defined yield point, *Y*, at which an increase in deformation occurs without an increase in stress, and the stress-strain curve has an abrupt flexure. The stress-strain curve for many materials continues to rise beyond the yield point along the line *YA* but at a slope that is much flatter than the slope in the elastic range. Materials for which the curve continues upward, although at a flatter slope, are said to strain harden.

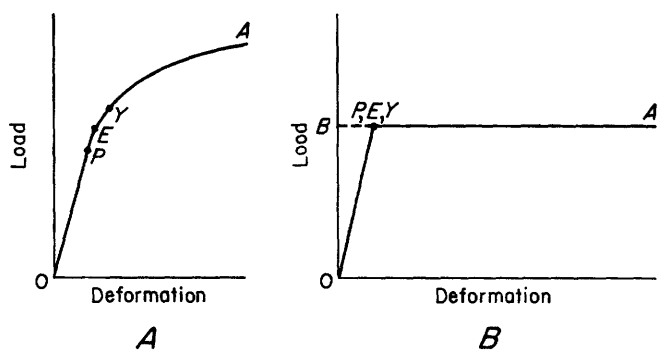

FIGURE 7.—Graphs of stress-strain relations. *A*, A real material under tension showing linear elasticity in the range *OP*. At *P*, the proportional limit, Hooke's law fails. Nonlinear elasticity may be shown in the range *PE*. Beyond *E*, the elastic limit, deformation is not fully recovered upon release of stress. The yield point, *Y*, defines the stress at which a specific amount of permanent deformation remains. Material work hardens in range *YA*. *B*, An ideal plastic material; deformation proceeds at a constant load, *B*. Elastic strain *BY* is negligible compared to plastic strain *YA*.

Strain hardening introduces considerable complication into the analytic analysis of plastic deformation. The theory of plastic deformation used in this paper has been most thoroughly developed for ideal materials that do not strain harden and that have stress-strain diagrams with abrupt flattening of the type shown in figure 7*B*. It will be assumed, simply for the purpose of simplifying the mathematics of analysis, that such ideally plastic material may represent the rocks in the South Silverton area to a rough first approximation; and further, that the elastic deformation *BY* is negligible compared to the permanent deformation *YA*.

Two other factors, derived largely from experimental observation, must enter into the concept of the ideal plastic state. The first is that crystalline metals do not undergo any appreciable permanent change of volume as the result of plastic deformation. This statement does not apply to particulate bodies, such as loose sand, but it will be assumed to hold for dense polycrystalline aggregates of minerals, and hence to the rocks of the South Silverton area. The second observation is that plastic deformation in crystalline solids is often accompanied by the appearance of physical discontinuities along which abrupt relative displacements occur. It will be assumed that the faults observed in the rocks of the South Silverton area are analogous to such "slip-lines" in deformed metals and that their arrangement may be determined by analysis of ideal plastic deformation.

Finally, the plastic state must be regarded as one in which continuous internal changes occur. If increase of stress is halted while a body is still in the elastic state all change ceases, and analyses may be made of the stresses and strains in that constant state. Furthermore, the work that has gone into producing elastic deformation can be recovered quantitatively. If the body is being deformed plastically, however, internal changes in the relative positions of particles may continue although the boundary loads are held constant. The work expended in plastic deformation, however, goes into producing disorder in lattices, into producing new surfaces, and into heat, and cannot be recovered. Even if deformation is so slow that inertial forces may be neglected, it is still necessary to use a quasi-dynamic approach to analysis; that is, the continuous changes in the internal geometry of the body from one particular stage to the next succeeding stage must be

considered. Evidently, then, the relations between stress and strain in the plastic state must be incremental in form and connect the stresses at each stage with small changes in deformation.

The basic concept of a plastic state has been outlined above in a rather unsophisticated fashion. It is now necessary to define more closely the conditions under which such a state may be reached and the properties of a body in that state. In the section that follows various criteria for defining the failure of elasticity are presented; next, the stress-strain relations used in the ideal plastic state are stated; and finally the method of computing slip-line fields is indicated.

CRITERIA OF FAILURE

Many criteria for expressing mathematically a state of plasticity or failure have been proposed by engineers and physicists. A few are manifestly more successful than others, but even the best are generally restricted in their application to certain broad classes of materials. No one theory appears to fit all the test results on all materials under all testing conditions. Some of the various criteria are briefly described below. For more details the reader is referred to Marin (1935), Nádai (1950), Hubbert (1951), and Robertson (1955).

1. Maximum principal-stress criterion

$$|\sigma_1| = K. \tag{9.1}$$

Failure occurs when the maximum principal stress reaches a certain value, whatever the other principal stresses may be, provided the latter are smaller in absolute value. This criterion is unsuccessful because, contrary to experience, it predicts failure under three equal compressive principal stresses (hydrostatic pressure) or three equal tensile principal stresses.

2. Maximum strain criterion. Failure occurs when the elastic strain reaches a certain value.

$$\epsilon_1 = K. \tag{9.2}$$

This criterion also appears faulty, if applied to material under hydrostatic pressure, because even very high hydrostatic pressures do not cause permanent deformation.

3. Maximum strain-energy-of-distortion criterion. Flow occurs at a constant maximum value of the strain energy of distortion. This quantity is obtained by subtracting the elastic energy of volume dilatation from the total elastic energy stored in the material.

$$(\sigma_1 - \sigma_2)^2 + (\sigma_2 - \sigma_3)^2 + (\sigma_3 - \sigma_1)^2 = 6k^2. \tag{9.3}$$

Nadái (1950, p. 210) expresses this criterion in terms of a quantity that he calls octahedral shear stress

$$\tau_o = \text{constant} = [(\sigma_1 - \sigma_2)^2 + (\sigma_2 - \sigma_3)^2 + (\sigma_3 - \sigma_1)^2]^{1/2}/3. \tag{9.4}$$

This criterion applies well to the yielding of ductile metals.

4. Maximum shear-stress criterion. Failure by flow or by rupture occurs when the maximum shear stress reaches a constant value, which is characteristic for each material.

$$\tau_{max} = (\sigma_1 - \sigma_3)/2 = k. \tag{9.5}$$

The intermediate principal stress can have any value between σ_1 and σ_3. This criterion agrees satisfactorily with the results of experiments on ductile metals. This is Tresca's criterion and is equivalent to Von Mises' criterion in plain strain.

5. Mohr's criterion. Failure occurs when the shear stress along the planes of potential slip reaches a certain value. This critical shear-stress value τ_c depends on the normal stress σ_n acting upon the same planes.

$$\tau_c = f(\sigma_n). \tag{9.6}$$

Mohr's criterion can be expressed in several ways, according to the type of function $f(\sigma_n)$ selected. One of the forms used widely, and more or less successfully, in the study of brittle, cohesive, or loose materials is that proposed long ago by Coulomb (1776). It states that the limiting or critical shear stress τ_c has a value of:

$$\tau_c = c + \sigma_n \tan \phi. \tag{9.7}$$

In this expression, c is regarded as a constant that is characteristic of the material and is often referred to as cohesion, σ_n is the normal compressive stress on a potential slip plane, and ϕ is the so-called angle of internal friction.

Figure 8 illustrates a state of stress at the inception of failure, according to the Coulomb criterion. Any state of stress represented by a circle that is tangent to the lines ED and ED' (fig. 8A) produces failure, whereas any state of stress represented by a circle wholly within the envelope DED' does not. Moreover, the orientation of planes along which failure occurs are defined by the points of tangency T_1 and T_2. These planes, shown in figure 8C as $P'T_1'$ and $P'T_2'$, are inclined at an angle of $45° - (\phi/2)$ with the axis of greatest pressure, σ_3. This may be readily seen because triangle OT_1E (fig. 8A) requires that

$$2\alpha + 90° + \phi = 180°,$$

or

$$\alpha = 45° - \frac{\phi}{2}. \tag{9.8}$$

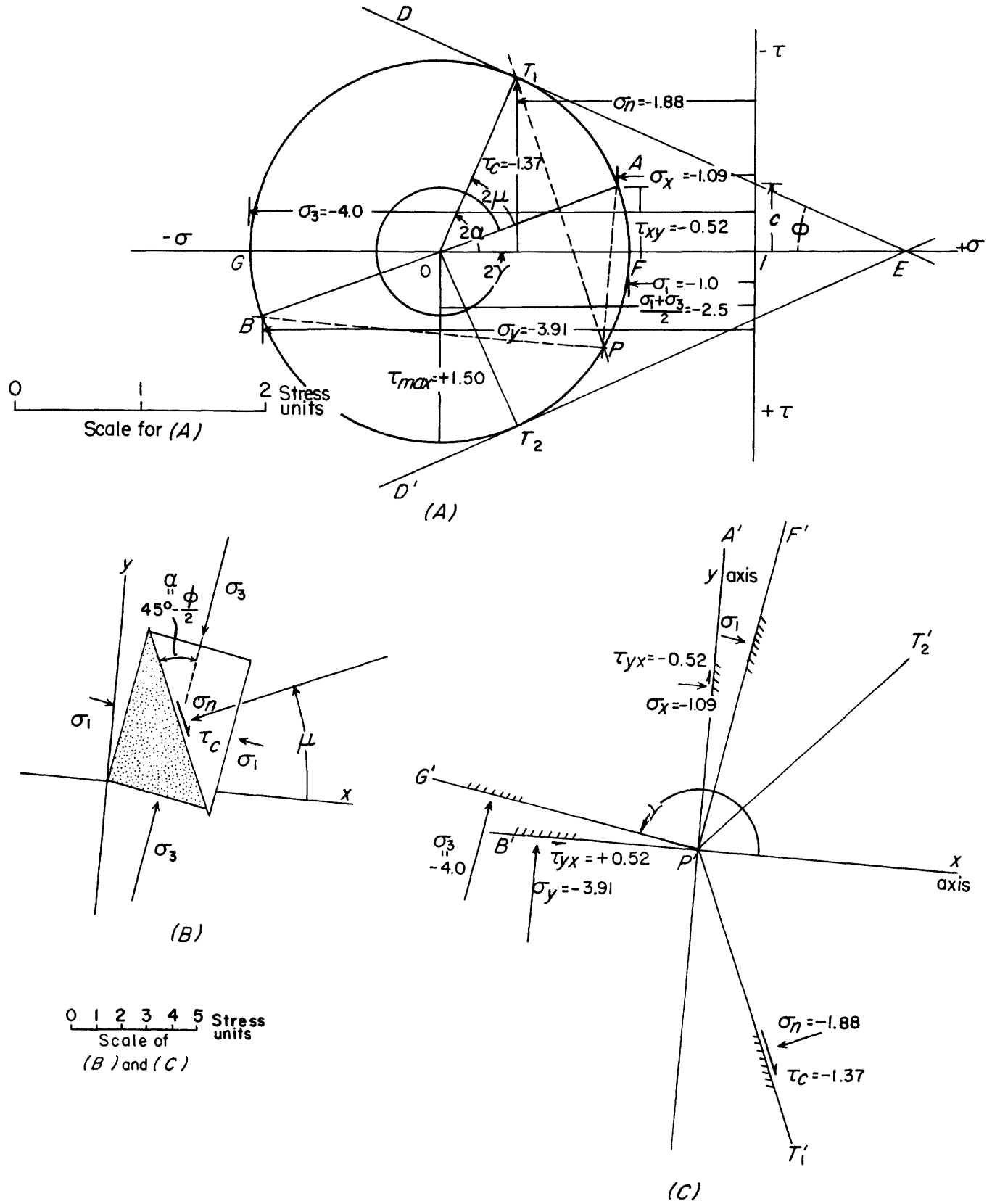

FIGURE 8.—State of stress at the inception of failure, according to the Coulomb criterion. *A*, Mohr's stress circle and envelope *DED'* of stress circles that produce failure. *B*, Diagram of a sample being sheared under stress system shown in *A*. *C*, Physical plane (x, y) corresponding to stress plane (σ, τ) of *A*.

In effect, failure does not occur along planes of maximum shear stress because there is too much frictional resistance along these planes. As the angle between the plane and the line of action of σ_3 is decreased, however, the frictional resistances due to σ_n decreases rapidly but the shear stress, although also decreasing, remains moderately high. At a certain angle, α, the shearing stress equals the sum of cohesion and frictional resistance and the system is no longer stable.

It is also assumed that the planes of failure are parallel to the axis of intermediate stress, σ_2, and that σ_2 has no effect upon the orientation of failure lines. Figure 8*B* shows some of the planes of figure 8*C* arranged into a triangular element (stippled) representing one-half of a specimen failing under compression.

The criterion of a straight-line envelope, of slope ϕ, becomes invalid near the point E. That is, brittle materials under tension, actually break at right angles to σ_1, the greatest tension, rather than obliquely to it, as they do under shear. Various other types of envelopes have been proposed to avoid this difficulty, for instance, the parabola shown in figure 9 would intersect the σ axis at a right angle, implying tensile fracture with $\gamma = 0$.

The maximum shear-stress criterion, in which the envelopes are horizontal lines, $\tau_{max} = \pm k$, is shown in figure 10.

6. Robertson's criterion. E. C. Robertson (1955, p. 1303–1305), pointed out that a fairly satisfactory expression for the rupture strength of silicate rocks is given by:

$$\tau_{max} \cong \sigma_m, \tag{9.9}$$

or

$$(\sigma_1 - \sigma_3) = k(\sigma_1 + \sigma_2 + \sigma_3)/3, \tag{9.10}$$

where σ_m is the mean stress and k is about equal to one, except for certain types of tests in which one of the principal stresses is zero.

7. Other criteria. Other criteria and mechanisms have been proposed by many workers. Among the better known is that of Griffith (see Nádai, 1950, p. 196–198; and Odé, 1956), who investigated the effect of small cracks, flaws, or foreign bodies upon the strength of amorphous materials. N. W. Taylor (1947) has also proposed a criterion that relates the stress required to break a brittle material under simple tension to the duration of application of stress.

It should be emphasized that the laws governing fracture and flow of solids are still imperfectly understood. Internal flaws and duration of stress are but two of many factors that influence fracture, in addition to the overall relations of principal stress. Temperature and chemical action of fluids have potent effects on the strength and on the mechanical type of failure of many geologic materials. All these factors well may have influenced the fracturing of rocks in the South Silverton mining district. Their significance in altering the theoretical fracture pattern can scarcely be estimated.

RELATION BETWEEN LOAD AND DEFORMATION IN THE PLASTIC STATE

The criteria of failure listed in the preceding section are concerned almost exclusively with relations between stresses at the time of yielding. They say nothing about possible modes of deformation after the plastic state is attained, nor do they make evident any particular relations between stresses and strains in the plastic state.

The relations between stress and strain in the plastic state are fundamentally different from those in the elastic state. The nature of those differences and the way in which plastic state stress-strain relations may allow for finite deformation has been clearly presented in a paper by Prager (1956, p. 64–66), to which the reader is referred.

There are two principal difficulties. The first is the mathematical complexity that arises when finite rather than infinitesimal strains are measured with reference to the stress-free state. The second is how to express strain when a body is undergoing both elastic and plastic deformation, particularly if deformations in the plastic zone are constrained by adjacent parts that have not yet reached the yield limit. The first difficulty is overcome by expressing the relation between stress and the rate of strain rather than between stress and strain itself. In this way stress is related to increments of strain produced between the instants t and $t + dt$ rather than the total strain since application of load. The second difficulty can be met by including both the recoverable and irrecoverable strains in a single relation to stress. Several such expressions have been used but they lead to rather formidable mathematical complications. In practice, the elastic-state strains are generally neglected, and in the simpler analyses it is assumed that the material does not work harden.

Some years before this study was made it was found that the problem of determining a plastic stress-strain relation was also related to the choice of a proper yield criterion and to the necessity of providing for discontinuities in deformation. Several relations between stress and increment of plastic strain have been proposed. The one that appears to satisfy the requirements most successfully, at

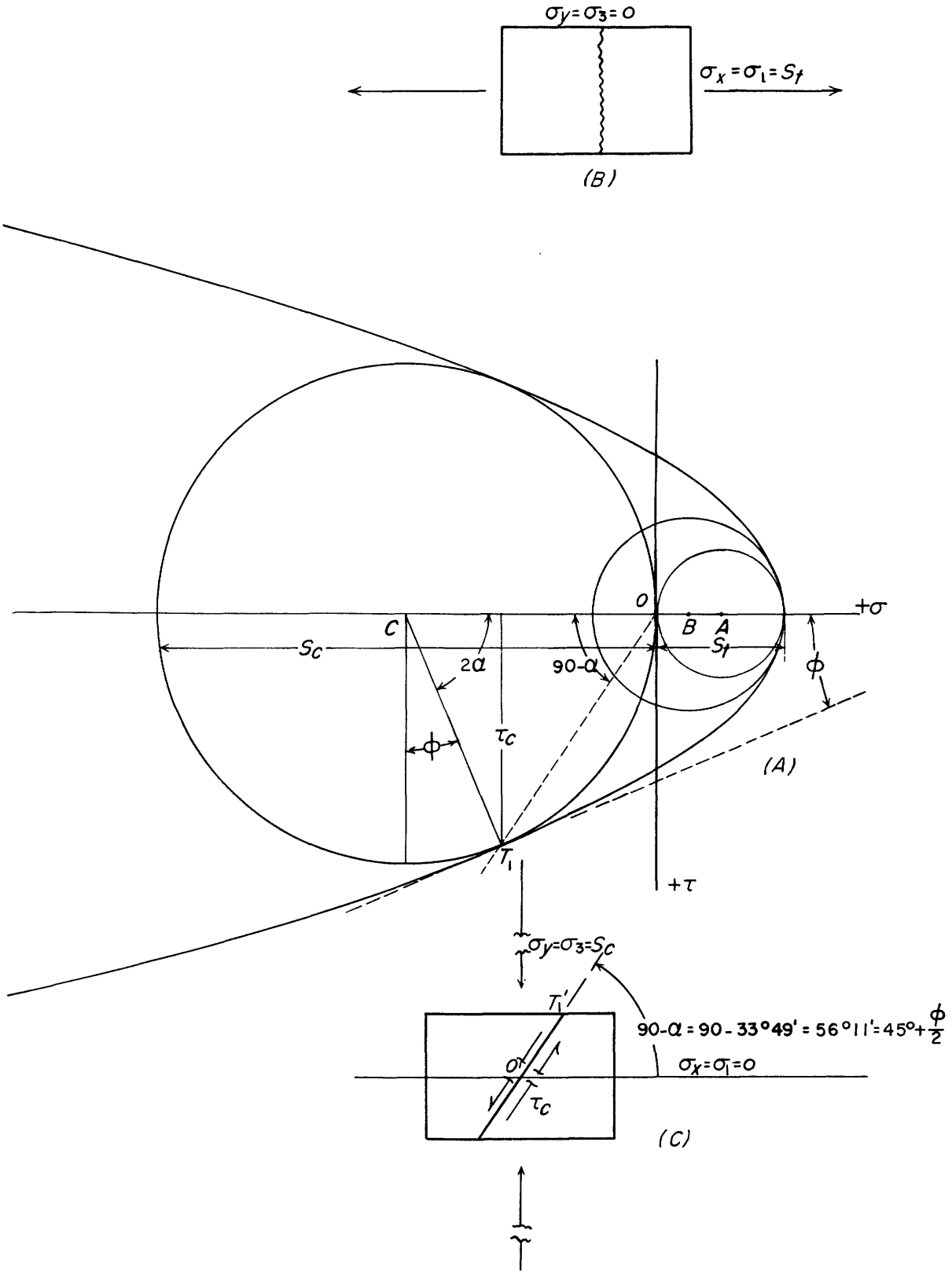

FIGURE 9.—*A*, Parabolic envelope of stress circles. Circle with center at *A* represents failure under tensile stress, $\sigma_1 = S_t$, $\sigma_3 = 0$ as shown in *B*. Stress circle for tensile failure is tangent to parabola at vertex. Circle with center at *B* has radius of curvature equal to that of parabola at vertex and is the largest stress circle for tensile failure. All larger circles contact parabola off the σ axis and represent failure due to shear. Circle with center at *C* represents failure under uniaxial compression. Failure occurs along on one or the other of two planes, say O' T_1' in *C*, which are inclined at $90 - \alpha$ to σ_1 axis. In this instance the ratio of strength in compression to strength in tension is $S_c/S_t = 3.95$.

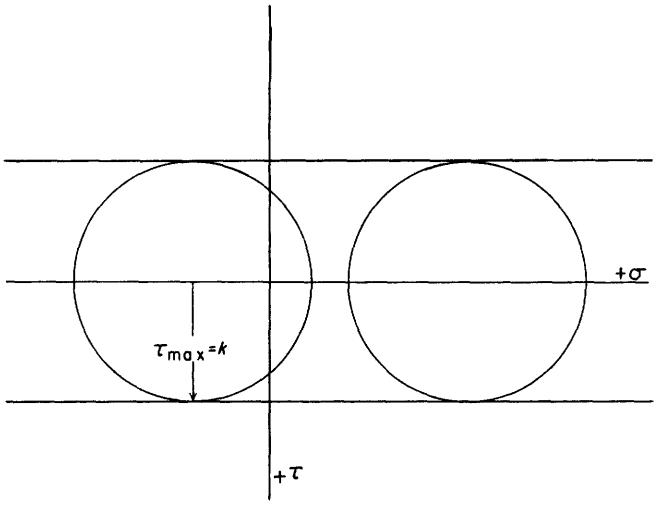

FIGURE 10.—Stress circle envelopes for criterion of constant maximum shear stress. Tresca's criterion or Von Mises' criterion for plane strain.

least when applied to unconstrained plane strain and when used with the yield criterion of maximum strain energy of distortion, is that of Lévy and Von Mises, already referred to. The Lévy-Mises' theory assumes (1) that the elastic-state part of strain is so small that it may be neglected relative to the permanent, or plastic state part, (2) plastic deformation does not result in a permanent change of volume, (3) the rate of change of the deviator part of strain is proportional to the deviator part of stress, and (4) the principal axis of stress deviators and strain-rate deviators remain parallel during the plastic deformation of isotropic material. The deviator of stress is that part of the stress tensor which remains after substraction of the hydrostatic part (average pressure or tension). Similarly, the deviator of strain is that part of the strain tensor remaining after subtraction of the average strain. Denoting elastic strains by one prime and plastic strains by a double prime, condition (1) above may be stated as:

$$\epsilon' = 0 \tag{10.1}$$

$$\text{total strain} = \epsilon = \epsilon' + \epsilon'' = \epsilon''. \tag{10.2}$$

Condition (2) may be stated as:

$$\epsilon_x'' + \epsilon_y'' + \epsilon_z'' = \epsilon_1'' + \epsilon_2'' + \epsilon_3'' = 0. \tag{10.3}$$

Condition (3) may be stated as:

$$\frac{d}{dt}\left(\epsilon_x'' - \frac{\epsilon_x'' + \epsilon_y'' + \epsilon_z''}{3}\right) = L\left(\sigma_x - \frac{\sigma_x + \sigma_y + \sigma_z}{3}\right), \tag{10.4}$$

in which L is a positive scalar quantity that may vary in space and time. L must be positive in order that work be done on rather than received from, the deforming body.

Writing $\dot{\epsilon}_x$ for $d\epsilon_x/dt$, s_x, and so on, for the components of the deviators of strain and stress, and inserting equation 10.3 gives for equation 10.4 and the other plastic stress-strain relations the following equations (Prager and Hodge, 1951, p. 30):

$$\begin{aligned} \dot{\epsilon}_x &= Ls_x & \dot{\gamma}_{yz} &= 2L\tau_{yz} \\ \dot{\epsilon}_y &= Ls_y & \dot{\gamma}_{zx} &= 2L\tau_{zx} \\ \dot{\epsilon}_z &= Ls_z & \dot{\gamma}_{xy} &= 2L\tau_{xy}. \end{aligned} \tag{10.5}$$

These are the plastic stress-strain relations that replace the elastic stress-strain relations of equations 5.1–5.3. The quantities $\dot{\epsilon}_x$, s_x, and so on, in each equation are vector components of the respective strain-rate and stress-deviator tensors. Their connection by means of a scalar variable requires that the vectors of strain rate and of stress deviation be parallel and that the tensors of strain rate and stress deviation be coaxial.

Strain-rate components are defined as below:

$$\dot{\epsilon}_x = \frac{d\epsilon_x}{dt} = \frac{d}{dt}\left(\frac{\partial u_x}{\partial x}\right) = \frac{\partial v_x}{\partial x},$$

and similarly,

$$\begin{aligned} \dot{\epsilon}_y &= \frac{\partial v_y}{\partial y} \\ \dot{\epsilon}_z &= \frac{\partial v_z}{\partial z} \end{aligned}$$

$$\begin{aligned} \dot{\gamma}_{yz} &= \frac{d\gamma_{yz}}{dt} = \frac{d}{dt}\left(\frac{\partial u_z}{\partial y} + \frac{\partial u_y}{\partial z}\right) = \frac{\partial v_z}{\partial y} + \frac{\partial v_y}{\partial z} \\ \dot{\gamma}_{zx} &= \frac{\partial v_x}{\partial z} + \frac{\partial v_z}{\partial x} \\ \dot{\gamma}_{xy} &= \frac{\partial v_y}{\partial x} + \frac{\partial v_x}{\partial y}. \end{aligned} \tag{10.6}$$

It will be noted that the plastic-strain-rate components are defined by the derivatives of velocity components in a manner exactly analogous to the definition of elastic strains in terms of derivatives of displacements. The element of time actually enters in only as a convenient parameter to express the progress of deformation, that is, to indicate an increment of strain at a particular point as deformation proceeds. This increment of strain applies to a particular point that is watched during deformation and is not to be confused with variations in strain that may be noted between the one (x, y) point and another at any instant of time. Any quantity, such as a particular dimension of the deforming body, that increases monotonously during the process of plastic deformation might be used instead of time.

For plane strain

$$\epsilon_z = 0,$$

therefore

$$\dot{\epsilon}_z = 0 \text{ and, since } L \neq 0$$

$$s_z = \frac{1}{L}\dot{\epsilon}_z = 0 = \sigma_z - \frac{\sigma_x + \sigma_y + \sigma_z}{3}$$

$$\sigma_z = \frac{\sigma_x + \sigma_y}{2}. \tag{10.7}$$

This is analogous to the corresponding expression for σ_z in the equations for elastic plane strain 7.1 if $\nu = \frac{1}{2}$. In fact, if Poisson's ratio ν is taken equal to one-half the elastic equations in three dimensions 5.3 lead to such expressions as

$$\epsilon_x = \frac{3}{2E} s_x \tag{10.8}$$

that superficially resemble their counterparts in 10.5. It would appear more logical, however, in analyzing a body of ideal plastic material with a sharp yield point to not attempt to interpret the plastic state as one in which the elastic constants ν and E have certain values or tend toward certain limits.

GENERALIZED EXPRESSION FOR SLIP LINES IN PLANE PLASTIC STRAIN (CARTESIAN COORDINATES)

In this section the method of determining principal shear-stress trajectories or "slip-lines" will be presented very briefly, under the assumptions that the body analyzed yields according to the criteria of maximum strain energy of distortion, and that the stress-strain relations are those of Lévy-Mises given in equations 10.5. In terms of stresses and velocities in plane strain we have the following relations and conditions to consider:

(a) Definitions of strain rates

$$\begin{aligned} \dot{\epsilon}_x &= \frac{\partial v_x}{\partial x} & \dot{\gamma}_{yz} &= \frac{\partial v_z}{\partial y} + \frac{\partial v_y}{\partial z} = 0 \\ \dot{\epsilon}_y &= \frac{\partial v_y}{\partial y} & \dot{\gamma}_{zx} &= \frac{\partial v_x}{\partial z} + \frac{\partial v_z}{\partial x} = 0 \\ \dot{\epsilon}_z &= \frac{\partial v_z}{\partial z} = 0 & \dot{\gamma}_{xy} &= \frac{\partial v_y}{\partial x} + \frac{\partial v_x}{\partial y} \end{aligned} \tag{11.1}$$

$$\frac{\partial}{\partial z}(v_x, v_y, v_z) = 0.$$

(b) Stress-strain rate relations

$$\begin{aligned} \dot{\epsilon}_x &= L s_x & \dot{\gamma}_{yz} &= 2L\,\tau_{yz} = 0 & \tau_{yz} &= 0 \\ \dot{\epsilon}_y &= L s_y & \dot{\gamma}_{zx} &= 2L\,\tau_{zx} = 0 & \tau_{zx} &= 0 \\ \dot{\epsilon}_z &= L s_z = 0 & \dot{\gamma}_{xy} &= 2L\,\tau_{xy} \\ s_z &= 0. \end{aligned} \tag{11.2}$$

(c) Definition of deviators of stress

$$\begin{aligned} s_x &= \sigma_x - \frac{\sigma_x + \sigma_y + \sigma_z}{3} = \frac{\sigma_x - \sigma_y}{2} \\ s_y &= \sigma_y - \frac{\sigma_x + \sigma_y + \sigma_z}{3} = \frac{\sigma_y - \sigma_x}{2} \\ s_z &= \sigma_z - \frac{\sigma_x + \sigma_y + \sigma_z}{3} = 0 \\ s_x &= -s_y. \end{aligned} \tag{11.3}$$

(d) Static equilibrium (neglecting body forces)

$$\begin{aligned} \frac{\partial \sigma_x}{\partial x} + \frac{\partial \tau_{xy}}{\partial y} &= 0 \\ \frac{\partial \sigma_y}{\partial y} + \frac{\partial \tau_{xy}}{\partial x} &= 0. \end{aligned} \tag{11.4}$$

(e) Yield condition. In the state of plane strain in which the z axis is normal to the plane being considered, σ_z is the intermediate principal stress and equation 9.3 becomes

$$\left(\frac{\sigma_1 - \sigma_3}{2}\right)^2 = k^2. \tag{11.5}$$

(f) Relations between principal stresses and coordinate stresses in a plane, same, respectively, as equations 2.9, 2.11 or 2.21, 2.22 and 2.18

$$\begin{aligned} \sigma_1 &= \frac{\sigma_x + \sigma_y}{2} + \frac{\sigma_x - \sigma_y}{2}\cos 2\gamma + \tau_{xy}\sin 2\gamma \\ \sigma_3 &= \frac{\sigma_x + \sigma_y}{2} - \frac{\sigma_x - \sigma_y}{2}\cos 2\gamma - \tau_{xy}\sin 2\gamma, \end{aligned} \tag{11.6}$$

or

$$\begin{aligned} \sigma_x &= \frac{\sigma_1 + \sigma_3}{2} + \frac{\sigma_1 - \sigma_3}{2}\cos 2\gamma \\ \sigma_y &= \frac{\sigma_1 + \sigma_3}{2} - \frac{\sigma_1 - \sigma_3}{2}\cos 2\gamma \\ \tau_{xy} &= \frac{\sigma_1 - \sigma_3}{2}\sin 2\gamma. \end{aligned} \tag{11.7}$$

(g) The angle γ is measured counterclockwise from the positive direction of the x axis to the line of action of σ_1, the algebraically largest principal stress.

In plane strain the yield criterion of maximum strain energy of distortion becomes the same as the maximum shear stress criterion, equation 9.5. In other words, the condition of plasticity is attained only if the shear stress is at a maximum, and this occurs only along trajectories of maximum shear stress. Therefore, plastic deformation, as herein defined, occurs only along trajectories of maximum shear.

The slope of the first shear trajectory is, as given in equation 2.28,

$$\frac{dy}{dx} = \frac{\cos 2\gamma}{1 - \sin 2\gamma}, \tag{2.28}$$

and the problem of constructing principal shear-stress trajectories reduces to the determination of γ as a function of x and y, so that equation 2.28 may be integrated.

For the determination of γ there are the two equilibrium equations 11.4, the yield condition equation 11.5, and the connections between γ and the stresses in equations 11.6 or 11.7. In order to reduce these six equations in six unknowns (σ_x, σ_y, τ_{xy}, σ_1, σ_3, γ) to one equation in γ, we introduce first a new variable ω, which denotes half the sum of the normal stresses. Making use of equation 2.20, ω may be written:

$$\omega = \frac{\sigma_x + \sigma_y}{2} = \frac{\sigma_1 + \sigma_3}{2}. \tag{11.8}$$

By use of the yield condition equation 11.5, equations 11.7 now become:

$$\sigma_x = \omega + k\cos 2\gamma \tag{11.9}$$

$$\sigma_y = \omega - k\cos 2\gamma \tag{11.10}$$

$$\tau_{xy} = k\sin 2\gamma. \tag{11.11}$$

In order that the reader may conveniently compare the results of the following section, on Prandtl's compressed strip, with those given by Nádai (1950, p. 533–538), the angle β, which is the angle that the first maximum shear trajectory makes with the x axis will be used instead of γ. The angle β is defined as in figure 3*B* by

$$\beta = \gamma + 45°. \tag{11.12}$$

Equations 11.9, 11.10 and 11.11 become

$$\sigma_x = \omega + k\sin 2\beta \tag{11.13}$$

$$\sigma_y = \omega - k\sin 2\beta \tag{11.14}$$

$$\tau_{xy} = -k\cos 2\beta. \tag{11.15}$$

These last three equations, when substituted into the equations of equilibrium, 11.4, give

$$\frac{\partial\omega}{\partial x} + k\frac{\partial}{\partial x}(\sin 2\beta) - k\frac{\partial}{\partial y}(\cos 2\beta) = 0 \tag{11.16}$$

$$\frac{\partial\omega}{\partial y} - k\frac{\partial}{\partial y}(\sin 2\beta) - k\frac{\partial}{\partial x}(\cos 2\beta) = 0. \tag{11.17}$$

Differentiating equation 11.16 with respect to y and equation 11.17 with respect to x and subtracting eliminates ω and gives:

$$2\frac{\partial^2}{\partial y\partial x}(\sin 2\beta) - \frac{\partial^2}{\partial y^2}(\cos 2\beta) + \frac{\partial^2}{\partial x^2}(\cos 2\beta) = 0 \tag{11.18}$$

or, in terms of stresses,

$$\frac{\partial^2}{\partial x\partial y}(\sigma_x - \sigma_y) + \frac{\partial^2}{\partial y^2}(\tau_{xy}) - \frac{\partial^2}{\partial x^2}(\tau_{xy}) = 0. \tag{11.19}$$

If the indicated differentiations are performed, equation 11.18 becomes

$$\sin 2\beta\frac{\partial^2\beta}{\partial x^2} - \sin 2\beta\frac{\partial^2\beta}{\partial y^2} - 2\cos 2\beta\frac{\partial^2\beta}{\partial x\partial y} + 2\cos 2\beta\left(\frac{\partial\beta}{\partial x}\right)^2 - 2\cos 2\beta\left(\frac{\partial\beta}{\partial y}\right)^2 + 4\sin 2\beta\frac{\partial\beta}{\partial x}\frac{\partial\beta}{\partial y} = 0. \tag{11.20}$$

This is a nonlinear partial differential equation of the second order. A solution of this equation that satisfies the prescribed boundary conditions generally presents great difficulty unless the angle β is some simple function of the coordinates. If the boundary conditions are in the form of prescribed stresses or velocities, the actual boundaries of the region undergoing plastic deformation are generally unknown, although the shape of the plastic-elastic boundary often may be inferred if the body and loads are symmetrical. Some useful solutions may be derived under the simplifying assumption that β (or τ_{xy}) is a function only of one or the other of the coordinates.

The equation of the first shear trajectory is determined through the relation that the slope of the trajectory is equal to the tangent of β.

$$\frac{dy}{dx} = \tan\beta = \frac{1-\cos 2\beta}{\sin 2\beta} = \frac{\sin 2\beta}{1+\cos 2\beta}. \tag{11.21}$$

If a relation between β and x and y can be found from equation 11.20, then substitution into equation 11.21 will give a relation between x and y which is the equation of one family of the slip-line field. It is usually neither feasible nor necessary to thus eliminate β. More commonly the equations are integrated with β left in, and the expressions for the slip lines are derived in parametric form, in which β (or γ) is the parameter.

PRANDTL'S COMPRESSED STRIP

STATEMENT OF THE PROBLEM

To illustrate the method of plastic analysis we will take the solution to Prandtl's problem of a compressed strip in which a plastic mass is squeezed between very long, perfectly rough, rigid, parallel plates in plane strain (Prandtl, 1923). The problems offered by fracturing in the South Silverton area may be regarded as complex variations of Prandtl's problem, in which the boundaries are inclined and curved.

The plastic mass is free to move only in the x and y plane, as shown in figure 11. The slip-line field will be examined in a region, R, that is sufficiently far removed from the y axis (where the movement changes direction) and from the ends (where the edges introduce complications) so that the mode of the deformation is more or less independent of the precise position of R along the x axis. Shear stress

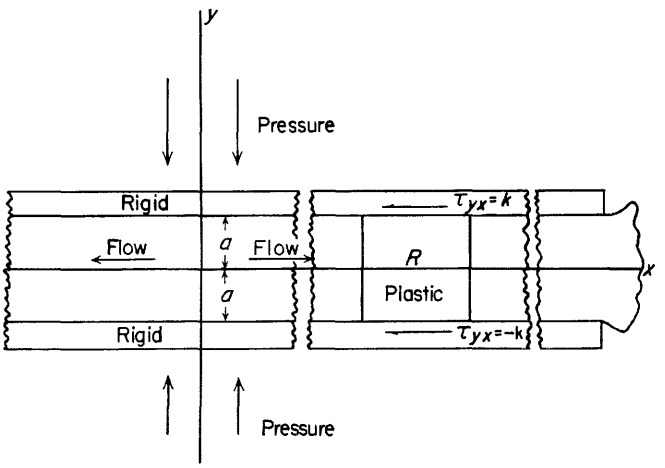

FIGURE 11.—Physical arrangement in Prandtl's plastic strip compressed between rigid plates. In the region R, considerably removed from either the center or the ends, the shearing stress next to the plates is constant and the region R is in a state of plane strain.

on the plates is at the maximum, and the convention for sign of shear stress gives

$$\tau_{yx} = +k,\ \tau_{xy} = -k, \text{ at } y = a$$
$$\tau_{yx} = -k,\ \tau_{xy} = +k, \text{ at } y = -a.$$

The shear stress is constant along the top and bottom surfaces of R. This is generalized by assuming that τ_{xy} is constant along any line parallel to the x axis; that is,

$$\frac{\partial \tau_{xy}}{\partial x} = 0. \tag{12.1}$$

From equations 11.15 and 12.1 we see that β must be a function of y only and equation 11.18 then reduces to

$$\frac{d^2}{dy^2}(\cos 2\beta) = 0 \tag{12.2}$$
$$\cos 2\beta = C_1 y + C_2. \tag{12.3}$$

Figure 12 shows the directions of maximum shear and principal stress on small rectangular elements in equilibrium lying next to each rigid plate and on the x axis. A first shear trajectory will have the orientation of side 1 of these rectangles and may be expected to form a continuous curve through points A, B, and C. At these points equation 12.3 has the respective values of:

Point A	$-1 = -C_1 a + C_2$
Point B	$0 = 0 + C_2$
Point C	$1 = C_1 a + C_2$.

The values $C_1 = 1/a$ and $C_2 = 0$, substituted into equation 12.3, give

$$\cos 2\beta = y/a. \tag{12.4}$$

SLIP LINES

Differentiating equation 12.4 gives

$$-2a \sin 2\beta d\beta = dy. \tag{13.1}$$

From equation 11.21, the differential equation of the first shear trajectory is

$$\left(\frac{dy}{dx}\right)_1 = \tan\beta = \frac{\sin 2\beta}{1 + \cos 2\beta}, \tag{13.2}$$

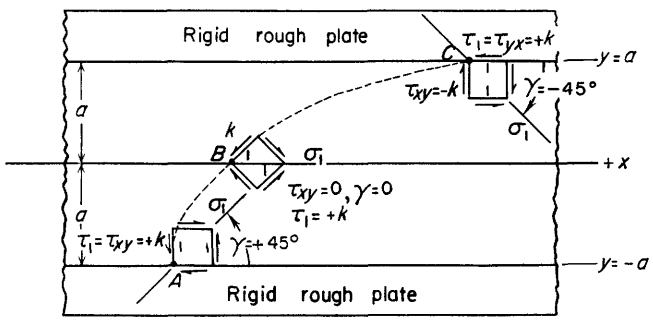

FIGURE 12.—Directions of principal stress and maximum shear on rectangular elements lying next to each rigid plate and on the x axis of Prandtl's compressed plastic strip. First maximum shear stress trajectory is indicated by 1.

in which the subscript indicates that the slope is of first shear trajectory.

In terms of the parameter β, and using equation 13.1, equation 13.2 may be written

$$dx = dy\,\frac{1 + \cos 2\beta}{\sin 2\beta} = -2a\,(1 + \cos 2\beta)\,d\beta.$$
$$x = -a\,(2\beta + \sin 2\beta) + \text{a constant},$$

and, as before,

$$y = a \cos 2\beta. \tag{13.3}$$

Equations 13.3 define families of half a cycloid described by a point on the circumference of a circle of radius a as it rolls to the right along the line $y = -a$, through half a revolution. The generating point starts on the line $y = -a$. The angle β varies from $+90°$ at $y = -a$ to $0°$ at $y = +a$.

The differential equation of the orthogonal second-shear trajectory is

$$\left(\frac{dy}{dx}\right)_2 = -\frac{1}{\left(\frac{dy}{dx}\right)_1}.$$

When integrated, the equations of the second-shear trajectory are

$$x = a\,(2\beta' - \sin 2\beta') + \text{a constant}$$
$$y = a \cos 2\beta', \tag{13.4}$$

in which

$$\beta' = \gamma - 45°$$

and β' varies from 0 at $y = -a$ to $-90°$ at $y = a$.

One member of each cycloidal set is generated for each value of the constants in equations 13.3 and 13.4. The center of the plate is taken at the point where a cycloid of the first shear trajectory, for which the value of the constant is zero, crosses the x axis. The center will then be at $x = -a\,[(\pi/2) + 1]$, $y = 0$.

The complete slip-line pattern is shown in figure 13.

STRESSES

From equations 11.15 and 12.4, we have

$$\tau_{xy} = -k\,\frac{y}{a},$$

which differentiated gives

$$\frac{d\tau_{xy}}{dy} = -k/a$$

and

$$\frac{\partial \tau_{xy}}{\partial x} = 0. \tag{14.1}$$

Placing these derivatives of τ_{xy} into the equations of equilibrium 11.4 and integrating gives

$$\sigma_x = kx/a + f_1(y) + D \tag{14.2}$$
$$\sigma_y = f_2(x) + E, \tag{14.3}$$

where D and E are constants of integration, and $f_1(y)$ and $f_2(x)$ are unknown functions of y and x.

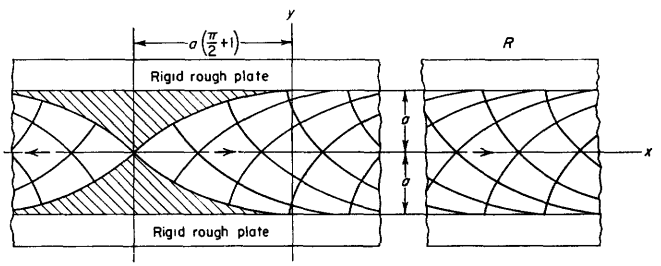

FIGURE 13.—Net of principal shear-stress trajectories in a strip of infinite length compressed in plane strain between rough rigid plates. In the region *R*, at some distance from center and the ends, $\partial\tau_{xy}/\partial x = 0$ and the curves are mutually orthogonal cycloids. Rigid wedges (ruled) remain at the center.

Subtracting equation 11.14 from equation 11.13 gives

$$\sigma_x - \sigma_y = 2k \sin 2\beta, \tag{14.4}$$

and substituting the expressions for σ_x and σ_y given by equations 14.2 and 14.3 into equation 14.4 yields

$$kx/a + f_1(y) - f_2(x) + D - E = 2k \sin 2\beta. \tag{14.5}$$

Because β is a function of y only, we have

$$f_1(y) = 2k \sin 2\beta \tag{14.6}$$

$$f_2(x) = kx/a \tag{14.7}$$

$$E = D,$$

and the expressions for stresses become

$$\sigma_x = kx/a + 2k \sin 2\beta + D \tag{14.8}$$

$$\sigma_y = kx/a + D \tag{14.9}$$

$$\tau_{xy} = -k \cos 2\beta, \tag{14.10}$$

or, in terms of x and y,

$$\sigma_x = kx/a + 2k\,(1 - y^2/a^2)^{1/2} + D \tag{14.11}$$

$$\sigma_y = kx/a + D \tag{14.12}$$

$$\tau_{xy} = -ky/a. \tag{14.13}$$

The stress deviations are, from equations 11.3, 14.8 and 14.9,

$$s_x = (\sigma_x - \sigma_y)/2 = +k\,(1 - y^2/a^2)^{1/2} \tag{14.14}$$

$$s_y = -s_x = -k\,(1 - y^2/a^2)^{1/2}. \tag{14.15}$$

The positive sign is chosen for the term to the one-half power in equations 14.11 and 14.14 because β varies between 90° and 0°, hence sin 2β is everywhere positive.

The expression for σ_y in equation 14.12 shows that σ_y consists of a tension that increases linearly with x, plus the constant D. Because the strip is specified to be under compression, D obviously must be negative and of greater magnitude than kx/a all along the bearing surface between the plates and the compressed strip. The pressure on the bearing surface thus decreases linearly going in the x direction, and becomes zero at some value of x that is determined by the value of D. In actual application of the method to the South Silverton area, the region in which tensile stress is not allowed will be defined, thereby fixing a lower limit on the constant of integration.

VELOCITY FIELD

The relative displacements and velocities of particles in a plastically deforming mass need also to be investigated before a field of principal shear-stress trajectories and the associated stress field can be regarded as valid during actual deformation. This phase of plasticity analysis has been largely neglected until recent years, but much present research, both theoretical and experimental, is devoted to defining velocity fields that are also compatible with slip-line fields and stress fields.

One of the principal difficulties lies in allowing for discontinuities in the velocities. The discontinuities are, of course, sites of abrupt differential movement, or faults, in the geologic sense. The differential equations which describe velocities may allow for such discontinuities only if the equations are "hyperbolic." A general discussion of hyperbolic equations is beyond the scope of this report; the reader is referred to Hill (1950), Prager and Hodge (1951) and to Odé (1960). However, the problem of providing for hyperbolic velocity equations becomes linked with stresses through the relations of stress to rate-of-strain. The stress equations are, in turn, determined by the equations of equilibrium and the yield condition. This has led to re-examination of yield conditions to see which will lead back, finally, to hyperbolic expressions for velocities. Problems of plane stress have proved considerably more difficult than problems of plane strain.

In plane strain, if Von Mises' yield condition and relations of stress to rate of strain are used, velocity discontinuities must coincide with lines of maximum shear stress. The converse, that all trajectories of maximum shear stress are also sites of differential displacement is not true. The particular principal shear-stress trajectories that coincide with faults are determined by the geometry of the body and the motions that are allowed or imposed upon its boundaries.

In short, all velocity discontinuities follow trajectories of maximum shear stress (or their envelopes) even though not all trajectories of maximum shear stress may become velocity discontinuities or faults. Hence the computation of lines of maximum shear stress (slip lines) appears to form only a reasonable starting point in the analysis of faulting. The determination of which trajectories of maximum shear stress are to become velocity discontinuities, or faults, at any particular stage of deformation remains largely unexplored as a field of research. But if faulting has already occurred, the determination of the pattern of maximum-shear-stress trajectories at the time of faulting may greatly aid in extending

the known fault pattern into covered areas and help interpret the observed differential displacements.

Prandtl's problem of the compressed strip has received particular attention from Hill (1950), Hodge (1950), Hill, Lee, and Tupper (1951), Green (1954), Alexander (1955) and many others. Prandtl did not consider the problem of displacements. These later workers found that the mode of internal deformation, including shape of the slip lines, the amount of differential displacement along slip lines, and the location of slip lines along which actual differential displacement may occur depend upon the conditions at the end of the strip, particularly the conditions of lateral restraint; upon the ratio of the length of the strip to its width; and upon the coefficient of friction along the contact with the pressing plates.

Prandtl's cycloidal principal shear-stress trajectories, or slip lines, lead to pressure distributions, except near the free edge, that are close to more accurate results obtained by Hill, Lee, and Tupper (1951) through numerical integration and by refined analytical methods. Prandtl's solution applies to a strip of infinite length with no commitments about the conditions of end restraint, whereas Hill, Lee, and Tupper analyzed a strip that overhangs the bearing plates and in which the length-width ratio of the region under compression is 6.72. The pattern of slip lines developed by Hill, Lee, and Tupper also appear to be cycloidal in form except near the free edge. These authors believed that Prandtl's solution could be made more satisfactory if stresses on the free edge were chosen so that their resultant was zero. Thus, some distance from the end, the Prandtl solution of pressure distribution would approach their solution in which the edge constraint actually was zero.

Now consider the velocity expressions that may be associated with Prandtl's cycloidal field of maximum shear-stress trajectories. The plates that squeeze the plastic mass must remain parallel and the velocities with which the upper plate moves downward and the lower plate moves upward are the constants $-U$ and U, respectively. Under these conditions of uniform movement of the plates in the y direction, we may expect that the y component of velocity within the deforming mass will be substantially independent of x at some distance from the center and ends. Assume, therefore, that, within the region R under consideration,

$$\frac{\partial v_y}{\partial x} = 0. \tag{15.1}$$

Therefore, v_y is some function of y only, say $f_1(y)$, and, from the relations in equations 11.1 and 11.2,

$$\frac{dv_y}{dy} = \frac{df_1(y)}{dy} = \dot{\epsilon}_y = Ls_y. \tag{15.2}$$

The factor L also must be a function of y only because s_y (equation 14.15) is a function of y only.

From the condition of no permanent volume change we have

$$\frac{\partial v_x}{\partial x} = -\frac{\partial v_y}{\partial y} = -\frac{df_1(y)}{dy}, \tag{15.3}$$

which, upon integration with respect to x, gives

$$v_x = -\frac{df_1(y)}{dy}x + f_2(y) + Q, \tag{15.4}$$

where $f_2(y)$ is another function of y, and Q is a constant. Differentiating equation 15.4, now, with respect to y yields

$$\frac{\partial v_x}{\partial y} = -x\frac{d^2f_1(y)}{dy^2} + \frac{df_2(y)}{dy}. \tag{15.5}$$

An expression for the partial derivative of v_x with respect to y may be found by another method through the relations of shear-stress to rate of strain, equation 11.2, and the expression for shear stress (14.13):

$$\frac{\partial v_x}{\partial y} = -2Lky/a. \tag{15.6}$$

If the expressions for $\partial v_x/\partial y$ in equations 15.5 and 15.6 are equated, we have

$$-x\frac{d^2f_1(y)}{dy^2} + \frac{df_2(y)}{dy} = -2Lky/a. \tag{15.7}$$

Because it has been established that L is not a function of x, the above equality is not valid unless the coefficient of x on the left side vanishes, giving

$$\frac{d^2f_1(y)}{dy^2} = \frac{d^2v_y}{dy^2} = 0, \tag{15.8}$$

which has the general solution

$$v_y = Ny + M,$$

where N and M are constants. The constants are determined by the boundary conditions

at $y = 0$ $\quad v_y = 0$ (by symmetry)
at $y = a$, $\quad v_y = -U$,

therefore,

$$M = 0$$
$$N = -U/a$$
$$f_1(y) = v_y = -Uy/a. \tag{15.9}$$

Expressions for L and v_x may now be developed. Equations 15.3 and 15.9 give

$$\frac{\partial v_x}{\partial x} = -\frac{\partial v_y}{\partial y} = \frac{U}{a}. \tag{15.10}$$

From equations 11.1, 11.2 and 14.14 we have

$$\frac{\partial v_x}{\partial x} = Ls_x = Lk\,(1 - y^2/a^2)^{1/2}. \tag{15.11}$$

Equating 15.10 and 15.11 gives

$$L = \frac{U}{ak\,(1 - y^2/a^2)^{1/2}}. \tag{15.12}$$

The coefficient of x vanished in equation 15.7, so substituting the value for L just obtained into equation 15.7 and integrating gives

$$f_2(y) = 2U\,(1 - y^2/a^2)^{1/2} + \text{a constant.} \qquad (15.13)$$

By letting the constant of equation 15.13 be absorbed by Q of equation 15.4 we have

$$v_x = Ux/a + 2U\,(1 - y^2/a^2)^{1/2} + Q \qquad (15.14)$$

$$v_y = -Uy/a. \qquad (15.15)$$

The above expressions for velocities are the same as those credited by Prager and Hodge (1951, p. 152) to Prandtl (1923), except that the equations as given by Prager and Hodge do not include the constant Q. Prager and Hodge do not, however, show a derivation of the velocity expressions, and the paper of Prandtl that they cite apparently does not mention velocities. Hill (1950, p. 233) gives, also without derivation, a possible expression for v_x similar to equation 15.14 that does include a constant, and which he credits to an unpublished work of Nádai. More recently, Green (1954) has shown, by the method of hodographs, that Nádai's proposed expression for v_x and, hence, equation 15.14 is unique for a region in which Prandtl's cyloids define the slip-line field.

The constant Q plays an important part in the expression of v_x, analogous to the constant D in the expression for stresses. Following the work of Hill (1950, p. 234), an expression for Q may be derived from the requirement that the rate of displacement of material across a vertical section at $x =$ a constant, say x_1, is equal to the rate at which material lying toward the center from the vertical section is displaced by the plates. This requires that

$$\int_0^a v_{x_1}\,dy = [x_1 + a\,(1 + \pi/2)]\,U, \qquad (15.16)$$

from which it may be shown that

$$Q/U = 1. \qquad (15.17)$$

The final expressions for velocity are then

$$v_x = U\,[(x/a) + 2\,(1 - y^2/a^2)^{1/2} + 1] \qquad (15.18)$$

$$v_y = -Uy/a \qquad (15.19)$$

at the edges $y = a$ and $y = -a$

$$v_x = U\,[(x/a) + 1], \qquad (15.20)$$

whereas in the adjacent rigid plate $v_x = 0$.

Thus the upper and lower contacts between the plates and the plastic strip are true velocity discontinuities across which the velocity v_x changes abruptly. The material slips along the plates, and particles in the interior that lay originally along a vertical line are displaced, as has been shown by Hill, into the arc of an ellipse.

Although the velocity equations may not be expected to hold near the center of the plate, the value of v_x at the point $y = 0$, $x = -a\,(1 + \pi/2)$, which is at the tips of the shaded central rigid wedges in figure 13, as computed from equation 15.18 is:

$$v_x = U\,(2 - \pi/2) = .43U. \qquad (15.21)$$

This non-zero value for v_x at the center of the block, although of doubtful validity, suggests that the points of the rigid wedges may become plastic as they are pressed together and that the newly generated plastic material moves away from the center.

FORMULAS IN POLAR COORDINATES

The mathematical expressions that describe the behavior of a stressed body have been given in reference to rectangular (x, y) cartesian coordinates because the operations using this type of coordinate system are simpler than those using any other. It is apparent, however, that the solution of boundary-value problems, in which information for the solution of differential equations is at hand only along certain physical boundaries, may be greatly simplified by making the coordinate system geometrically similar to the boundaries of the body to be analyzed. The areas of interest in the South Silverton problem can be solved most readily by the use of (r, θ) polar coordinates. The results obtained so far in cartesian coordinates need modification in order to be used in the polar-coordinate system.

STRESS NOTATION AND EQUILIBRIUM EQUATIONS

The notation for two-dimensional stresses in the polar coordinate system is analogous to the notation for those in the rectangular cartesian coordinate system. The positive direction of normal stresses, the positive direction of $\tau_{r\theta}$, and a trajectory of first maximum-shear-stress are shown in figure 14.

As in the cartesian coordinate system, shears on adjoining faces of a rectangular element are equal

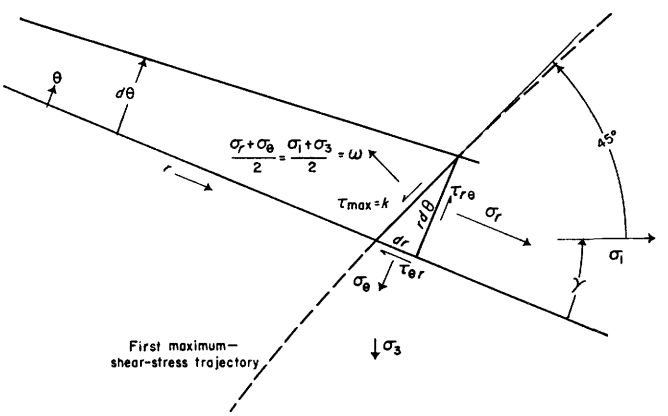

FIGURE 14.—Stresses on a small triangular element in polar coordinates, showing orientation of positive normal stress, positive shear stress, $\tau_{r\theta}$, and a first trajectory of maximum shear stress.

in magnitude and opposite in sign, $\tau_{\theta r} = -\tau_{r\theta}$. The distance r is measured positively away from the origin and the angle θ must be measured counterclockwise from the reference radius at $\theta = 0°$.

All expressions pertaining to stress at a point can be obtained simply by substituting σ_r for σ_x and σ_θ for σ_y. In particular, the expressions for the variation of stress with orientation of the plane on which it is measured, equations 2.21, 2.22 and 2.18, become

$$\sigma_r = \frac{\sigma_1 + \sigma_3}{2} + \frac{\sigma_1 - \sigma_3}{2}\cos 2\gamma \tag{16.1}$$

$$\sigma_\theta = \frac{\sigma_1 + \sigma_3}{2} - \frac{\sigma_1 - \sigma_3}{2}\cos 2\gamma \tag{16.2}$$

$$\tau_{r\theta} = \frac{\sigma_1 - \sigma_3}{2}\sin 2\gamma, \tag{16.3}$$

where γ is the angle measured counterclockwise from the direction of r to the direction of action of σ_1. Equations 2.20 and 11.8 become

$$\sigma_1 + \sigma_3 = \sigma_r + \sigma_\theta = 2\omega. \tag{16.4}$$

The expressions for the change of stress from point to point, that is, the equations of equilibrium, are of somewhat different form in polar coordinates. If body forces are not included, the equations are

$$r\frac{\partial \sigma_r}{\partial r} + \frac{\partial \tau_{r\theta}}{\partial \theta} + \sigma_r - \sigma_\theta = 0 \tag{16.5}$$

$$\frac{\partial \sigma_\theta}{\partial \theta} + r\frac{\partial \tau_{r\theta}}{\partial r} + 2\tau_{r\theta} = 0. \tag{16.6}$$

Although the derivation of these equations will not be given here, the method used is basically the same as that used for cartesian coordinates. Total forces acting on a quadrilateral element in the r direction are equated to give equation 16.5 and total forces acting in the θ direction are equated to give equations 16.6. The expressions are somewhat more complicated than those for cartesian coordinates, owing to the curved and inclined boundaries. Many texts give this derivation, but that presented by Frocht (1941, p. 51–54) can be especially recommended for its clarity.

STRAIN AND VELOCITIES

If the components of displacement in the r and θ directions are called u_r and u_θ, respectively, the components of strain are then

$$\epsilon_r = \frac{\partial u_r}{\partial r} \tag{17.1}$$

$$\epsilon_\theta = \frac{u_r}{r} + \frac{\partial u_\theta}{r\partial \theta} \tag{17.2}$$

$$\gamma_{r\theta} = \frac{\partial u_r}{r\partial \theta} + \frac{\partial u_\theta}{\partial r} - \frac{u_\theta}{r}. \tag{17.3}$$

A derivation of these strain components is given by Timoshenko (1934, p. 62–63).

Velocities and strain rates are given by

$$v_r = \frac{du_r}{dt} \tag{17.4}$$

$$v_\theta = \frac{du_\theta}{dt} \tag{17.5}$$

$$\dot{\epsilon}_r = \frac{\partial v_r}{\partial r} \tag{17.6}$$

$$\dot{\epsilon}_\theta = \frac{v_r}{r} + \frac{\partial v_\theta}{r\partial \theta} \tag{17.7}$$

$$\dot{\gamma}_{r\theta} = \frac{\partial v_r}{r\partial \theta} + \frac{\partial v_\theta}{\partial r} - \frac{v_\theta}{r}. \tag{17.8}$$

RELATIONS OF PLASTIC STRESS TO RATE OF STRAIN IN PLANE STRAIN

The relations of plastic-stress deviation to rate of strain for plane strain in terms of polar coordinates are taken to be analogous to equation 11.2 and are written as:

$$\dot{\epsilon}_r = \frac{\partial v_r}{\partial r} = Ls_r \tag{18.1}$$

$$\dot{\epsilon}_\theta = \frac{v_r}{r} + \frac{\partial v_\theta}{rd\theta} = Ls_\theta \tag{18.2}$$

$$\dot{\gamma}_{r\theta} = \frac{\partial v_r}{rd\theta} + \frac{\partial v_\theta}{\partial r} - \frac{v_\theta}{r} = 2L\tau_{r\theta}, \tag{18.3}$$

in which

$$s_r = \sigma_r - \frac{\sigma_r + \sigma_\theta + \sigma_z}{3} = \frac{\sigma_r - \sigma_\theta}{2} \tag{18.4}$$

$$s_\theta = \sigma_\theta - \frac{\sigma_r + \sigma_\theta + \sigma_z}{3} = -\frac{\sigma_r - \sigma_\theta}{2}. \tag{18.5}$$

This manner of writing relations of plastic stress to rate of strain in terms of polar coordinates does not appear explicitly in the textbooks examined, but it would seem to be a logical extension from the cartesian form.

Von Mises' yield criterion in plane strain remains

$$\left(\frac{\sigma_1 - \sigma_3}{2}\right)^2 = k^2. \tag{18.6}$$

Substitution of equation 18.6 into equation 16.1 to 16.3 and 18.1 to 18.5 gives

$$s_r = k\cos 2\gamma = \frac{\dot{\epsilon}_r}{L} \tag{18.7}$$

$$s_\theta = -k\cos 2\gamma = \frac{\dot{\epsilon}_\theta}{L} \tag{18.8}$$

$$\tau_{r\theta} = k\sin 2\gamma = \frac{\dot{\gamma}_{r\theta}}{2L}. \tag{18.9}$$

Thus,

$$\dot{\epsilon}_r - \dot{\epsilon}_\theta = 2kL\cos 2\gamma \tag{18.10}$$

$$\dot{\gamma}_{r\theta} = 2kL\sin 2\gamma \tag{18.11}$$

$$\frac{\dot{\gamma}_{r\theta}}{\dot{\epsilon}_r - \dot{\epsilon}_\theta} = \tan 2\gamma. \tag{18.12}$$

Where γ is a function of θ only, equation 18.12

requires that if $\dot{\gamma}_{r\theta}$ and $(\dot{\epsilon}_r - \dot{\epsilon}_\theta)$ contain r at all, they must contain it as a factor that will cancel in their quotient. Thus,

$$2kL \sin 2\gamma = \dot{\gamma}_{r\theta} = Af_1(\theta)f_1(r) \tag{18.13}$$

$$2kL \cos 2\gamma = \dot{\epsilon}_r - \dot{\epsilon}_\theta = Af_2(\theta)f_1(r). \tag{18.14}$$

And thus:

$$L = \frac{Af_1(\theta)f_1(r)}{2k \sin 2\gamma} = \frac{Af_2(\theta)f_1(r)}{2k \cos 2\gamma}, \tag{18.15}$$

and, if γ is a function of r only or of θ only, L may, in either case be a product (some function of θ only) times (some function of r only).

GENERALIZED EXPRESSIONS FOR SLIP LINES IN PLANE PLASTIC STRAIN

By use of equations 16.1, 16.2, 16.3, 16.4 and 18.6, the expressions for stresses in plane plastic strain become

$$\sigma_r = \omega + k \cos 2\gamma \tag{19.1}$$

$$\sigma_\theta = \omega - k \cos 2\gamma \tag{19.2}$$

$$\tau_{r\theta} = k \sin 2\gamma. \tag{19.3}$$

Substitution of the above expressions in to the equations of equilibrium 16.5 and 16.6 gives

$$r\frac{\partial}{\partial r}(\omega + k \cos 2\gamma) + \frac{\partial}{\partial \theta}(k \sin 2\gamma) + 2k \cos 2\gamma = 0 \tag{19.4}$$

and

$$\frac{\partial}{\partial \theta}(\omega - k \cos 2\gamma) + r\frac{\partial}{\partial r}(k \sin 2\gamma) + k \sin 2\gamma = 0. \tag{19.5}$$

Differentiating equations 19.4 with respect to θ and equation 19.5 with respect to r gives

$$r\frac{\partial^2 \omega}{\partial \theta \partial r} + rk\frac{\partial^2}{\partial \theta \partial r}(\cos 2\gamma) + k\frac{\partial^2}{\partial \theta^2}(\sin 2\gamma) + 2k\frac{\partial}{\partial \theta}(\cos 2\gamma) = 0, \tag{19.6}$$

and

$$\frac{\partial^2 \omega}{\partial r \partial \theta} - k\frac{\partial^2}{\partial r \partial \theta}(\cos 2\gamma) + kr\frac{\partial^2}{\partial r^2}(\sin 2\gamma) + k\frac{\partial}{\partial r}(\sin 2\gamma) + 2k\frac{\partial}{\partial r}(\sin 2\gamma) = 0. \tag{19.7}$$

Dividing equation 19.6 by r and subtracting equation 19.7 eliminates ω; k cancels out, giving

$$-r\frac{\partial^2}{\partial r^2}(\sin 2\gamma) + 2\frac{\partial^2}{\partial r \partial \theta}(\cos 2\gamma) + \frac{1}{r}\frac{\partial^2}{\partial \theta^2}(\sin 2\gamma) - 3\frac{\partial}{\partial r}(\sin 2\gamma) + \frac{2}{r}\frac{\partial}{\partial \theta}(\cos 2\gamma) = 0. \tag{19.8}$$

A solution to this equation in the form $\gamma = f(r, \theta)$ is valid throughout the plastic region. The angle γ is also related to the slope of the first principal-shear trajectory because the slope of first slip line $= r\frac{d\theta}{dr} = \tan \beta = \tan(\gamma + 45°)$. (19.9)

By trigonometric relations,

$$\tan(\gamma + 45°) = \frac{1 + \sin 2\gamma}{\cos 2\gamma} \text{ or } = \frac{\cos 2\gamma}{1 - \sin 2\gamma}; \tag{19.10}$$

therefore,

$$d\theta = \frac{1 + \sin 2\gamma}{\cos 2\gamma}\frac{dr}{r}, \tag{19.11a}$$

or

$$d\theta = \frac{\cos 2\gamma}{1 - \sin 2\gamma}\frac{dr}{r}. \tag{19.11b}$$

The integration of equation 19.11 leads to the relation between r and θ along the first family of slip lines; that is, to the equation of these lines in reference to polar coordinates. This integration is evidently considerably simplified if γ in equation 19.11 is either a function of r only or of θ only, because the variables r and θ can then be completely separated.

The analyses of the western and eastern parts of the South Silverton area, described in the section on application, are made, respectively, under the assumptions that γ is a function of θ only and that γ is a function of r only. The nature of these functions is determined by equation 19.8. Since these particular examples will be used farther along, the consequences of the two assumptions are examined in some detail below.

If γ (and thus $\tau_{r\theta}$) is assumed to be a function of θ only, then

$$\frac{\partial \gamma}{\partial r} = 0, \qquad \frac{\partial \tau_{r\theta}}{\partial r} = 0, \tag{19.12}$$

and equation 19.8 reduces to

$$\frac{d}{d\theta}\left(2 \cos 2\gamma \frac{d\gamma}{d\theta} + 2 \cos 2\gamma\right) = 0. \tag{19.13}$$

Integrating equation 19.13 once gives

$$d\theta = \frac{\cos 2\gamma d\gamma}{C - \cos 2\gamma}, \; C \text{ is a constant.} \tag{19.14}$$

From equation 19.11b we know that along the first slip line

$$\frac{dr_1}{r_1} = \frac{d\theta\,(1 - \sin 2\gamma)}{\cos 2\gamma}. \tag{19.15}$$

Substitution of equation 19.14 into equation 19.15 eliminates $d\theta$ and gives

$$\frac{dr_1}{r_1} = \frac{1}{2}\frac{2d\gamma}{C - \cos 2\gamma} - \frac{1}{2}\frac{(\sin 2\gamma)2d\gamma}{C - \cos 2\gamma}, \tag{19.16a}$$

or

$$\frac{dr_1}{r_1} = \frac{1}{2}\frac{2d\gamma}{C - \cos 2\gamma} + \frac{1}{2}\frac{(\sin 2\gamma)2d\gamma}{\cos 2\gamma - C}. \tag{19.16b}$$

Equations 19.14 and 19.16 are the differential equations of the first family of slip lines in plane plastic strain in terms of γ, under the assumption that γ (and therefore $\tau_{r\theta}$) is a function of θ only.

Equation 19.14 may be transformed (Pierce, 1929, p. 42 formula 304) into

$$\int d\theta = \theta + D = -\gamma + \frac{C}{2}\int \frac{2d\gamma}{C - \cos 2\gamma}, \quad (19.17)$$

where D is constant. The constant D will always be associated with the complete integration of the terms in equations 19.17, and only those. Because expressions involving several integrals in various combinations will become common farther along, care must be taken to associate each integration with its own constant.

The remaining integral in equation 19.17 may be evaluated, again according to Pierce (1929, p. 41, formula 300), as

$$\int \frac{2d\gamma}{C - \cos 2\gamma} = \frac{2}{\sqrt{C^2 - 1}} \tan^{-1} \frac{\sqrt{C^2 - 1}\tan\gamma}{C - 1} \quad (19.18)$$

$$= \frac{1}{\sqrt{1 - C^2}} \log_e \frac{\sqrt{1 - C^2}\tan\gamma + C - 1}{\sqrt{1 - C^2}\tan\gamma - C + 1} \quad (19.19)$$

$$= \frac{2}{\sqrt{1 - C^2}} \tanh^{-1} \frac{\sqrt{1 - C^2}\tan\gamma}{C - 1} \quad (19.20)$$

$$= \frac{2}{\sqrt{1 - C^2}} \operatorname{ctnh}^{-1} \frac{\sqrt{1 - C^2}\tan\gamma}{C - 1}. \quad (19.21)$$

These formulas are valid in the range

$$-\pi < 2\gamma < \pi.$$

The one that is to be used depends upon the value of C for the particular problem at hand; if C is greater than one, equation 19.18 should be used to avoid having negative quantities under the radical sign. The restriction that 2γ must lie between $-\pi$ and $+\pi$ presents no problem because the angle between any point on Mohr's circle and the $+\sigma$ axis will be found to be either less than π if measured counterclockwise, or no more negative than $-\pi$ if measured clockwise.

The integration of equation 19.16 leads to

$$\ln r_1 - \ln M + \ln \sqrt{\pm(C - \cos 2\gamma)} = \frac{1}{2}\int \frac{2d\gamma}{C - \cos 2\gamma},$$

in which M is an arbitrary constant associated only with the integration of terms of the left side of the above equations and ln denotes the natural, or Napierian logarithm. The plus–or–minus sign under the radical sign indicates that either the plus sign or the minus sign may be chosen, depending upon the relative values of C and $\cos 2\gamma$, so that $(C - \cos 2\gamma)$ is always positive and the square root is real. Taking the exponential of both sides of the above equation reduces the equation to

$$\text{First shear line } r_1 = \frac{M}{\sqrt{\pm(C - \cos 2\gamma)}} \exp\left[\tfrac{1}{2}\int \frac{2d\gamma}{C - \cos 2\gamma}\right] \quad (19.22)$$

which expresses r in terms of γ along the first family of slip lines under the condition that $\partial\gamma/\partial r = 0$. This formula again contains the integral that takes various forms, and the generalized derivation for this case is now carried as far as it can be until further information on C can be supplied.

Along the second shear line we have

$$\text{slope of second shear line} = r_2 \frac{d\theta}{dr_2} = \tan\alpha = \tan(\gamma - 45°). \quad (19.23)$$

By trigonometric relations

$$\tan(\gamma - 45°) = -\frac{\cos 2\gamma}{1 + \sin 2\gamma} = -\frac{1 - \sin 2\gamma}{\cos 2\gamma}. \quad (19.24)$$

Therefore,

$$d\theta = -\frac{\cos 2\gamma}{1 + \sin 2\gamma}\frac{dr_2}{r_2},$$

or

$$= -\frac{1 - \sin 2\gamma}{\cos 2\gamma}\frac{dr_2}{r_2}, \quad (19.25)$$

and

$$\frac{dr_2}{r_2} = -\frac{1 + \sin 2\gamma}{\cos 2\gamma} d\theta, \quad (19.26a)$$

or

$$\frac{dr_2}{r_2} = -\frac{\cos 2\gamma}{1 - \sin 2\gamma} d\theta. \quad (19.26b)$$

Substituting the value $d\theta$ from equations 19.14 into equation 19.26a gives

$$\frac{dr_2}{r_2} = -\frac{1}{2}\frac{2d\gamma}{C - \cos 2\gamma} - \frac{1}{2}\frac{(\sin 2\gamma)\,2d\gamma}{C - \cos 2\gamma} \quad (19.27a)$$

or

$$= -\frac{1}{2}\frac{2d\gamma}{C - \cos 2\gamma} + \frac{(\sin 2\gamma)\,2d\gamma}{\cos 2\gamma - C}, \quad (19.27b)$$

which, when integrated, gives for the second slip line

$$r_2 = \frac{M}{\sqrt{\pm(C - \cos 2\gamma)}} \exp\left[-\frac{1}{2}\int \frac{2d\gamma}{C - \cos 2\gamma}\right]. \quad (19.28)$$

The parametric expression for θ is the same (19.17) for both the first and the second shear lines.

If γ (or $\tau_{r\theta}$) is assumed to be a function of r only, then

$$\frac{\partial\gamma}{\partial\theta} = 0, \quad \frac{\partial\tau_{r\theta}}{\partial\theta} = 0, \quad (19.29)$$

and (19.8) reduces to

$$r\frac{d^2}{dr^2}(\sin 2\gamma) + 3\frac{d}{dr}(\sin 2\gamma) = 0. \quad (19.30)$$

Equation 19.30 may be integrated completely to give

$$\sin 2\gamma = (G/r^2) + H, \quad (19.31)$$

where G and H are constants.

Differentiating equation 19.31 once with respect to r gives

$$-\frac{\cos 2\gamma d\gamma}{\sin 2\gamma - H} = \frac{dr}{r}. \quad (19.32)$$

Substitution of equation 19.32 into first equation of 19.11 gives

$$2d\theta = -\frac{2d\gamma}{\sin 2\gamma - H} - \frac{(\sin 2\gamma)\, 2d\gamma}{\sin 2\gamma - H} \qquad (19.33$$

along the first slip line.

Equation 19.33 can be altered somewhat to give

$$\theta + N = \frac{\pi}{4} - \gamma - \frac{1+H}{2}\int \frac{2d\gamma}{\sin 2\gamma - H} \qquad (19.34)$$

along the first slip line. Here N is a constant. The remaining integral, like that of equation 19.17, can take several forms depending upon the value of H. The integration of equation 19.34 is valid only in the range $-\pi < 2\gamma < \pi$.

The equation of the second shear line can be obtained by substituting equation 19.32 into equation 19.26b instead of into 19.11. This gives

$$2d\theta = \frac{2d\gamma}{\sin 2\gamma - H} - \frac{2\sin 2\gamma d\gamma}{\sin 2\gamma - H} \qquad (19.35)$$

along the second shear line,
which may be reduced to

$$\theta + P = \frac{\pi}{4} - \gamma - \frac{H-1}{2}\int \frac{2d\gamma}{\sin 2\gamma - H}, \qquad (19.36)$$

along the second shear line.

GENERALIZED EXPRESSIONS FOR STRESSES IN PLANE PLASTIC STRAIN

As shown by equations 19.1 to 19.3, expressions for stresses in terms of r and θ can be written if ω and γ are given in terms of r and θ. The preceding section has shown how to obtain a differential relation between γ and θ (equation 19.14) if γ is a function of θ only, or a simple relation between γ and r (equation 19.31) if γ is a function of r only. The corresponding relations between ω and r and θ will be shown in this section.

If γ is a function of r only, equation 19.6 reduces to

$$r\frac{\partial^2\omega}{\partial\theta\partial r} = 0, \qquad (20.1)$$

and, if γ is a function of θ only, equation 19.7 reduces to

$$\frac{\partial^2\omega}{\partial r\partial\theta} = 0. \qquad (20.2)$$

So, in either case, ω is some function that satisfies equation 20.2, provided that $r \neq 0$, if γ is a function of r only.
The general solution of equation 20.2 is

$$\omega = (\text{function of } r) + (\text{function of } \theta). \qquad (20.3)$$

If γ is a function of r only, ω can be of the form

$$\omega = (\text{function of } r, \text{ or } \gamma, \text{ or both}) + (\text{function of } \theta). \qquad (20.4)$$

and, if γ is a function of θ only, ω can be of the form

$$\omega = (\text{function of } r) + (\text{function of } \theta, \text{ or } \gamma, \text{ or both}). \qquad (20.5)$$

These relations are useful as a check on the form of expressions for ω in the solution of particular problems.

We can go considerably farther in determining the nature of the functions in equations 20.3 to 20.5 by integrating equations 19.4 and 19.5.

Under the assumption that γ is a function of θ only, equation 19.4 becomes

$$r\frac{\partial\omega}{\partial r} + 2k\cos 2\gamma\left(\frac{d\gamma}{d\theta} + 1\right) = 0. \qquad (20.6)$$

Substituting the value of $\frac{d\gamma}{d\theta}$ from equation 19.14 into equation 20.6 gives

$$\frac{\partial\omega}{\partial r} = -2kC/r. \qquad (20.7)$$

Also, if γ is a function of θ only, equation 19.5 becomes

$$\frac{\partial\omega}{\partial\theta} = -2kC\sin 2\gamma/\cos 2\gamma. \qquad (20.8)$$

The total differential of ω is

$$d\omega = \frac{\partial\omega}{\partial r}dr + \frac{\partial\omega}{\partial\theta}d\theta. \qquad (20.9)$$

Substituting equations 20.7, 20.8, and 19.14 into equation 20.9 gives

$$d\omega = -2kC\frac{dr}{r} - kC\frac{2\sin 2\gamma d\gamma}{C - \cos 2\gamma}, \qquad (20.10)$$

which may be integrated directly to give

$$\omega + 2kE = -2Ck\ln r - Ck\ln[\pm(C - \cos 2\gamma)], \left(\frac{\partial\gamma}{\partial r} = 0\right) \qquad (20.11)$$

where $2kE$ is another constant.

Equation 20.11 evidently is of the form predicted by equation 20.5. Having this expression for ω, one may compute σ_r and σ_θ from equations 19.1 and 19.2.

If γ is a function of r only, equations 19.4 and 19.5 become, respectively

$$r\frac{\partial\omega}{\partial r} - 2kr\sin 2\gamma\frac{d\gamma}{dr} + 2k\cos 2\gamma = 0, \qquad (20.12)$$

and

$$\frac{\partial\omega}{\partial\theta} + 2kr\cos 2\gamma\frac{d\gamma}{dr} + 2k\sin 2\gamma = 0. \qquad (20.13)$$

Substituting the expression for $d\gamma/dr$ from equation 19.32 into equation 20.13 gives

$$\frac{\partial\omega}{\partial\theta} = -2kH. \qquad (20.14)$$

Rearranging equation 20.12 gives

$$\frac{\partial\omega}{\partial r} = 2k\sin 2\gamma\frac{d\gamma}{dr} - 2\frac{k}{r}\cos 2\gamma. \qquad (20.15)$$

Substitution of equations 20.14 and 20.15, and 19.32 into equation 20.9 yields

$$d\omega = -2kHd\theta + 2k\sin 2\gamma d\gamma + 2k\frac{\cos^2 2\gamma d\gamma}{\sin 2\gamma - H}. \qquad (20.16)$$

Integration of equation 20.16 gives

$$\frac{\omega}{k} + 2F = -2H\theta - \cos 2\gamma + \int \frac{(\cos^2 2\gamma)\, 2d\gamma}{\sin 2\gamma - H}, \text{ if } \frac{\partial \gamma}{\partial \theta} = 0, \tag{20.17}$$

which may be reduced to the more tractable form

$$\frac{\omega}{k} + 2F = -2H(\theta + \gamma) + \frac{H\pi}{2} + (1 - H^2)\int \frac{2d\gamma}{\sin 2\gamma - H}. \tag{20.18}$$

This expression contains the many-form integral of the equation 19.34, and again the final integration must be left until the boundary values of γ are known for a particular problem.

There is a strong similarity between the expressions for slip lines and the expressions for stresses, which is due to a fundamental property of slip lines that is worth discussing.

For example, when γ is a function of θ only, we have, from equation 20.10,

$$d\omega = -2kC\frac{dr}{r} - kC\frac{2\sin 2\gamma d\gamma}{C - \cos 2\gamma}. \tag{20.10}$$

But from equations 19.16*a* and 19.27*a* we have

$$\frac{dr}{r} = \pm\frac{1}{2}\frac{2d\gamma}{C - \cos 2\gamma} - \frac{1}{2}\frac{2\sin 2\gamma d\gamma}{C - \cos 2\gamma}, \tag{20.19}$$

where the upper sign, of the plus–or–minus sign, is associated with the first family of slip lines; and the lower sign, with the second. If equation 20.19 is substituted into equation 20.10, we obtain

$$\int d\omega = \mp kC\int \frac{2d\gamma}{C - \cos 2\gamma} \quad \text{along slip lines.} \tag{20.20}$$

But from equation 19.17 we have

$$2\theta + 2D + 2\gamma = C\int \frac{2d\gamma}{C - \cos 2\gamma},$$

hence

$$\omega + 2kE = \mp k(2\theta + 2D + 2\gamma),$$

where E is the constant of equation 20.11 resulting from the integration of $d\omega$. Rearranged, this gives

$$\frac{\omega}{2k} + (\theta + \gamma) = -D - E \tag{20.21}$$

along the first slip lines, and

$$\frac{\omega}{2k} - (\theta + \gamma) = -D - E \tag{20.22}$$

along the second slip lines.

Similar operations when γ is a function of r only lead to

$$\frac{\omega}{2k} + (\theta + \gamma) = \frac{\pi}{4} - N - E \tag{20.23}$$

along the first slip lines, and

$$\frac{\omega}{2k} - (\theta + \gamma) = -\left(\frac{\pi}{4} - N\right) - E \tag{20.24}$$

along the second slip lines.

These remarkable relations between average stress and the inclinations of slip lines appear to be special cases of more general relations, generally attributed to Hencky (1923), which state that

$$\frac{\omega}{2k} + \phi = \text{a constant on a first slip line,} \tag{20.25}$$

and

$$\frac{\omega}{2k} - \phi = \text{a constant on a second slip line,} \tag{20.26}$$

where ϕ is the angle measured from any fixed direction to the tangent of the first slip line (Hill, 1950, p. 135). In terms of γ, and setting the fixed direction in polar coordinates to be the line $\theta = 0$, Hencky's relations become the same as those derived above, that is,

$$\frac{\omega}{2k} + \left(\theta + \gamma + \frac{\pi}{4}\right) = \text{a constant along a first slip line} \tag{20.27}$$

and

$$\frac{\omega}{2k} - \left(\theta + \gamma - \frac{\pi}{4}\right) = \text{a constant along a second slip line.} \tag{20.28}$$

The Hencky relations lead to interesting geometric properties of slip lines, which have attracted considerable attention from stress analysts, mathematicians, and geometers (Hill, 1950, p. 136–140; Nádai, 1950, p. 545; and Prager and Hodge, 1951, p. 130–134). Because these properties may be useful in the analysis of geologic structures some of them are briefly given below, as paraphrased from various sources.

GEOMETRIC PROPERTIES OF SLIP LINES

1. Hencky's first theorem. The angle formed by the tangents of two fixed slip lines of one family where they are intersected by a slip line of the other family is constant along their length and does not depend on the choice of the intersecting slip line of the other family.
2. Hencky's second theorem. As a slip line of one family is followed, the radii of curvature of the other family decrease or increase by the length of arc travelled.
3. If the slip line followed is straight, the slip lines of the curved orthogonal family are circular arcs near the intersection.
4. The envelope of the shear lines of one family is the natural boundary of the analytic solution and a limiting line across which the shear lines of the other family cannot be continued.
5. If a segment AB of a slip line is straight, then all members of that slip-line family are straight between the two members of the other family which pass through A and B.

6. Two or more adjacent slip-line fields corresponding to analytic solutions that are valid for adjacent regions may be patched together, subject to the conditions that the boundaries are slip lines common to the adjacent fields, the normal stress across the boundaries is continuous, and the velocity normal to the boundaries is continuous.

APPLICATION TO THE SOUTH SILVERTON AREA

GENERAL STATEMENT

The application of the theory of plasticity to the South Silverton area is concerned primarily with determining if the trajectories of maximum shear-stress or slip lines constructed according to Von Mises' theory in any way resemble the fault pattern as mapped in the field. Construction of the whole theoretical pattern is based upon assumptions regarding the mode of deformation and the shape of the plastic domain, and upon direct knowledge of part of the fault pattern. The orientation of selected slip lines rather than stresses or displacements form the boundary conditions for solution of the equations. Only very general assumptions regarding the distribution of normal stress are made in setting up the problems. The exact distribution of stresses that is necessary to produce the pattern of slip lines is then computed to see whether the distribution is geologically reasonable.

The dominant feature of the regional structure is a subsided block, within the Silverton caldera, or volcanic basin, which is bounded by a zone of normal faults called the ring-fault zone, as shown in figure 15.

The area to be analyzed lies adjacent to the south-

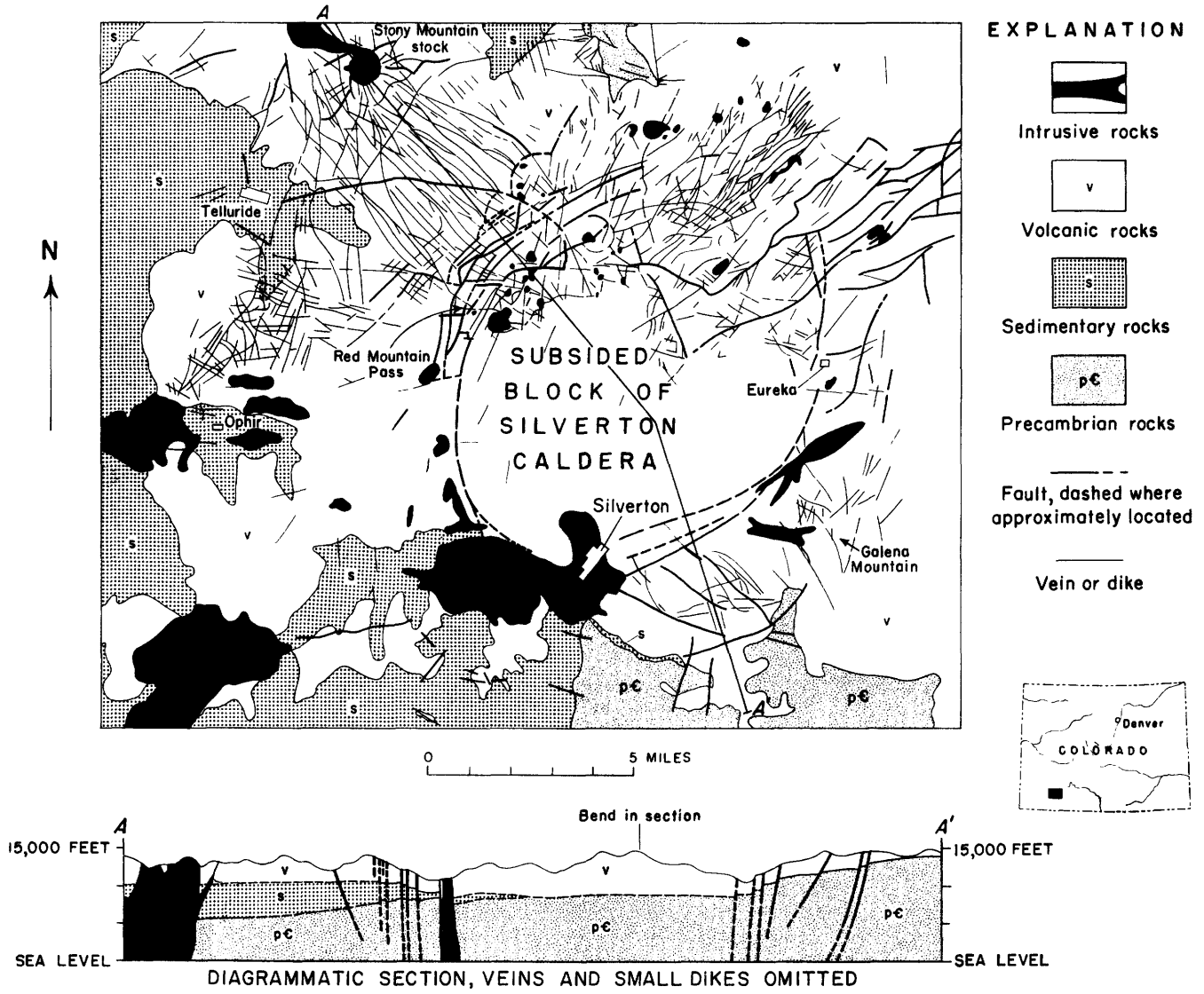

FIGURE 15.—Generalized geologic map of part of the Silverton caldera area showing the subsided block. Adapted from Burbank, Eckel, and Varnes (1947, p. 28).

ern periphery of the subsided block, southeast of the town of Silverton, and is shown in more detail in figure 16.

The production of ores in the area southeast of Silverton has come almost entirely from veins in a complexly fractured zone that lies to the south and southeast of the ring-fault zone. The most intense fracturing and strongest mineralization occurred in a roughly triangular area, shown in figure 16, which is bounded by the ring-fault zone on the north, by the northwestward-trending Titusville vein on the southwest, and by an arcuate shear zone (3*a*) on the east and southeast. Geologic data in the eastern and western quarters of figure 16 are taken from the Silverton folio (Cross, Howe, and Ransome, 1905); data for the central part are derived from the geologic map that accompanies Professional Paper 378–A. In order to better show their true strike, the courses of many faults, veins, and dikes have been modified somewhat before plotting on figure 16 to remove the effect of topography.

Three systems of fractures may be recognized within the triangular area: (1) a system that is more or less concentric with and 1½ to 2½ miles south of the southern border of the caldera; (2) a system of shear fractures and related tension fractures in the western part; and (3) a system of shear fractures in the eastern part.

The second or western shear system of figure 16 includes three groups of fractures. Each can be identified by its trend; 2*a*, a northwestward-trending group of shear fractures; 2*b*, a northeastward-trending group of shear fractures; and 2*c*, a group of diagonal tension fractures trending somewhat west of north. The eastern system is tentatively divided into three groups: 3*a*, an eastern arcuate group of shear fractures, partly filled with granite porphyry dikes, which extends from Galena Mountain to Kendall Gulch, together with several other northward-trending fractures lying east of Cunningham Creek; 3*b*, northwestward-trending fractures on both sides of Cunningham Creek; and 3*c*, fractures that apparently are approximately radial to the ring-fault zone. There are, in addition to these seven main groups, numerous smaller fractures, narrow veins, and a few dikes that do not fit into any easily recognized system or group. These appear to have lesser significance, either in the regional structure or in the mineral deposits.

Several of the groups of fractures shown in figure 16 are not considered in the analysis of the dominant shearing deformation. The first group is eliminated because it is almost surely of tensile origin and is definitely older than the northwestward- and northeastward-trending faults in the western part of the area. The fractures of group 1 are filled by dikes, as are most of the major faults, but they show no evidence of either lateral or vertical displacement and are themselves cut and displaced by the faults. They were apparently not reopened after injection of dike material and are virtually unmineralized.

Group 2*c* is eliminated from analysis because it includes only tension fractures that formed as a result of continued movement along fractures of group 2*b*, in the manner explained by Burbank (1933, fig. 2). The analysis of the western system thus applies only to the conjugate set of shears, groups 2*a* and 2*b*.

The groups 3*a*, 3*b*, and 3*c* of the eastern system are less well defined because this part of the area has not been mapped in detail. The radial fractures of group 3*c* were eliminated from the analysis because descriptions by Ransome (1901) and observations by the writer (made on the Pride of the West vein only), show no evidence that lateral shear has occurred on any of them. There is good field evidence for right lateral movement on the Green Mountain vein and for left lateral movement along the eastern arcuate group of fractures (3*a*). A simplified structural pattern, from which the groups 1, 2*c* and 3*c* have been eliminated, and on which some of the veins mentioned above are identified, is shown in figure 17. Several groups of fractures that were mapped by Ransome near the northeast corner of the map are retained because there is little or no information available to indicate whether they should be included in the analysis of shearing.

The western part is contained within a wedge-shaped area bounded on the north by the ring-fault zone and on the southwest by the Titusville vein. The Titusville is regarded as a master fracture that formed before the fractures within the wedge-shaped area. It is along a projection of a straight part of the southwestern border of the subsided block west of Silverton, and may have formed as a shear fracture off the southwest end of the subsided block at an early stage in the subsidence. The directions of relative movement along the shear fractures shown by arrows, indicate an axis of compression oriented north or northwest. Fault patterns in the eastern and western parts of the South Silverton district appear to be different; therefore, analysis of these parts will be taken up separately.

The entire analysis is based upon the hypothesis that the observed fault pattern has resulted from radial compression directed outward from the sub-

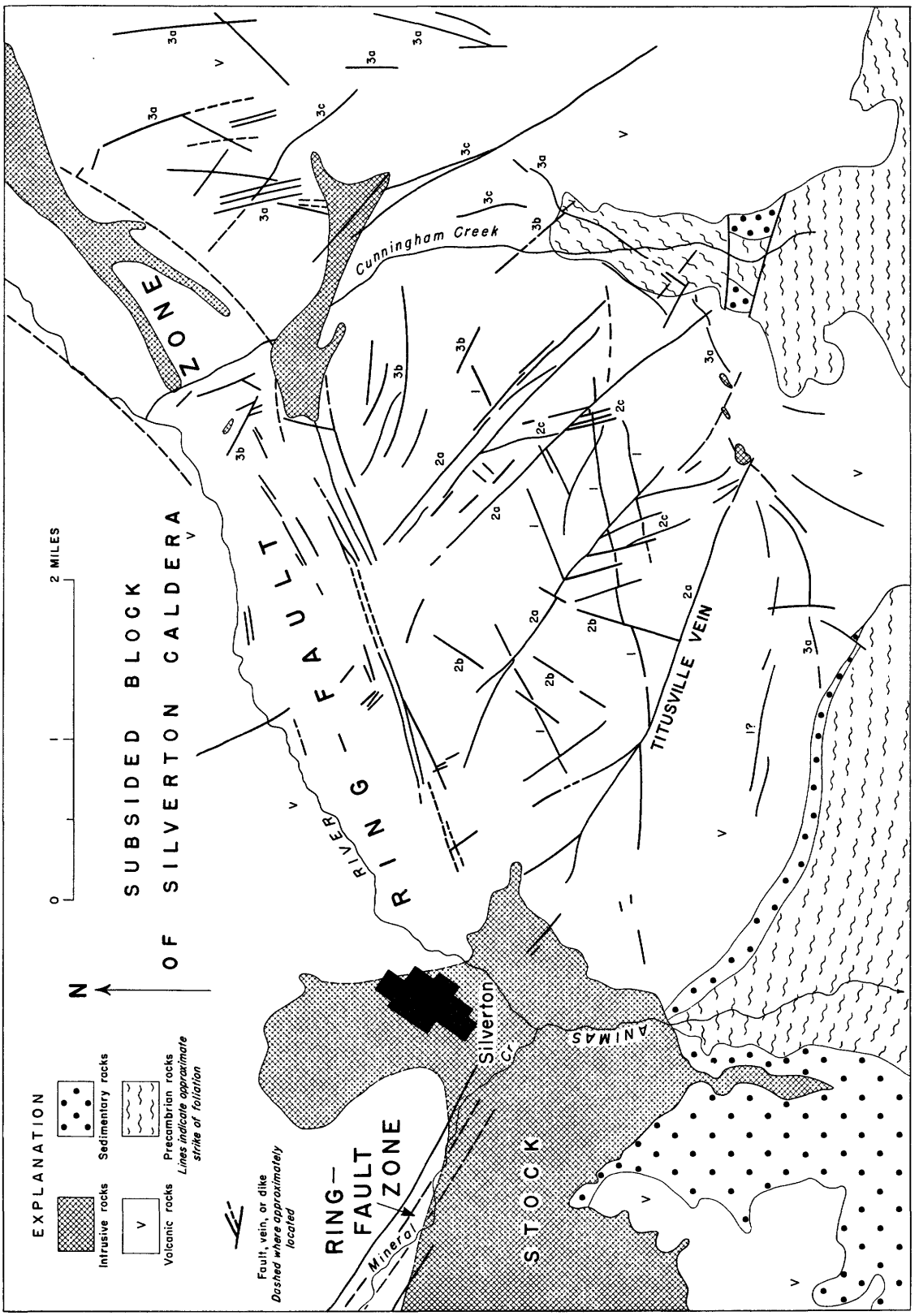

FIGURE 16.— Sketch of the principal fracture systems of the South Silverton mining area. The courses of the fractures have been modified somewhat from their actual trend of outcrop in order to remove the effect of topographic relief. 1. Concentric system. 2. Western shear system consisting of: *2a*, northwestward-trending faults, *2b*, northeastward-trending faults, and *2c*, diagonal tension fractures. 3. Eastern system consisting of: *3a*, eastern arcuate group of shear fractures, *3b*, northwestward-trending fractures, and *3c*, fractures that are approximately radial to the ring-fault zone.

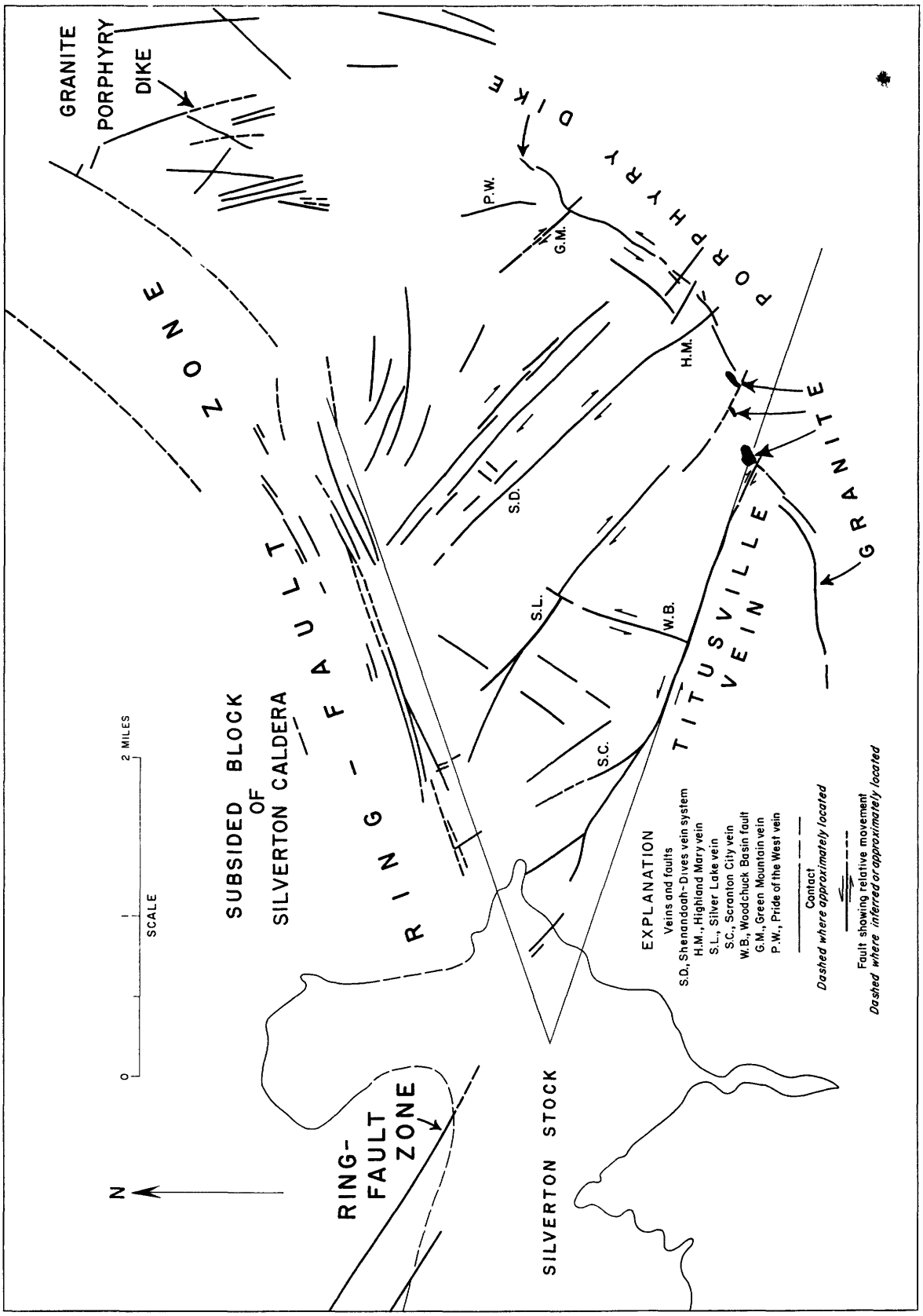

FIGURE 17.—Simplified structural pattern of the South Silverton district. Arrows show observed relative direction of lateral movement along faults. The principal faults of the western shear system are within the wedge shown by light lines.

sided block and resisted by rigid material outside the deformed periphery. If the ring faults that bound the subsided block dip slightly inward, radial compression would have been generated by the block as it sank as a tapered plug. Support for the central block presumably was removed when magma and volatile material escaped to the surface during eruptions, or into peripheral areas to form stocks, dikes, and veins. Although the ring faults dip 75° to 85° N. near the mouth of Arrastra Gulch, in other places where the ring faults can be observed around the border of the subsided block their dip is almost vertical. Much of the ring-fault zone is so obscured by alluvium, moraine, and alteration of the rocks that the average dip of the faults is uncertain. Subsided cauldrons, in general, have been interpreted to have outward-dipping boundary faults, according to the analysis of the British Tertiary volcanic centers presented by Anderson (1936).

Inward dip of the ring faults may not have been a necessary condition for generation of radial pressure. As suggested by Burbank (written communication, 1957), the central block may have been broken and the open fractures filled by magma during eruptive stages; thereby the upper part would have expanded so much that outward pressure would be generated during withdrawal of magma from below. Wedging due to a graben structure at the northeast end of the subsided block, to be considered later in connection with analysis of the eastern part, possibly contributed to local concentration of outwardly directed pressure.

The assumptions under which analyses are made of the fault systems, according to Von Mises' theory of plane plastic strain, are here repeated.

1. The entire plastic zone is assumed to be isotropic, homogeneous, and perfectly plastic. Elastic strains are neglected under the assumption that they are at least an order of magnitude smaller than the permanent plastic strains. For the meaning of perfect plasticity the reader is referred to earlier sections of this report, to Prager and Hodge (1951), and to Hill (1950).
2. The mode of deformation is by plane strain; that is, deformation takes place only in the horizontal (r, θ) planes, and these remain plane during deformation. This requires that the intermediate principal stress, σ_2, be oriented vertically.
3. Stress acting normal to the horizontal (r, θ) plane, that is, the intermediate principal stress, including the body force of gravity, is assumed to have no influence on the orientation of the trajectories of principal shear stress. This assumption necessarily follows from the assumption of plane strain.
4. The expressions of stress components in terms of principal stresses in two dimensions are:

$$\sigma_r = \frac{\sigma_1 + \sigma_3}{2} + \frac{\sigma_1 - \sigma_3}{2} \cos 2\gamma$$

$$\sigma_\theta = \frac{\sigma_1 + \sigma_3}{2} - \frac{\sigma_1 - \sigma_3}{2} \cos 2\gamma$$

$$\tau_{r\theta} = \frac{\sigma_1 - \sigma_3}{2} \sin 2\gamma,$$

   in which σ_r designates normal stress in the radial direction, σ_θ designates normal stress in the θ or tangential direction, σ_1 is the algebraically largest principal stress (tension is positive), σ_3 is the algebraically least stress, $\tau_{r\theta}$ is shear stress measured in the coordinate directions, and γ is the angle measured positively counterclockwise from the radial direction to the direction of action of σ_1. Figure 14 shows the positive directions of normal coordinate stresses, the positive direction of $\tau_{r\theta}$ and the angle γ.
5. Equilibrium of internal elements is maintained; that is, each small element is assumed to be in static equilibrium under the forces to which it is subjected. This requires that

$$r \frac{\partial \sigma_r}{\partial r} + \frac{\partial \tau_{r\theta}}{\partial \theta} + \sigma_r - \sigma_\theta = 0$$

$$\frac{\partial \sigma_\theta}{\partial \theta} + r \frac{\partial \tau_{r\theta}}{\partial r} + 2\tau_{r\theta} = 0.$$

6. The velocity of deformation is assumed to be so small that inertial forces may be neglected.
7. The stresses in the wedge are not influenced by the loading path; that is, they depend only on the final state, and not upon the succession of events through elastic deformation and plastic failure prior to the state that is analyzed. This follows from the basic assumption of unrestricted deformation in a perfectly plastic solid.
8. The shear strength of the material is a constant k. This is Von Mises' criterion for plastic deformation in plane strain.

$$\tau_{max} = (\sigma_1 - \sigma_3)/2 = k.$$

The analyses of the western and eastern parts of the South Silverton district that follow are made, respectively, under the additional assumptions $\partial\gamma/\partial r = 0$ and $\partial\gamma/\partial\theta = 0$, for which generalized expressions for slip lines and stresses were previously derived.

ANALYSIS OF THE WESTERN SHEAR SYSTEM

STATEMENT OF THE PROBLEM

The western part of the South Silverton area is analyzed as a compressed wedge, and the theoretical

pattern of maximum-shear-stress trajectories will be compared farther on with that of the faults as mapped in the field. The wedge is assumed to be compressed from the north against a rigid buttress south of the Titusville vein. The apex of the wedge is to the west, just south of the town of Silverton; the axis of the wedge trends due east. The eastern base of the wedge cannot be closely defined but is near Cunningham Creek (fig. 16).

The method used here for determining the internal stresses and trajectories of principal shear stress in a compressed wedge follows that developed by Nádai (1924) and briefly referred to in his more recent text (1950, p. 542) and by Hill (1950, p. 209). Nádai's solution was directed toward the study of plastic flow and extrusion of ductile metal through the opening at the apex of a wedge-shaped die. The analysis was made, using polar coordinates, and taking the apex of the wedge as the origin, under the assumption that, at some distance from the apex, the shear stress $\tau_{r\theta}$ is independent of the distance r from the apex; that is, $\partial\tau_{r\theta}/\partial r = 0$. From equations 19.3 we see also that $\partial\gamma/\partial r = 0$. This assumption is analogous to the assumption, in the analysis of Prandtl's compressed strip (Prandtl, 1923), that τ_{xy} is independent of x. In other words, Nádai's solution for the wedge is an adaptation of Prandtl's problem as applied to inclined plates. The procedure he followed in deriving expressions for slip lines is practically the same as that used to derive equation 19.16, with the integration completed to fit his requirements for boundary conditions. The pattern of slip lines that he developed is shown in figure 18.

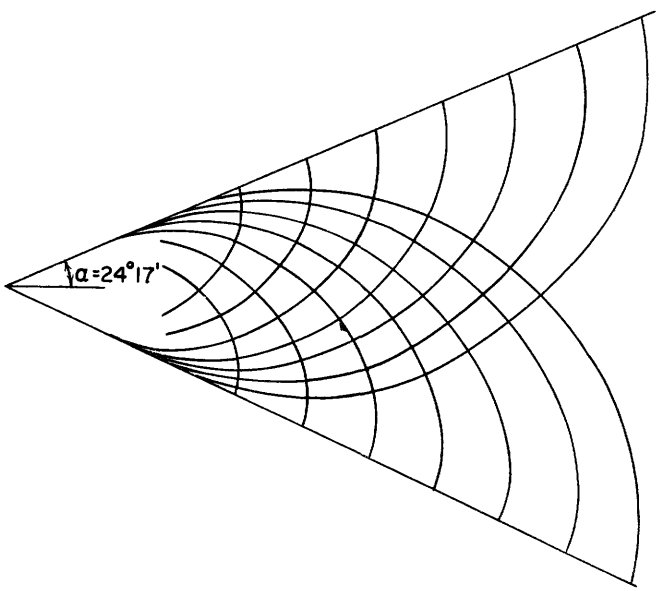

FIGURE 18.—Slip lines having two inclined straight lines as their envelopes. Plastic flow is directed toward the apex of the wedge. From Nádai (1924, fig. 28).

Nádai's problem differs in several respects from that presented by the compressed wedge at Silverton. First, in Nádai's problem the material in the wedge is forced to flow toward and out of an opening at the apex; in the Silverton analysis the apex is considered to be closed and the material is assumed to move from the apex and toward the large end of the wedge. The sense of shear stress on the boundaries is thus opposite to that of Nádai's problem. This radically alters the trajectories of principal shear stress. Second, maximum shear stress acts on the upper face of Nádai's wedge. It is assumed that the north side of the Silverton wedge did not sustain the maximum possible horizontal shear stress because there is no field evidence that horizontal displacement occurred along the southern border of the ring-fault zone. There was, of course, considerable vertical differential displacement along the ring-fault zone, but this need not be considered in the analysis of plane strain in the horizontal plane. Third, the angle of opening of Nádai's wedge, 48° 34′, for which he calculated a solution, is too large for the Silverton wedge, which has an angle of opening of 38°.

The basic assumptions made in the analysis of the western shear system are those listed in the general statement at the beginning of the section on application plus:

9. In the region under consideration, the shear stress does not vary with the distance from the apex of the wedge.

All these assumptions are incorporated into the derivation of the generalized expressions for slip lines, equation 19.16 and stresses equation 20.11, which may be put to direct application when the geometry and boundary conditions of the problem are specified. These are presented in figure 19.

DERIVATION OF SLIP LINES

The derivation of generalized expressions for the families of slip lines, under the assumption $\partial\gamma/\partial r = 0$, ended with the expressions equations 19.14, 19.22, and 19.28, repeated below

$$d\theta = \frac{\cos 2\gamma d\gamma}{C - \cos 2\gamma}, \qquad (21.1)$$

and

$$r = \frac{M}{\sqrt{\pm(C - \cos 2\gamma)}} \exp\left[\pm \frac{1}{2}\int \frac{2d\gamma}{C - \cos 2\gamma}\right], \qquad (21.2)$$

where the sign in the exponential is positive for the first family of slip lines and negative for the second. Integration of the expression $d\gamma/(C-\cos 2\gamma)$ cannot be made until the value of C is given. In order to determine C and a second constant D, which results

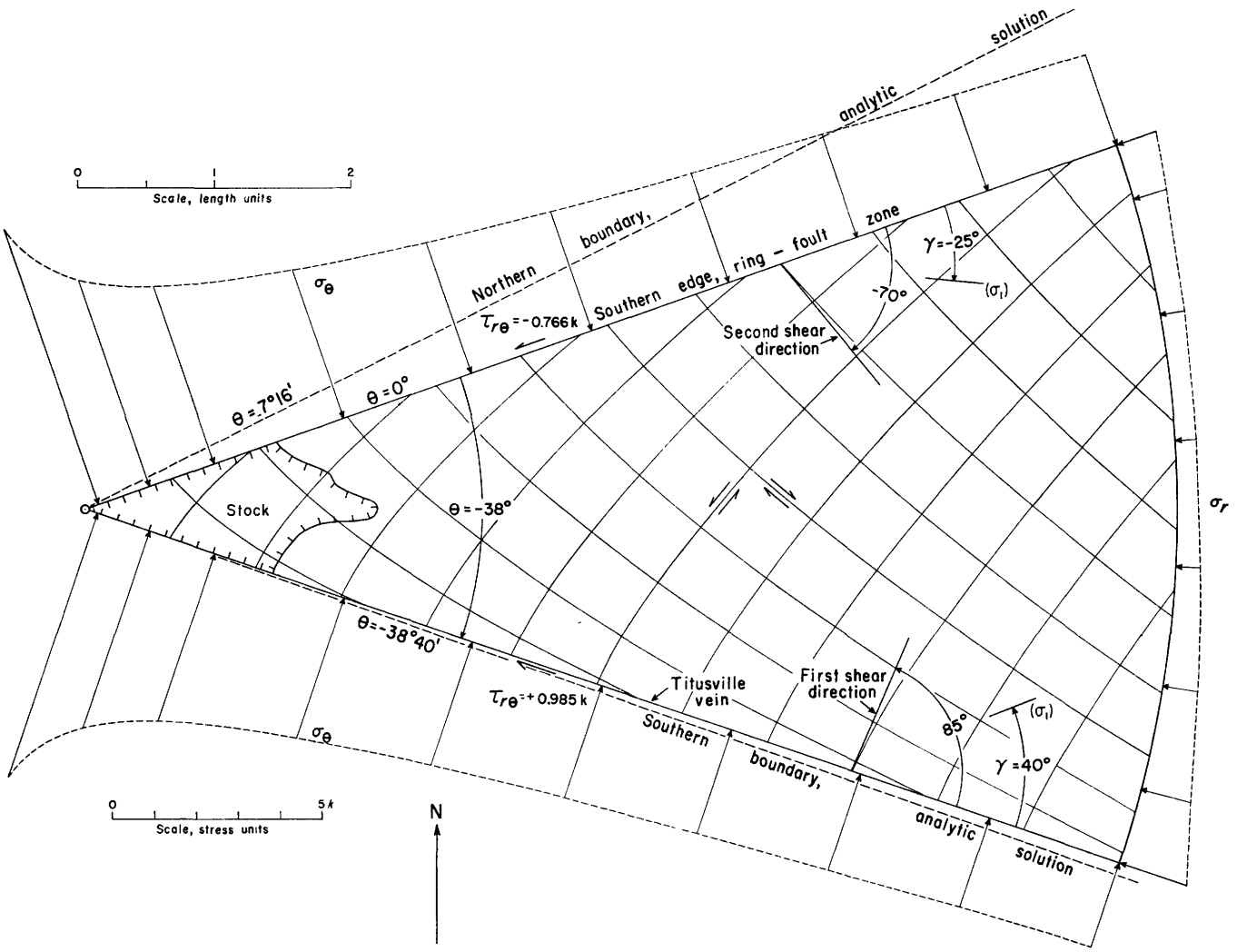

FIGURE 19.—Compressed wedge: idealization of the western part of the South Silverton district. Network of curves in the wedge are principal shear-stress trajectories (slip lines). Boundary conditions are that σ_1 acts at angles of $-25°$ and $+40°$ to the radius at the upper and lower faces, respectively. Computed values of stresses σ_θ and σ_r are shown on boundaries. Normal stress σ_θ becomes infinite at apex of wedge.

from integration of equation 21.1, it is necessary to specify γ for two values of θ. For this purpose, the angle γ will be specified at the ring-fault zone ($\theta = 0°$) and at the Titusville vein ($\theta = -38°$).

Field evidence, the strikes of observed faults, is used to determine the value of γ at the boundaries. The principal northwestward- and northeastward-trending faults rarely can be observed at the boundaries. A reasonable estimate was made concerning the angle at which the northwestward-trending faults and veins (second set of maximum-shear-stress trajectories) would meet the ring-fault zone if they were prolonged a short distance. This angle was estimated to be $-70°$. An angle of $-5°$ between these members of the second set and the Titusville vein was chosen so that the northwestward-trending set could join the Titusville envelope without an unduly long approach to tangency. As a result, the angle between the first shear direction and the Titusville vein is 85°. These boundary conditions are shown on figure 19. The real boundary conditions are, of course, not determined by γ itself but by the orientation of faults that are assumed to be maximum shear stress trajectories oriented at ($\gamma + 45°$) to the radius.

The Titusville fault and vein is regarded, for all practical purposes, as an envelope and a limiting boundary for the mathematical solution, even though the first and second sets of principal shear–stress trajectories are not made to meet it exactly orthogonally and tangentially. Shear stress along the Titusville fault as computed from equation 19.3, therefore comes out to be $0.985k$, slightly less than the amount necessary for slip. In reality, there is

evidence for horizontal displacement along the Titusville vein of as much as several hundred feet in its middle course. The actual boundary for the mathematical solution lies just south of the Titusville fault.

The direction of principal normal stress will bisect the right angles included between the trajectories of principal shear stress, hence, with the assumed values of $\gamma + 45°$ or $\gamma - 45°$ at the boundaries, the direction of action of σ_1 at the boundaries is as shown in figure 19. The corresponding boundary conditions for γ are:

at

$$\begin{aligned} \theta &= 0° \\ \gamma &= -25° = -0.4363 \text{ radians} \\ 2\gamma &= -50° = -0.8727 \text{ radians}, \end{aligned} \tag{21.3}$$

at

$$\begin{aligned} \theta &= -38° = -0.6632 \text{ radians}; \\ \gamma &= +40° = +0.6981 \text{ radians} \\ 2\gamma &= +80° = +1.3963 \text{ radians}. \end{aligned} \tag{21.4}$$

Knowing θ and γ for two values of θ makes the solution for C and D in equations 19.17 to 19.21 theoretically possible. However, these equations are quite complicated, and at the outset there is no indication concerning which is to be used. Nádai avoided this problem simply by choosing a value of 2 for C that was convenient for computation. He let that choice determine the angle of opening of the wedge, since the precise angle of the wedge was of no concern for his generalized analysis. However, that choice limited him to the use of equation 19.18. In the South Silverton analysis it is necessary to perform the more complicated inverse and determine C from the angle of the wedge and the values of γ at the boundaries.

The first step is to determine, if possible, whether C is negative or positive and its approximate magnitude so that the choice of equations to use is narrowed. Note first that, as θ increases from $-38°$ to $0°$, γ decreases from $40°$ to $-25°$ so the ratio $d\gamma/d\theta$ is probably everywhere negative, while $\cos 2\gamma$ is always positive. From equation 19.14 we have

$$\frac{d\gamma}{d\theta}\ (-) = \frac{C - \cos 2\gamma}{\cos 2\gamma\ (+)}, \tag{21.5}$$

where the signs in parentheses indicate the sign of the term. Hence,

$$C - \cos 2\gamma = \text{a negative number}. \tag{21.6}$$

From equation 21.6 the inference is that either: C is a negative number or, C is a positive number with a magnitude less than the smallest value of $\cos 2\gamma$ ($\cos 80° = 0.174$). In order to decide which of these two assumptions is more probably correct, equation 21.5 can be used as an approximate expression for finite differences. The total change in γ is $-65°$ while θ changes $+38°$. An average value for γ of $10°$ is taken. Used thus, equation 21.5 becomes

$$\begin{aligned} \frac{\Delta\gamma}{\Delta\theta} &\approx \frac{C - \cos 2\gamma}{\cos 2\gamma} \\ -\frac{65}{38} &\approx \frac{C - 0.9397}{0.9397} \\ C &\approx -0.67. \end{aligned} \tag{21.7}$$

These results indicate that C probably lies between -1 and 0, hence equation 19.18 should not be used to evaluate C because imaginary quantities would result from the radical. Equation 19.20 appears to be the simplest alternative, and it gives

$$\theta + D = -\gamma + \frac{C}{\sqrt{1 - C^2}} \tanh^{-1} \frac{\sqrt{1 - C^2}\tan\gamma}{C - 1}. \tag{21.8}$$

Using the known radian values of the angle γ at the radian values of $\theta = 0°$ and $\theta = -38°$, equation 21.8 reduces to

$$-0.4712 = \frac{C}{\sqrt{1 - C^2}}\left[\tanh^{-1}\left(\frac{-0.4663\sqrt{1 - C^2}}{C - 1}\right) - \tanh^{-1}\left(\frac{0.8391\sqrt{1 - C^2}}{C - 1}\right)\right]. \tag{21.9}$$

A direct solution for an approximate value of C in equation 21.9 may be obtained by putting the $\tanh^{-1}$ expression in the form of an infinite series. That is,

$$\tanh^{-1} x = x + \frac{x^3}{3} + \frac{x^5}{5} + \ldots \text{ if } [x^2 < 1]\ . \tag{21.10}$$

Using only the first two terms of the series, equation 21.9 can be recast into a form that reduces to the quadratic equation

$$0.6032C^2 - 0.5940C - 0.4712 = 0 \tag{21.11}$$

that has the two solutions

$$C = -0.52 \tag{21.12}$$

$$C = +1.513. \tag{21.13}$$

The second solution is not valid for the present problem. With the approximate value of -0.52 for C, one may easily determine, by trial and the use graphs, the precise value of C that satisfies equation 21.9. Once C is obtained, D can be found from (21.8) at $\theta = 0$. The values are:

$$\begin{aligned} C &= -0.513 \\ D &= +0.274 \end{aligned} \tag{21.14}$$

The resulting expressions for θ (from equation 21.8) and r (from equations 19.22 and 19.28) are

$$\theta = -0.274 - \gamma + .598 \tanh^{-1}(0.567 \tan\gamma) \tag{21.15}$$

$$\frac{r}{M} = \frac{1}{\sqrt{\cos 2\gamma + .513}} \exp\left[\pm 1.165 \tanh^{-1}(0.567 \tan\gamma)\right] \tag{21.16}$$

where the — sign in the exponential term in equation 21.16 is associated with the first family of slip lines and the + sign with the second family. One pair of slip lines is generated for each value of M. The sign before the quantity $(C - \cos 2\gamma)$ in equations 19.22 and 19.28 is taken to be minus because $(C - \cos 2\gamma)$ is itself negative in the present instance.

The next step is to draw a section of the wedge and plot the first and second families of slip lines at some arbitrary scale. The size of this initial drawing does not matter—it may be enlarged or reduced to fit the area of interest on the geologic map. But it is necessary to plot enough slip lines so that an adequate diagram is formed. The slip lines are shown in figure 19.

NORMAL STRESSES

In this section expressions for the normal stresses within and on the faces of the compressed wedge are developed. The shear stress on the boundaries is determined by the choice of the angle γ on the boundaries through equation

$$\tau_{r\theta} = k \sin 2\gamma \qquad (19.3)$$

The above equation, and the requirement that shear stress is to vary only with θ,

$$\frac{\partial \tau_{r\theta}}{\partial r} = 0 \qquad (19.12)$$

use up the arbitrary choices that can be made. The normal stresses, σ_θ and σ_r, cannot now be arbitrarily chosen. They can only be computed; however, some control over their magnitude is possible by adjusting constants that will appear in the solution.

Return now to equation 20.11, the generalized expression for ω under the condition $\partial\gamma/\partial r = 0$, and to equations 19.1 and 19.2, which give σ_r and σ_θ in terms of ω and γ.

$$\sigma_r = \omega + k \cos 2\gamma \qquad (19.1)$$

$$\sigma_\theta = \omega - k \cos 2\gamma \qquad (19.2)$$

$$\omega + 2kE = -2Ck \ln r - Ck \ln (\cos 2\gamma - C). \qquad (22.1)$$

In rewriting equation 20.11 as equation 22.1, the minus sign is to be selected in the second logarithmic term of equation 20.11 because $(C - \cos 2\gamma)$ is negative. Substitution of equation 22.1 into equations 19.1 and 19.2 gives

$$\frac{\sigma_r}{k} = -2C \ln r - C \ln (\cos 2\gamma - C) + \cos 2\gamma - 2E, \qquad (22.2)$$

$$\frac{\sigma_\theta}{k} = -2C \ln r - C \ln (\cos 2\gamma - C) - \cos 2\gamma - 2E. \qquad (22.3)$$

These equations are the same as those given by Hill (1950, p. 211) and credited to Nádai (1924, p. 125). Nádai's equations are in a slightly different form, for example,

$$\sigma_r = -k \ln \frac{r^2 (C \mp \cos 2\gamma)}{a^2} \pm k \cos 2\gamma, \qquad (22.4)$$

in which the constant "a" is related to E of equation 22.2 thus

$$C \ln a^2 = -2E. \qquad (22.5)$$

When the value of C is inserted into the expressions for stresses, they become

$$\frac{\sigma_r}{k} = 1.026 \ln r + 0.513 \ln (\cos 2\gamma + 0.513) + \cos 2\gamma - 2E \qquad (22.6)$$

$$\frac{\sigma_\theta}{k} = 1.026 \ln r + 0.513 \ln (\cos 2\gamma + 0.513) - \cos 2\gamma - 2E \qquad (22.7)$$

$$\frac{\omega}{k} = 1.026 \ln r + 0.513 \ln (\cos 2\gamma + 0.513) - 2E \qquad (22.8)$$

$$\frac{\tau_{r\theta}}{k} = \sin 2\gamma. \qquad (22.9)$$

It is apparent that as r increases, σ_r, σ_θ, and ω are each positive and increasing, and that σ_r and ω reach a maximum when γ is zero. The variable parts in the expression for ω lead to positive stresses. The average stress in the compressed wedge is to be kept negative (compression throughout), therefore the constant $-2E$ must be dominant over all the other terms. This constant is analogous to the constant D met in the analysis of Prandtl's compressed strip and explained in the discussion of equation 14.14. In evaluating E we must decide what part of the wedge is to be used for analysis and whether or not tension is to be allowed upon the boundaries.

The base (eastern border) of the wedge is taken to be at $r = 8$ units and the most positive stress on the base, $\sigma_r = \sigma_1$ at $\gamma = 0°$, is taken to be a compression of $-0.5k$. All parts of the wedge are thus assumed to be under compression and the complicating possibility of fracture by tension is avoided. There is no field evidence for tensile failure at this stage of deformation in the western system.

Under these assumptions, from equation 22.6 at $r = 8$, $\gamma = 0$,

$$-0.5 - 1.026 \ln 8 + .513 \ln (1.513) + 1 - 2E$$

$$E = 1.92. \qquad (22.10)$$

Values of the stresses on the boundaries are also shown in figure 19. Although the tangential stress σ_θ remains fairly constant along the greater part of the wedge, it becomes infinite at r equals zero. This is a singular point in the solution of the differential equations and should be excluded from consideration. As a matter of fact, the apex of the wedge is occupied by the east end of the Silverton stock. Much of the stock was intruded into the ring-fault zone and, so far as can be determined, the ring faults in the adjacent volcanic rocks continue but feebly, if at all, into the stock. There are many joints and some veins in

the stock, but it does not seem to have been sheared nearly as intensely as the volcanic rocks in the wedge. It may be inferred that the stock was intruded rather late in the process of deformation and that its location may have been determined by a crushed zone near the apex of the wedge where the ring-fault zone veers abruptly in strike.

The stresses now are:

$$\frac{\sigma_r}{k} = 1.026 \ln r + 0.513 \ln (\cos 2\gamma + 0.513) + \cos 2\gamma - 3.845 \quad (22.11)$$

$$\frac{\sigma_\theta}{k} = 1.026 \ln r + 0.513 \ln (\cos 2\gamma + 0.513) - \cos 2\gamma - 3.845 \quad (22.12)$$

$$\frac{\omega}{k} = 1.026 \ln r + 0.513 \ln (\cos 2\gamma + 0.513) - 3.845 \quad (22.13)$$

$$\frac{\tau_{r\theta}}{k} = \sin 2\gamma. \quad (22.14)$$

VELOCITIES

The next problem is to see if the stress field and slip-line pattern that were developed for the compressed wedge can be associated with velocities that are compatible with the behavior of a perfectly plastic wedge.

The basic relations to be used are those of equations 18.1 to 18.3 that combined with equations 18.7 to 18.9 become

$$\dot{e}_r = \frac{\partial v_r}{\partial r} = Ls_r = Lk \cos 2\gamma \quad (23.1)$$

$$\dot{e}_\theta = \frac{v_r}{r} + \frac{\partial v_\theta}{r\partial\theta} = Ls_\theta = -Lk \cos 2\gamma \quad (23.2)$$

$$\dot{\gamma}_{r\theta} = \frac{\partial v_r}{r\partial\theta} + \frac{\partial v_\theta}{\partial r} - \frac{v_\theta}{r} = 2L\tau_{r\theta} = 2Lk \sin 2\gamma. \quad (23.3)$$

These three equations by themselves may not be sufficient for the derivation of expressions for the three variables v_r, v_θ, and L. They may, however, limit to a considerable degree the possible forms which these variables can take.

A full investigation of velocity expressions that may satisfy equations 23.1 to 23.3 will not be made. Instead, the problem will be restricted to the example in which the material southwest of the Titusville vein remains rigid and immovable and the subsiding block north of the ring-fault zone presses against the north side of the wedge in such a way that the ring-fault zone moves southeastward with a constant velocity in a direction normal to the ring faults while remaining parallel to its preceding positions, as shown in figure 20. The angle of opening of the wedge thus remains constant. The constant C, which is determined in part by the angle of the wedge, will in this example remain constant with time. Other modes of deformation, in which the ring-fault zone rotates or becomes curved, would require C to vary during deformation and would be considerably more difficult to analyze.

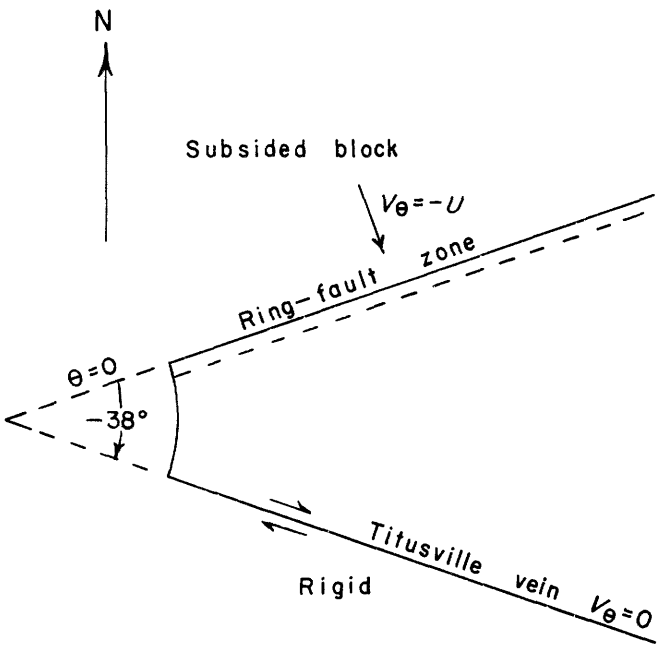

FIGURE 20.—Compression of the wedge under the assumption $\partial v_\theta/\partial r = 0$. The southwestern boundary is assumed to remain rigid. The northwestern boundary moves southeastward at a constant velocity $-U$ while remaining parallel to its original position.

If the ring-fault zone remains straight and does not rotate, v_θ will be independent of r along the northern border; it will also be independent of r along the rigid southern border. It will be assumed, therefore, that v_θ is independent of r everywhere in the interior of the wedge. This may be stated as

$$\partial v_\theta/\partial_r = 0. \quad (23.4)$$

Equations 23.1 to 23.3 become, respectively

$$\frac{\partial v_r}{\partial r} = Lk \cos 2\gamma \quad (23.5)$$

$$v_r + \frac{dv_\theta}{d\theta} = Lkr \cos 2\gamma \quad (23.6)$$

$$\frac{\partial v_r}{\partial \theta} - v_\theta = 2Lkr \sin 2\gamma. \quad (23.7)$$

Taking the derivative of equation 23.6 with respect to r and equating the result to equation 23.5 gives

$$-2L = r\frac{\partial L}{\partial r}. \quad (23.8)$$

Taking the derivative of equation 23.5 with respect to θ and of equation 23.7 with respect to r, equating the results, and using equation 23.8, gives

$$\frac{\partial L}{\partial \theta} = -2 \tan 2\gamma \left(1 - \frac{d\gamma}{d\theta}\right) L. \quad (23.9)$$

From (23.8)

$$\frac{\partial L}{\partial r} = -\frac{2L}{r}. \quad (23.10)$$

The total differential of L is

$$dL = \frac{\partial L}{\partial r}\, dr + \frac{\partial L}{\partial \theta}\, d\theta, \tag{23.11}$$

which becomes, with substitution of equation 23.9 and 23.10,

$$\frac{dL}{L} = -2\,\frac{dr}{r} - \frac{2\sin 2\gamma d\theta}{\cos 2\gamma} + 2\tan 2\gamma d\gamma. \tag{23.12}$$

When equation 19.14 is used to express $d\theta$, equation 23.12 becomes

$$\int \frac{dL}{L} = -2\int \frac{dr}{r} - \int \frac{-2\sin 2\gamma d\gamma}{\cos 2\gamma - C} + \int \tan 2\gamma 2 d\gamma, \tag{23.13}$$

which may be completely integrated to give

$$\ln L = -\ln r^2 - \ln(\cos 2\gamma - C) - \ln\cos 2\gamma + \ln A$$

$$L = \frac{A}{\cos 2\gamma\,(\cos 2\gamma - C)\, r^2}. \tag{23.14}$$

All quantities in the denominator of equation 23.14 are positive and the constant of integration, A, is positive because it has a real logarithm. Thus, L as here derived, is positive. This satisfies a basic requirement that L must be positive in order to assure that positive work is done on the plastically deforming material.

We now return to derivation of velocities from equations 23.5 to 23.7. The new expression for L makes these equations read

$$\frac{\partial v_r}{\partial r} = \frac{Ak}{(\cos 2\gamma - C)\, r^2} \tag{23.15}$$

$$v_r + \frac{dv_\theta}{d\theta} = -\frac{Ak}{(\cos 2\gamma - C)\, r} \tag{23.16}$$

$$\frac{\partial v_r}{\partial \theta} - v_\theta = \frac{2Ak\tan 2\gamma}{(\cos 2\gamma - C)\, r}. \tag{23.17}$$

The derivative of equation 23.16 with respect to θ is

$$\frac{\partial v_r}{\partial \theta} = -\frac{d^2 v_\theta}{d\theta^2} - \frac{Ak}{r}\left[\frac{2\sin 2\gamma}{(\cos 2\gamma - C)^2}\frac{d\gamma}{d\theta}\right]. \tag{23.18}$$

Substitution of this expression for $\partial v_r/\partial\theta$ into equation 23.17 gives

$$\frac{d^2 v_\theta}{d\theta^2} + v_\theta = 0. \tag{23.19}$$

The general solution to equation 23.19 is

$$v_\theta = B\cos\theta + D\sin\theta. \tag{23.20}$$

Using equations 23.20 and 23.16 gives

$$v_r = B\sin\theta - D\cos\theta - \frac{Ak}{(\cos 2\gamma - C)\, r}. \tag{23.21}$$

The constants B and D may be evaluated from the boundary conditions:

at

$$\theta = 0, \qquad v_\theta = -U; \tag{23.22}$$

and at

$$\theta = -38°, \quad v_\theta = 0. \tag{23.23}$$

Hence,

$$B = -U, \tag{23.24}$$

$$D = -1.28U, \tag{23.25}$$

$$v_\theta = -U(\cos\theta + 1.28\sin\theta), \tag{23.26}$$

and

$$v_r = U(-\sin\theta + 1.28\cos\theta) - \frac{Ak}{(\cos 2\gamma - C)\, r} \tag{23.27}$$

The above derivation indicates that expressions for velocity may be found for the assumed mode of deformation. Hence, the formal requirement, often neglected, that a derived slip-line field have a compatible velocity field, is here fulfilled. No claim is made that the velocity field is unique.

Equation 23.17 indicates that $\partial v_r/\partial\theta$ becomes infinite only if γ becomes equal to $\pm 45°$ or if r becomes zero. Disregarding the singular point $r = 0$, this means that the radial velocity is discontinuous across a radius only if that radius is an envelope of the slip lines. Such discontinuities occur at the limits of the analytic solution (fig. 19). The implications that arise from the northern boundary of the wedge not being at the analytic boundary of the solution are dealt with in the section on discussion of results and conclusions.

ANALYSIS OF THE EASTERN SHEAR SYSTEM

STATEMENT OF THE PROBLEM

The analysis of the eastern part of the South Silverton area proceeds from the assumption that the granite porphyry dike occupies a typical fault in the shear system. The known outcrop of the dike indicates that its northern terminus is at the edge of the subsided block and is oriented at a right angle to the ring faults. From this point it veers southward and southwestward in a great arc, and its southern terminus is parallel to the southern border of the subsided block (fig. 17). This arrangement suggests that the shear system, of which the dike is a part, lies within an annular ring around the subsided block, and that one set of maximum-shear-stress trajectories meets the inner boundary at a right angle and the outer boundary tangentially. The other set is tangent to the inner boundary and normal to the outer boundary.

A sketch of such a slip-line field has been given by Nádai (1950, fig. 37–14), but he does not develop the expressions for stresses or the equations for the lines. He simply states that such a pattern consists of epicycloids and hypocycloids and arises from assuming that the shear stress $\tau_{r\theta}$ depends only on r, the distance from the center of the circular arcs that bound the ring, and that $\tau_{r\theta}$ has the value of $-k$ and $+k$ on the inner and outer boundaries, respectively.

The shearing in the eastern part of the South Silverton area will be analyzed under the assumption that it simulates Nádai's problem with the boundary conditions as shown in figure 21. For simplicity the ring-fault zone will be assumed to be an arc of a circle rather than its more probable true shape, the arc of an oval or ellipse. In the South Silverton analysis the outer boundary of the ring-fault zone marks the limit of the plastic domain. Outward pressure from the subsiding block cannot produce shear in the same sense all the way around a continuous ring without causing circulation of the matter in the ring. Hence, this must be a local feature limited to just a sector of the periphery of the subsided block. Displacement to the northeast and north of the area analyzed must be in the opposite direction.

The assumptions made in the mathematical analysis are the same as those made for the analysis of the western part, except that $\tau_{r\theta}$ is taken as a function of r only:

$$\partial\tau_{r\theta}/\partial\theta = 0$$
$$\partial\gamma/\partial\theta = 0.$$

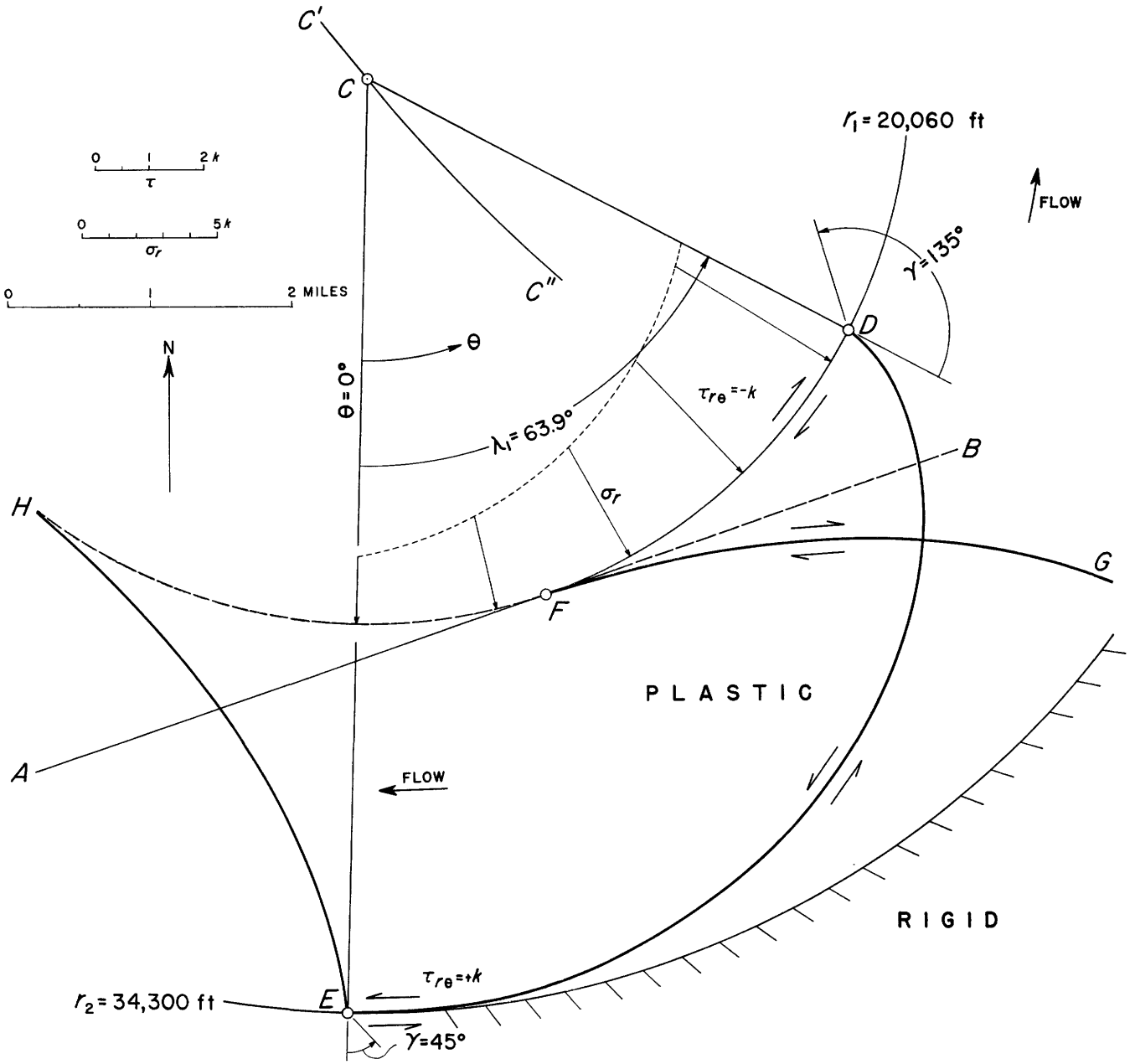

FIGURE 21.—Compressed annular ring; idealization of the eastern part of the South Silverton district. Boundary conditions are that $\gamma = 135°$ on the inner boundary r_1, and $\gamma = 45°$ on the outer boundary r_2. The slip lines are epicycloids and hypocycloids, for example DE and FG, respectively.

DERIVATION OF SLIP LINES

If $\tau_{r\theta}$ is taken to be a function of r only, the generalized relation between γ and r in equation 19.31 is

$$\sin 2\gamma = \frac{G}{r^2} + H, \tag{24.1}$$

and the relation between θ and r along the first set of slip lines is equation 19.34:

$$\theta + N = \frac{\pi}{4} - \gamma - \frac{1+H}{2}\int \frac{2d\gamma}{\sin 2\gamma - H}. \tag{24.2}$$

Further information on the magnitude of H is needed in order to determine the integral of equation 24.2.

Expressions for G and H may be derived from the boundary conditions:

at $r = r_1$

$$\gamma = +135°; \tag{24.3}$$

at $r = r_2$,

$$\gamma = +45°. \tag{24.4}$$

Hence, from equation 24.1,

$$-1 = \frac{G}{r_1^2} + H$$

$$1 = \frac{G}{r_2^2} + H,$$

and

$$G = -\frac{2r_1^2 r_2^2}{r_2^2 - r_1^2} \tag{24.5}$$

$$H = \frac{r_1^2 + r_2^2}{r_2^2 - r_1^2}. \tag{24.6}$$

In the present instance, r_2 is larger than r_1, so H is a positive number and greater than one.

At this point, however, a further complication is produced because integrals of equation 24.2 are valid only if 2γ lies between $-\pi$ and $+\pi$. At the inner radius, γ has a value of 135° or −45°, depending in which direction the angle γ is measured from the radius to the line of action of σ_1. If a first shear direction is followed from the outer circle to the inner circle, the angle γ is seen to increase continuously from 45° to 135°, so 135° is the proper value at the inner circle. The value of 2γ is here $3\pi/2$, hence a substitution of another variable is necessary; let

$$\nu = 2\gamma - \pi/2 \tag{24.7}$$

$$\sin \nu = -\cos 2\gamma$$

$$\cos \nu = \sin 2\gamma$$

$$d\nu = 2d\gamma$$

and equation 19.34 becomes

$$\theta + N = \frac{\pi}{4} - \frac{1}{2}\left(\nu + \frac{\pi}{2}\right) - \frac{1+H}{2}\int \frac{d\nu}{\cos \nu - H}. \tag{24.8}$$

If $H > 1$, the proper integral of equation 24.8 is, according to Pierce (1929, formula 300):

$$\theta + N = -\frac{\nu}{2} - \frac{1+H}{\sqrt{H^2-1}} \tan^{-1} \frac{\sqrt{H^2-1}\tan\frac{\nu}{2}}{1-H}. \tag{24.9}$$

On resubstitution of γ, equation 24.9 becomes

$$\theta + N = \frac{\pi}{4} - \gamma - \frac{1+H}{\sqrt{H^2-1}} \tan^{-1} \frac{\sqrt{H^2-1}\tan\left(\gamma - \frac{\pi}{4}\right)}{1-H}. \tag{24.10}$$

The constant N may be evaluated by the boundary condition at $\theta = 0$, for a slip line of the first family that starts at E,

$$\gamma = 45°,$$

so

$$N = 0. \tag{24.11}$$

The next step is the evaluation of G and H and the determination of numerical values of r_1 and r_2. A geometrical construction in figure 21 is necessary to locate the center of coordinates, which represents the center of the subsided block, and to determine numerical values for r_1 and r_2. The center will not be located from the outline of the block on figure 15 but rather from the following facts and inferences that pertain only to the southeast periphery. (a). The points D and E on figure 21 are fixed by field mapping. Field evidence indicates that they lie on a single line. (b). It is assumed that the plastic domain is an annular ring, hence the maximum-shear-stress trajectory between D and E is an epicycloid. (c). The epicycloid is assumed to complete half its cycle between E and D after passing through a polar angle of λ_1. (d). The inner bounding circle through D is tangent to AB, the northern straight boundary of the western wedge, prolonged as may be necessary. (e). The strike of the dike at D and E could not be determined accurately enough in the field to allow radial lines to be drawn. (f). The locus of centers of all circles that may be drawn through D and tangent to AB is a parabola C'–C'', which has D as focus and AB as directrix.

It is now possible, after some trial and error, to select a center C on the parabola, which will allow generation of an epicycloid DE that has approximately the same strike at E as the average observed strike of the dike in this vicinity. Several trials were necessary to find the best location for C; however, the labor is not great because the actual curve DE need not be plotted each time.

As the reader may recall, an epicycloid is generated by a point on one circle of diameter $r_2 - r_1$ which rolls without slipping around the outside of a circle of radius r_1. A hypocycloid is generated if the

smaller circle rolls on the inside of the circle with radius r_2. Hence, if λ_1 is the angle DCE,

$$\lambda_1 = 90° \left(\frac{r_2 - r_1}{r_1}\right). \tag{24.14}$$

The distances r_1 and r_2 and the angle λ_1 are all fixed by each choice of C. The position of C that makes equation 24.14 an equality can be most easily found by trial. The resulting values are:

$$r_1 = 20{,}060 \text{ feet} \tag{24.15}$$

$$r_2 = 34{,}300 \text{ feet} \tag{24.16}$$

$$\gamma_1 = 63.9° \tag{24.17}$$

$$G = -12.232 \times 10^8 \tag{24.18}$$

$$H = 2.0397 \tag{24.19}$$

$$\sqrt{H^2 - 1} = 1.7778 \tag{24.20}$$

$$\frac{1 + H}{\sqrt{H^2 - 1}} = 1.7099 \tag{24.21}$$

$$\frac{\sqrt{H^2 - 1}}{1 - H} = -1.7099. \tag{24.22}$$

Equations 24.10 and 24.1 now become

$$\theta = 45° - \gamma - 1.7099 \tan^{-1} [-1.7099 \tan (\gamma - 45°)] \tag{24.23}$$

$$\sin 2\gamma = \frac{-12.223 \times 10^8}{r^2} + 2.0397. \tag{24.24}$$

Equations 24.23 and 24.24 are the parametric equations of the first set of principal-shear-stress trajectories of the eastern system. It is not at all apparent that these equations represent an epicycloid. The most direct demonstration is to plot the curve from equations 24.23 and 24.24 and compare it with an epicycloid plotted from the standard formulas for an epicycloid in cartesian coordinates (James and James, 1949, p. 130):

$$x = (a + b) \cos \phi - a \cos \frac{a + b}{a} \phi \tag{24.25}$$

$$y = (a + b) \sin \phi - a \sin \frac{a + b}{a} \phi, \tag{24.26}$$

in which ϕ is the angle subtended at the origin of coordinates by the arc already traveled by the center of the rolling circle, b is the radius of the inner circle, and a is the radius of the rolling circle. The curves plotted from equations 24.23–24.24 and from equations 24.25–24.26 coincide exactly. I am also indebted to Mr. Odé (written communication, 1956) for the mathematical proof of equivalence.

The second set of slip lines (hypocycloids) may be derived in a similar manner. Since they are orthogonal to the first set, their slope is equal to the negative reciprocal of the first set. This leads to

$$\theta + P = \frac{\pi}{4} - \gamma - \frac{H - 1}{2} \int \frac{2d\gamma}{\sin 2\gamma - H}. \tag{19.36}$$

After integration of equation 19.36, again using the intermediate variable ν, we get

$$\theta + P = 45° - \gamma - 0.585 \tan^{-1} [-1.71 \tan (\gamma - 45°)]. \tag{24.27}$$

In order to evaluate P it is assumed that a hypocycloid HE passes through point E in figure 21. Then at

$$\theta = 0,$$
$$\gamma = 45°,$$
$$P = 0. \tag{24.28}$$

The two epicycloid and hypocycloid curves are shown in figure 21. These are but two examples of the infinite number of epicycloidal and hypocycloidal slip lines in the eastern system.

It is not necessary actually to plot the equations of the slip lines in each area where comparison with the fault pattern is desired. For this purpose, a cardboard template, at the scale of the geologic map, was cut in the shape $HFDE$. It has a full epicycloidal edge on the right edge and bottom, a hypocycloid on the left edge, and a segment of the inner circle at the top. By sliding the template around the inner circle, which was drawn on the geologic map, the strike of actual faults could be compared with the theoretical orientation at any location and segments of the theoretical lines could be drawn for reference using the edges of the template. This comparison will be deferred to a later section.

NORMAL STRESSES

The generalized expression for average normal stress, ω, under the condition that γ is a function of r only, is given by equation 20.18.

The necessary integration has already been discussed under the section on slip lines, equations 24.8 and 24.9. Using equations 19.1 and 19.2 the expressions for normal stresses become

$$\frac{\sigma_r}{k} = \frac{\omega}{k} + \cos 2\gamma \tag{25.1}$$

$$\frac{\sigma_\theta}{k} = \frac{\omega}{k} - \cos 2\gamma \tag{25.2}$$

$$\frac{\tau_{r\theta}}{k} = \sin 2\gamma \tag{25.3}$$

$$\frac{\omega}{k} = -2H\left(\theta + \gamma - \frac{\pi}{4}\right) - 2\sqrt{H^2 - 1} \tan^{-1}\left[\frac{\sqrt{H^2 - 1} \tan\left(\gamma - \frac{\pi}{4}\right)}{1 - H}\right] - 2F. \tag{25.4}$$

These expressions for stress satisfy the equations of equilibrium, equations 16.5 and 16.6.

The next step is to locate the point of greatest positive stress and regulate the constant of integration, F in this equation, so that this point, together with all other parts of the eastern system, remain

in compression. Since $\sigma_1 = \omega + k$, σ_1 will be most positive where ω is most positive. One may see from (25.4) that, at constant γ or r, ω is most positive at $\theta = 0$, the arbitrary western border of the eastern system. The point along the radius $\theta = 0$ at which ω reaches a maximum is determined by the conditions

$$\frac{\partial \omega}{\partial r} = 0 \tag{25.5}$$

and

$$\frac{\partial^2 \omega}{\partial r^2} < 0. \tag{25.6}$$

It may be determined that ω reaches a maximum along the line $\theta = 0°$ where γ has the value 75°20′. The actual value of ω at this maximum is

$$\frac{\omega}{k} = 0.631 - 2F. \tag{25.7}$$

The constant F is adjusted so that the most positive value of σ_1 is zero and the most positive value of ω is $-1.0k$. Hence

$$2F = 1.631. \tag{25.8}$$

The final expressions for normal stresses become

$$\sigma_r = \omega + k \cos 2\gamma \tag{25.9}$$

$$\sigma_\theta = \omega - k \cos 2\gamma \tag{25.10}$$

$$\frac{\omega}{k} = -4.079\left(\theta + \gamma - \frac{\pi}{4}\right) - 1.631 - 3.556 \tan^{-1}\left[-1.71 \tan\left(\gamma - \frac{\pi}{4}\right)\right]. \tag{25.11}$$

The values for σ_r along the ring-fault zone at several values of θ, plotted to an arbitrary scale (reduced compared to the scale for $\tau_{r\theta}$), are shown on figure 21.

The computed normal stress on the ring-fault zone increases steadily counterclockwise around the southeastern border of the caldera to a maximum near the granite porphyry dike. A possible explanation for this pattern of stress increase is given below.

Figure 15 shows a boot-shaped area, bounded by faults, that extends well into the northeast side of the subsided block. According to Burbank, this area is a graben that forms part of a system of graben blocks and faults extending northeastward from the Silverton subsidence to another volcanic center near Lake City. Referring to the boot-shaped area Burbank wrote (1951, p. 295):

> As shown by geologic cross sections across both the foot and leg of the graben, the volcanic formations are tilted away from the graben on all sides. This tilt indicates probably that while the graben was being formed there were periods of alternate tensional and compressional stresses that operated like the opening and closing of the jaws of a crusher. As the jaws opened, the central block wedged downward and when the jaws closed, it tended to force outward and to tilt the bounding volcanic beds and flows. The causes of this action may be related to the repeated welling up of molten rock at depth, followed by loss of pressure and subsidence of the earth's crust. The final result of these repeated actions was the formation of a crude arch of the volcanic formations with a downfaulted keystone block in the center. The downward sinking of the keystone blocks produced a wedging action on the surrounding rocks.

Figure 22 shows the outline of the subsided block and the graben area. The estimated center of coordinates, C, for analysis of the eastern part of the South Silverton district is also plotted. It is very close to the actual geometric center of the area of subsidence.

If the graben area acted as a wedge, strong local stresses should act on the eastern periphery of the larger subsided block and also on the northern and northwestern periphery. The values of σ_r thus generated might be difficult to compute, particularly as the graben structure also continues through the periphery. The net displacement in the graben area appears, however, to be greatest within the ring-fault zone (Burbank, 1951, p. 291). In any event, it is reasonable to suppose that radial displacement of the border and, hence, radial pressure would increase southward from the graben area—as indicated by

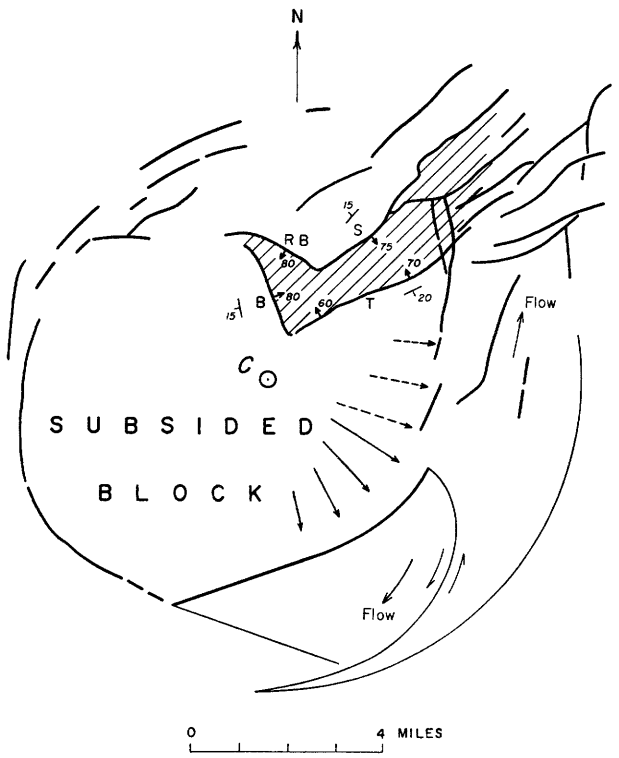

FIGURE 22.—Sketch map of the subsided block of the Silverton caldera. Graben area at northeast corner (after Burbank, 1951, figs. 1 and 2) is ruled. Outward tilting of adjacent rocks is shown by dip symbols. The principal structures are the Ross Basin (R. B.), Sunnyside (S.), Toltec (T.), and Bonita (B.) faults. The circle at C is the center of the polar coordinates for the analysis of the eastern part of the South Silverton district. Stresses computed from this analysis are shown as solid lines; inferred stresses farther north are shown as dashed lines.

dashed lines representing stresses on figure 22—reach a maximum at or somewhat north of the point where the granite porphyry dike enters the ring-fault zone, and then diminish farther southwestward. This last decrease in normal stress toward the southwest agrees qualitatively with the distribution of stress that was found necessary to produce the shear-stress trajectories of the eastern part of the South Silverton district.

No attempt was made to analyze displacements and velocities in the eastern shear system.

COMPARISON OF SLIP-LINE FIELDS AND ACTUAL FAULT PATTERNS

The fault pattern shown on figure 17 has been reproduced in figure 23, together with a number of trajectories of principal shear stress shown by dotted lines. The position and spacing of the dotted lines is, of course, arbitrary; only enough were put in to furnish a basis for comparison.

WESTERN PART

The agreement between actual and theoretical strikes of the northwestward-trending faults is generally good, for instance at *A*, *B*, and *C* of figure 23. There seems to be some departure to the south at the southeast end of some northwestward-trending faults, as a *D*, but others, as at *B* and *E*, seem to veer, as they should in theory, toward the trend of the Titusville vein or envelope. The splitting at the northwest end of the Titusville vein is unexplained; in particular, the split *F* (Scranton City vein) may well belong with oblique secondary fractures shown by 2*c* on figure 16, rather than with the main northwest shear faults. There is no field evidence for or against lateral movement along the Scranton City vein.

The northeastward-trending structures are poorly represented in the whole pattern. A pair of dikes at *G* follow the theoretical strike closely. One member of the northeastward-trending set, the Whale Basin fault at *H*, diverges northward off the predicted course.

All observed directions of relative lateral movement along the faults agree with the theoretical directions of movement.

EASTERN PART

The northwestward-trending hypocycloidal set of faults of the eastern system appears not to have been well developed. A number of fractures near *I* show general agreement. A fault at *J* that branches off from the ring-fault zone and caused some puzzlement during mapping, fits now as the beginning of a hypocycloid. The Green Mountain vein at *K* may be either a hypocycloid of the eastern system or a northwestward-trending vein of the western system. It appears to have been displaced by left-lateral movement on the epicycloid set. The Pride of the West vein at *L* doesn't conform with any theoretical direction. No lateral displacement has been proved along this vein, and it may not properly belong with the other faults shown.

The agreement between the actual course of the granite porphyry dike and its theoretical trend is striking, considering that only the two ends were used to control the geometry of the slip-line field. Between these two ends, through a distance of 7 miles, the dikes curve in strike about 154°, and pass through rocks as diverse as the nearly vertically foliated Precambrian schist and gneiss and the flat volcanic flows and breccias, yet the maximum departure from the theoretical course is only about 400 yards. This occurs at *M*, where the strike of individual en-echelon-dike segments is askew to the general trend of the dike system.

It is not known if the granite porphyry dike is present in the central section around *N*. Cross, Howe, and Ransome (1905) did not show it here, but neither did they map the mile or more of the dike farther north at *P*. The author did not examine the area around *N* during the course of mapping the area to the west. Study of aerial photographs has not helped to settle the question here owing to the prevalence of grass cover, although in many places elsewhere the white dike can be traced as it cuts through darker rocks.

Some other veins mapped by Ransome (1901) or detected on aerial photographs are shown at *Q*, *R*, and *S*. Their strikes conform reasonably well with those postulated by the theory. An andesite dike at *T* has an epicycloidal trend, but this may be fortuitous. Field data are lacking concerning possible lateral movement along it.

DISCUSSION OF RESULTS

The practical results of analysis of the fault pattern in the South Silverton mining district depend more upon the recognition of a pattern of conjugate shears, and knowledge of the relative movements along faults and consequent internal structures of the vein systems, than upon the precise configuration of the pattern itself.

Several questions regarding the theoretical analysis have been raised by some who have read either this report or an abbreviated preliminary version. One question is that of uniqueness. The question really consists of two parts: (1) Do the assumed boundary conditions admit any solutions other than

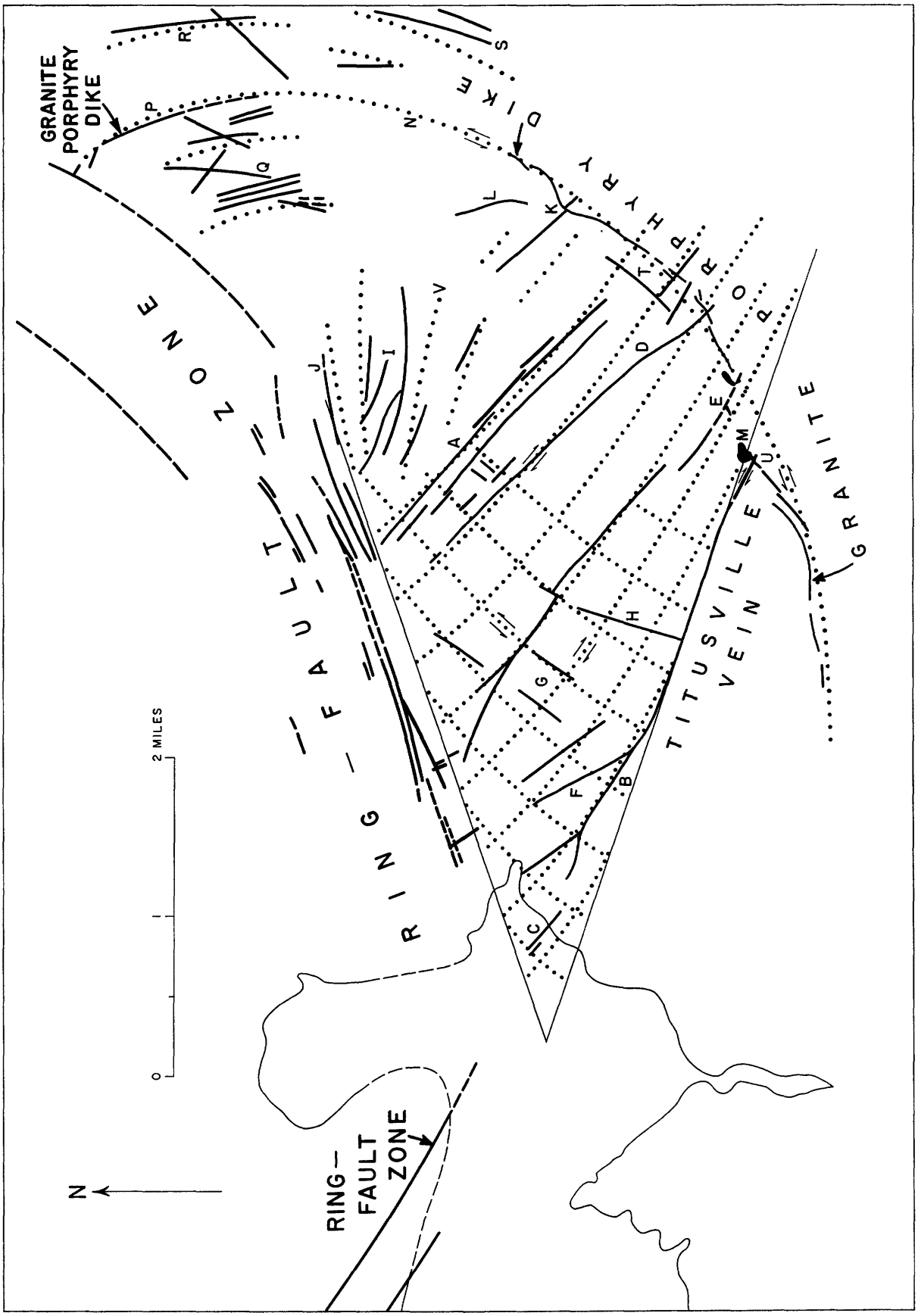

FIGURE 23.—Comparison of actual faults (solid lines) in the South Silverton district with theoretical pattern of principal shear-stress trajectories (dotted lines). Localities shown by letters are discussed in the text.

the ones derived? and (2) Could the observed fault patterns have been produced by other mechanisms, for example, by different boundary conditions, or by the combination of local doming and fracturing?

The answer to the first part is that the pattern of potential faults, as determined by the angle γ in the interior of the analyzed domain, is uniquely determined by the external boundary conditions. The expressions for internal stresses are also determined by the boundary conditions, except for constant multipliers or constant additive terms. The answer to the second part of the question is that no claim is made for uniqueness in the larger sense. The only applicable remark is that the solutions presented for the eastern and western systems are each a possible solution, not necessarily the only solution, and that each encompasses as much ground as possible under a single concept. No doubt, refinements could be made by dividing either or both the western and eastern systems into units, but only at the cost of increasing complexity, and with the necessity of matching boundary conditions of the subunits within each of the two systems.

The division of the area into western and eastern parts, each having independent boundary conditions, has also been questioned. There is no definite answer. The division was made somewhat subjectively, because the granite porphyry dike is unique, both in its lithologic character and its great curvature. It simply does not seem to belong with the nearly straight, andesite-filled fractures of the western system. The relation in age between the western and eastern shear systems is uncertain. There is no field evidence that the two systems formed simultaneously. According to the way in which the two theoretical systems were set up and analyzed, it would be unlikely, perhaps impossible, for them to operate contemporaneously. Hence, no effort has been made to adjust the theoretical boundary stresses into agreement where the two systems merge. The only pertinent bit of evidence is at *U* on figure 23. At this point the Titusville vein, here a barren fault, offsets the granite porphyry dike about 55 feet, the northeast side of the fault having moved to the southeast. Yet, this indicates only the nature of the last movement after the dike was emplaced and tells nothing about the relative times at which faulting began in the two systems.

Although correspondence between the theoretical fault pattern and field observation is gratifying, it does not necessarily imply that all the assumptions made in the analysis, particularly those concerning the physical properties of the rocks, are themselves correct. It is hard to tell what the assumption $\tau_{max} = k$ in plane strain means regarding the behavior of rock in a real three-dimensional-stress distribution. For this reason it would be unwise to infer that the rocks near Silverton were deformed in a region of extremely high hydrostatic pressure, where the envelopes of Mohr's circles are thought to become parallel horizontal lines. The depth below original ground surface of the plane on which analysis was made was not stated, nor can it be estimated with any assurance. Scanty geologic evidence suggests that 2 miles seems to be a fair maximum estimate, but perhaps the depth was much less.

The most important question is whether Von Mises' theory for plane plastic strain can be applied validly to the analysis of three-dimensional geologic problems. This question can hardly be answered in full until a theory of plasticity applicable to geology is developed for three dimensions. Such a theory would need to include the body force of gravity. The slip-line pattern on a horizontal cut through the three-dimensional model then should be compared with the pattern in a horizontal plane given by the simpler analysis in plane strain. The three-dimensional analysis would yield information on dips of the slip surfaces, but the pattern made by these surfaces on a horizontal plane might well be similar to or even identical with the pattern of slip lines formed under the simple assumption of plane strain. This is a matter that needs further investigation.

Another field in which advances may be expected in the theory of plasticity, and in which the theory can be of real service to structural geology, is the determination of the trajectories of maximum shear stress that may be expected to become velocity discontinuities. It may be hoped that one or another of the theories of permanent deformation, controlled by basic geological laboratory and field research, will eventually be able to predict where faults should occur, and their dip, as well as their general trend.

Meanwhile, judging from the results presented in this paper, the incomplete theory for plane plastic strain seems to offer a fair starting point for analyses of some fault patterns, and a rational means whereby scattered field observations may be correlated to obtain a coherent picture.

REFERENCES CITED

Alexander, J. M., 1955, The effect of Coulomb friction in the plane-strain compression of a plastic rigid material: Jour. Mechanics and Physics of Solids, v. 3, p. 233–245.

Anderson, E. M., 1936, The dynamics of the formation of cone-sheets, ring-dykes, and cauldron-subsidences: Royal Soc. Edinburgh Proc., v. 56, p. 128–157.

Burbank, W. S., 1933, Vein systems of the Arrastre Basin and regional geologic structure in the Silverton and Telluride quadrangles, Colorado: Colorado Sci. Soc. Proc., v. 13, no. 5, p. 136–214.

——— 1951, The Sunnyside, Ross Basin, and Bonita fault systems, and their associated ore deposits, San Juan County, Colorado: Colorado Sci. Soc. Proc., v. 15, no. 7, p. 285–304.

Burbank, W. S., Eckel, E. B., and Varnes, D. J., 1947, The San Juan region [Colorado]: Colorado Mineral Resources Board Bull., p. 396–446.

Coulomb, C. A., 1776, Essai sur une application de régles de maximis et minimis à quelques problèmes de statique, relatifs à l'architecture: Mem. Acad. Sci. (Savants Estrang.), v. 7, p. 343–382. Paris.

Cross, C. W., Howe, Ernest, and Ransome, F. L., 1905, Description of the Silverton quadrangle [Colorado]: U. S. Geol. Survey Geol. Atlas, Silverton folio, no. 120.

Frocht, M. M., 1941, Photoelasticity: New York, John Wiley and Sons, v. 1, 411 p.

Green, A. P., 1954, On the use of hodographs in problems of plane plastic strain: Jour. Mechanics and Physics of Solids, v. 2, p. 73–80.

Hafner, Willy, 1951, Stress distributions and faulting: Geol. Soc. America Bull., v. 62, p. 373–398.

Hencky, Heinrich, 1923, Über einige statisch bestimmte Fälle des Gleichgewichts in plastischen Körpern: Zeitschr. angew. Mathematik u. Mechanik, v. 3, p. 241–251.

Hill, Rodney, 1950, The mathematical theory of plasticity. London, Oxford Univ. Press, 356 p.

Hill, Rodney, Lee, E. H., and Tupper, S. J., 1951, A method of numerical analysis of plastic flow in plane strain and its application to the compression of a ductile material between rough plates: Jour. Appl. Mechanics, v. 18, p. 46–52.

Hodge, P. C., Jr., 1950, Approximate solutions of problems of plane plastic flow: Jour. Appl. Mechanics, v. 17, p. 257–264.

Hubbert, M. K., 1951, Mechanical basis for certain familiar geologic structures: Geol. Soc. America Bull., v. 62, p. 355–372.

Jaeger, J. C., 1956, Elasticity, fracture and flow, with engineering and geological applications: London, Methuen and Co., 152 p.

James, Glenn, and James, R. C., 1949, Mathematics dictionary. New York, D. Van Nostrand Co., 432 p.

Lévy, Maurice, 1870, Memoíre sur les équations générales des mouvements intérieurs des corps solides ductiles au delà des limites où l'elasticité pourrait les ramener à leur premier état: Acad. Sci. Paris comptes rendus, v. 70, p. 1323–1325.

Love, A. E. H., 1944, A treatise on the mathematical theory of elasticity: New York, Dover Publication, 4th ed., 643 p.

Marin, Joseph, 1935, Failure theories of materials subjected to combined stresses: Am. Soc. Civil Engineers Proc., v. 61, p. 851–867.

Mises, R. von, 1913, Mechanik der festen Körper im plastisch-deformablen Zustand: Göttinger Nachr., math.-phys. Kl., p. 582–592.

Mohr, Otto, 1882, Ueber die Darstellung des Spannungzustandes und des Deformationzustandes eines Körperelementes und über die Anwendung derselben in der Festigkeitslehre: Zivilingenieur, v. 28, p. 113–156.

Nádai, Arpad, 1924, Über die Gleit- und Verzweigungsflächen einiger Gleichgewichtzustände bildsamer Massen und die Nachspannungen bleibend verzerrter Körper: Zeitschr. Physik, v. 30, p. 106–138.

——— 1931, Plasticity, a mechanics of the plastic state of matter: New York, McGraw-Hill Book Co., 349 p.

——— 1950, Theory of flow and fracture of solids: New York, McGraw-Hill Book Co., 572 p.

Odé, Helmer, 1956, A note concerning the mechanism of artificial and natural hydraulic fracture systems, *in* Symposium on rock mechanics: Colorado School Mines Quart., v. 51, p. 21–29.

——— 1960, Faulting as a velocity discontinuity in plastic deformation, *in* David Griggs and John Handin, eds., Rock deformation—a symposium: Geol. Soc. America, Mem. 79, p. 293–321.

Pierce, B. O., 1929, A short table of integrals: Boston, Ginn and Co., 3d ed., 156 p.

Prager, William, 1956, Finite plastic deformation, p. 63–96, *in* Rheology, theory and applications: F. R. Eirich, ed. New York Academic Press, v. 1, 761 p.

Prager, William, and Hodge, P. G., Jr., 1951, The theory of perfectly plastic solids: New York, John Wiley, 264 p.

Prandtl, Ludwig, 1923, Anwendungsbeispiele zu einem Henckyschen Satz über das plastische Gleichgewicht: Zeitschr. angew. Mathematik u. Mechanik, v. 3, p. 401–407.

Ransome, F. L., 1901, A report on the economic geology of the Silverton quadrangle, Colorado: U. S. Geol. Survey Bull. 182.

Robertson, E. C., 1955, Experimental study of the strength of rocks: Geol. Soc. America Bull., v. 66, p. 1275–1314.

Taylor, N. W., 1947, Mechanism of fracture of glass and similar brittle solids: Jour. Appl. Physics, v. 18, p. 943–955.

Timoshenko, S. P., 1934, Theory of elasticity: New York, McGraw-Hill Book Co., 416 p.

☆ U. S. GOVERNMENT PRINTING OFFICE: 1962—602793